ABSTRACT

Title of Dissertation: **CHARACTERIZATION OF THE COWPOX AND MOUSEPOX HOMOLOGS OF THE SMALLPOX VIRUS B22 PROTEIN AND THEIR ROLES IN MOUSE DISEASE MODELS**

Sara Elizabeth Reynolds, Doctor of Philosophy, 2016

Dissertation directed by: Dr. Bernard Moss, Adjunct Professor, National Institutes of Health
and Dr. James Culver, Professor, Biological Sciences Program

Poxviruses are an important family of viruses with members capable of infecting humans including variola virus, the causative agent of smallpox. Homologs of the variola virus B22 protein are found in almost all chordopoxviruses and have estimated masses of greater than 200 kDa, making them the largest known poxvirus proteins, and leading to our initial interest in the role of this protein family. Most homologs are found in the variable region of the poxviral genome where less conserved host-interaction proteins are found, however, B22 homologs are remarkably well conserved, missing only from the parapox subfamily and vaccinia virus, and sometimes even found in multiples (crocodilepox, canarypox) despite their large size. We showed that the cowpox homolog, CPXV219, was expressed early during infection and cleaved into fragments that remained associated. CPXV219 was observed in the secretory pathway and at the plasma membrane with the majority of

the protein extracellular. However, mutants that did not express CPXV219 replicated normally in cell culture and retained virulence in a mouse respiratory infection model. Next, we investigated the importance of the ectromelia virus homolog C15 in the natural infection model, mousepox. In the absence of C15 following footpad infection of BALB/c mice, there was less mortality and at high doses all mice survived, whereas none survived infection with wildtype virus. Similar virus loads were present at the site of infection with mutant or control virus whereas there was less virus in popliteal and inguinal lymph nodes, spleen and liver, key organs in mousepox disease, indicating decreased virus spread and replication in the absence of C15. Decreased spread was not the result of an intrinsic viral function of C15 as the survival of infected mice was dependent on host CD4+ and CD8+ T cells during infection. These results highlight the importance of choosing an appropriate animal model. The influence of B22 homologs displays a species-specificity as observed in the natural virus-host model of ectromelia virus, which provides an excellent model for the study of such host-defense molecules during poxvirus infection. Future work should focus on determining the mechanism of action of these homologs.

CHARACTERIZATION OF THE COWPOX AND MOUSEPOX HOMOLOGS OF THE SMALLPOX VIRUS B22 PROTEIN AND THEIR ROLES IN MOUSE DISEASE MODELS

by

Sara Elizabeth Reynolds

Dissertation submitted to the Faculty of the Graduate School of the
University of Maryland, College Park, in partial fulfillment
of the requirements for the degree of
Doctor of Philosophy
2016

Advisory Committee:
Professor James Culver, Chair
Dr. Bernard Moss, Co-chair
Dr. Eric Freed
Professor David Mosser
Assistant Professor George Belov

Dedication

I would like to dedicate this thesis to the many people who have influenced me, encouraged me and supported me throughout the years. To my Dad, Craig Reynolds, who inspired my love of science, teaching, and has been a role model all of my life. My Mom, Della Reynolds, who has always believed that I could do anything, be anything, and meet any challenge. To my grandmother, Betty Naylor (Mom-Mom), who taught me to always remember the important things in life; love, family, and honesty. To my sisters, Chantal and Elizabeth who challenge me in new and important ways, but always remind me to keep life fun. And lastly, my husband, William Hardie, who has inspired me to always be a better, happier, stronger, and kinder person. William has stood beside me and encouraged me to take new risks and meet new challenges, again and again. I would not have been able to do so much, or be where I am today without his steadfast presence.

Thank you to you all.

Acknowledgements

Thank you to Bernie Moss for the opportunity to study in his fantastic lab, for the time spent mentoring as well as the time spent letting me make my own mistakes, and for all of the other opportunities I was allowed to experience in my pursuit of personal and professional growth.

I am also thankful to all the other members of my advisory committee, James Culver, Eric Freed, David Mosser, and George Belov, for their time, guidance, and support.

A very special thank you to the entire Moss lab who have been valuable teammates and friends. I'd especially like to thank Pat Earl for her patience, guidance and mentoring, Cat Cotter for her expertise and countless cells, Jeff Americo for his assistance and dedication to excellence, Carey Stuart for his friendship, and all the other members of journal club throughout the years.

I would like to thank Paul Kennedy, the LVD office at NIH, and the BISI office at University of Maryland for administrative support. The tireless efforts of so many animal technicians have made the many animal experiments in this work feasible. The select agent committee and all the dedicated individuals on the team have ensured a safe working environment for me and my colleagues. The Graduate Partnership Program at the NIH has facilitated my ability to work at such a prestigious institution and provided a bounty of additional opportunities.

Lastly, I would like to thank the many scientists who have given me the opportunity to learn, try new things, and grow in their labs. I have worked with many inspiring (and patient) individuals who deserve a ton of gratitude for the opportunities they afforded me.

Table of Contents

List of Tables

List of Figures

List of Abbreviations

AIM2 absent in melanoma 2

AP1 activator protein 1

AraC cytosine arabinoside

ATI A-type inclusion

Bcl-2 B-cell lymphoma 2

BCR B cell receptor

BFA Brefeldin A

BP Binding Protein

C Crescent

cGAS cyclic GMP-AMP synthase

Clr-b C-type lectin related protein b

CPXV Cowpox virus

CTL Cytolytic T cell

DAI DNA-dependent activator of IFN-regulatory factors/Z-DNA-binding protein 1

DC Dendritic cell

DDX3 DEAD-box RNA helicase 3

DPI Days Post-Infection

DNA-PK DNA dependent protein kinase

dsDNA Double-stranded deoxyribonucleic acid

dsRNA double stranded ribonucleic acid

ECTV Ectromelia virus

EFC Entry fusion complex

eIF2α eukaryotic translation initiation factor 2α

ER Endoplasmic reticulum

ERGIC ER Golgi intermediate compartment

EV Enveloped extracellular virus

FasL Fas ligand

HPI Hours post-infection

IFN Interferon

IFNAR interferon α/β receptor

IκBα inhibitor of κB

IKK inhibitor of κB kinase

IRF Interferon Response Factor

IRAK2 IL-1R-associated kinase 2

ISG Interferon Stimulated Genes

ITR Inverted terminal repeat

IV Immature virus

JAK Janus kinase

Kbp Kilobase pairs

LD_{50} 50% Lethal Dose

LN Lymph node

MAL MyD88 adaptor-like

MDA5 melanoma differentiation antigen 5

MOCV Molluscum contagiosum virus

MOS Moscow strain

MPXV Monkeypox virus

MV Intracellular mature virus

MyD88 Myeloid Differentiation Primary Response

NCLDV Nucleo-cytoplasmic large DNA viruses

NF-κB nuclear factor kappa-light-chain-enhancer of activated B cells

NK Natural Killer

NKC Natural Killer cell gene complex

NLRP nucleotide-binding domain, leucine-rich repeat and pyrin domain containing protein

OAS 2′-5′-oligoadenylate synthase

OPXV Orthopox virus

ORF Open reading frame

PAMP Pathogen Associated Molecular Pattern

PFU Plaque Forming Unit

PKR protein kinase R

PRR Pattern Recognition Receptor

RAP94 RNA polymerase-associated protein of 94kDa

RIG-I retinoic acid inducible gene I

RLR RIG-I-like receptors

rmp Resistance to Mousepox gene

Serpin serine protease inhibitor

SP Signal Peptide

SPI-2 serine proteinase inhibitor 2

STAT1 signal transducers and activators of transcription 1

STING Stimulator of Interferon Genes

T1-IFN Type I Interferons

TAP Transporter associated with antigen processing protein

TBK1 TANK-binding kinase 1

TCR T cell Receptor

TGN Trans-Golgi network

Th T helper cell

TIR Toll/IL-1R

TM Transmembrane domain

TRAF tumor necrosis factor receptor-associated factor

TRAM TRIF-related adaptor molecule

TRIF TIR-domain-containing adaptor-inducting IFN-β

TLR Toll-like Receptors

TNF(R) Tumor Necrosis Factor (Receptor)

VACV Vaccinia virus

VARV Variola virus

vCCI CC chemokine inhibitor

vCKBP viral chemokine binding receptor

VETF VACV early transcription factor

VMAP viral membrane assembly proteins

WHO World Health Organization

WV Wrapped virus

Chapter 1: Introduction

Smallpox is one of the most devastating diseases in human history. Variola virus is the causative agent of smallpox and a member of the Orthopoxviridae (OPXV) which contains multiple double stranded DNA viruses capable of infecting humans. The smallpox epidemic was finally brought under control by the development of the first vaccine, a live attenuated vaccinia virus. Introduced by Edward Jenner in 1796, material from the lesion of a dairymaid, presumably cowpox, was demonstrated to protect against smallpox. A worldwide vaccination campaign was launched in 1966 using the presumed viral descendant, vaccinia virus (VACV), by the World Health Organization and eventually led to the eradication of smallpox disease in the natural world by 1980. Rare, but serious complication led to the cessation of regular vaccination for the general populous and currently only military and research personnel are regularly vaccinated (1, 2).

There is a need for continued research and a better understanding of poxviruses in general as there are ongoing OPXV epidemics in humans and animals around the world (3), as well as a potential for new emerging zoonotic poxviruses capable of infecting humans, and the potential use of smallpox for bioterrorism (2). VACV, the smallpox vaccine, has been the best characterized poxvirus but repeated passaging and attenuation has led to many deletions and changes in the genome (4).

The primary goal of this dissertation was to characterize a large family of proteins present in almost all chordopoxviruses, the B22 family of proteins. Homologs of the variola virus B22 protein represent the largest poxviral genes, typically greater than 200 kDa in size, and are found in all chordopoxviridae, with the exception of the parapox genus and VACV. This conservation is despite being found most commonly in the variable region of the genome among genes that encode primarily host-interaction proteins. Along with its absence in the attenuated VACV, the lack of prior research, strong conservation and large size of these proteins made B22 homologs an interesting subject to study.

Cowpox virus (CPXV), another member of the OPXV and possible parental virus of the smallpox vaccine VACV, contains all of the open reading frames represented within the OPXV (5). As such, CPXV presents an opportunity to study genes absent from VACV and in the presence of all other OPXV proteins. The B22 family member in CPXV is open reading frame 219 (CPXV219) and was found to be expressed early during infection and trafficks to the surface of infected cells. The majority of the protein is extracellular and thus poised to interact with the host immune response, however, absence of CPXV219 did not affect disease pathogenesis in laboratory mice as discussed in Chapter 3.

Ectromelia virus (ECTV) the causative agent of mousepox, is a unique member of the OPXV with a known natural host of laboratory mouse strains such as BALB/c. In Chapter 4, the use of this known virus/host paired model is used to better examine the role of the B22 family member, C15, during disease. The footpad infection model, intended to represent a natural route of infection in mice, allowed

examination of the virus spread in the presence or absence of C15 and the host response to infection. Absence of C15 resulted in complete host survival at high viral doses dependent on the presence of CD4+ or CD8+ T cells. Virus replication at the site of infection was not affected by the absence of C15, but viral dissemination and replication in key organs such as lymph nodes, liver and spleen was reduced.

Altogether, the findings of this work provide a picture of how B22 homologs influence disease outcome during poxvirus infection and highlight the importance of carefully choosing a disease model. Our work with ECTV suggests B22 homologs may influence the immune response in a T cell-dependent and species-specific manner. Future work is needed to better understand how the B22 family of proteins interact with and influence the host immune response to poxviral infection and how this may vary in efficacy or species-specificity between viruses and hosts.

Chapter 3 includes work that has been previously published in the journal Virology. Laboratory experiments were performed by me, and experimental designs and publication was achieved through collaborative efforts with my supervisor, Bernard Moss. Adapted from: Reynolds, S. E. and Moss, B. Characterization of a large, proteolytically processed cowpox virus membrane glycoprotein conserved in most chordopoxviruses. Virology. 2015 Sep;483:209-17 Copyright © Elsevier

Chapter 2: Literature Review

2.1 The Poxviridae

2.1.1 Classification

The *Poxviridae* are a family of large, enveloped, double-stranded DNA (dsDNA) viruses that replicate in the cytoplasm of host cells. These brick-shaped viruses contain enzymes that synthesize mRNA and a dsDNA genome of 134-300 kilobase pairs (kbp) organized with a hairpin loop at both ends. Subfamilies are divided based on host range. The subfamily *Chordopoxvirinae* infect vertebrate hosts, and the *Entomopoxvirinae* infect insect hosts. Despite distinct host ranges, DNA sequences and bioinformatics confirm the genetic relationship between these two subfamilies (6, 7), and also suggest that the *Poxviridae* may be distantly related to *Asfaviridae, Iridoviridae, Phycodnaviridae* (8) and *Mimiviruses* (9), other large DNA viruses that replicate in the cytoplasm. Together these viruses have been named the Nucleo-Cytoplasmic Large DNA Viruses (NCLDV) and likely share a common ancestor (8).

The *Chordopoxvirinae* subfamily contains 10 genera (International Committee on Taxonomy of Viruses 2015 (10)): *Avipoxvirus, Caporipoxvirus, Cervidpoxvirus, Crocodylidpoxvirus, Leporipoxvirus, Molluscipoxvirus, Orthopoxvirus (OPXV), Parapoxvirus, Suipoxvirus, and Yatapoxvirus* (Fig 2.1) along with the unassigned *Squirrelpox virus (11)* and *Salmon Gill poxvirus* (12). New

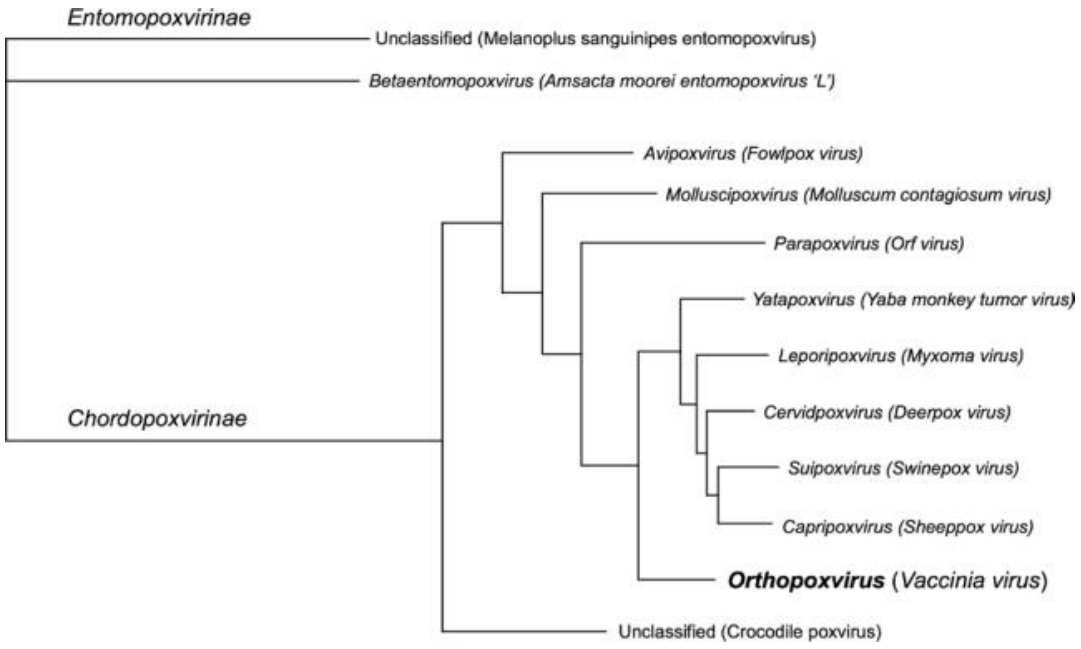

Figure 2.1 Phylogenetic relationship between Poxviruses

Amino acid alignment of 20 conserved genes is used in determination of phylogenetic relationships by Hendrick, R.C. et al. (4). This prediction represents one possible tree, however, other comparative methods have generated slightly different evolutionary relationships. Predicted tree is represented with branches labeled by genus name and the prototypic species for each genus in parentheses. Unclassified viruses have not yet been assigned to a taxon. Figure reprinted with permission under the shared creative commons attribution license.

poxviruses continue to be identified on a regular basis (12-14) and expand the diversity of this family. Classification of viral species within each genera is based upon criteria such as host range, genetic similarity, particle morphology and antigenic relatedness (10, 15). Among these only OPXV and *Molluscipoxvirus* contain obligate human pathogens, variola virus (VARV) and molluscum contagiosum virus (MOCV), respectively. Additional viruses from OPXV, *Parapoxvirus* and *Yatapoxvirus* genera can infect humans via zoonosis (Table 2.1, (16)).

Genus	Species	Clinical sign	Host
Parapox virus	orfvirus	Orf; ecthyma contagiosum	sheep, goat, wild ruminant
	pseudo cowpox virus	Melker's nodule	cattle
	parapox in cattle (stomatitis papulosa virus of the cattle)	local infections	cattle
	seal parapox virus (SPPV)	local infections	seal
	reindeer parapox virus	local infections	reindeer
Molluscipoxvirus	molluscum contagiosum virus	non-malignant tumours	human
Yatapoxvirus	yaba monkey tumour virus	yaba monkey tumour	monkey
	tanapoxvirus	tanapox	monkey (rodent)

Table 2.1 Non-Orthopoxviruses that can infect humans

Outside of the OPXV genus, only three genera are known to be capable of infecting humans. Of these, only MOCV is an obligate human pathogen. Clinical signs of disease in humans and host species for each virus are listed in columns three and four, respectively. Table reprinted with permission from Pauli, G. et al. (16).

2.1.2 Orthopoxviridae

The OPXV genus includes multiple viruses capable of infecting humans and has thus been the most extensively studied. The most famous member is the variola virus (VARV), causative agent of smallpox, perhaps the most devastating disease in human history. There is no way to accurately estimate the toll of smallpox throughout human history but it is clearly an ancient and devastating disease. Indeed, the mummified remains of Ramses V (died 1156 BC) bear the marks of the disease (17), VARV contaminated blankets were used as the first examples of biological warfare during the French-Indian war (1754-1767) (18), and in 1777 George Washington had ordered the American army variolated (19).

The process of variolation describes the use of material from a fresh smallpox pustule to intentionally inoculate a patient and was practiced in Africa, India and China long before the 18th century. The goal is to induce a mild, localized form of the disease that results in life-long protection from reinfection, however, it does pose a risk for developing the full smallpox disease course and possibly death.

In 1797, Edward Jenner published his findings that a similar inoculation using material from the pustule of dairy maids resulted in the same level of protection, but without the risks of using VARV. The material used was likely a cowpox virus (CPXV) and as the Latin word for cow is *vacca*, thus vaccinia virus (VACV) and the term *vaccine* (1). Over the next two centuries this material was passaged through many people, and later cows, resulting in the phylogenetically distinct VACV species used during the final eradication campaign of smallpox. As VARV is an obligate human pathogen, the eradication campaign orchestrated by the World Health

Organization (WHO) was able to use localized VACV vaccination campaigns to halt the person-to-person transmission of VARV. Efforts were aided by the life-long protection of vaccination or surviving smallpox, and the scarring that results from pustules marks individuals who are protected. Ultimately, in 1977 WHO achieved the first ever eradication of a disease from the natural world (2).

Although vaccination against smallpox has ceased, interest in VACV as a vector for new vaccines or therapeutics for a variety of infectious agents and cancer has emerged (20, 21). However, lack of smallpox vaccination has left behind a more susceptible population of human hosts (2, 22) and a variety of other OPXV have the potential to infect non-vaccinated humans (Table 2.2). Zoonotic transmissions have appeared with monkeypox virus (MPXV) in Africa and, for the first time, in the United States in 2003. Concerns about bioterrorism have emerged due to the similarity in appearance of this disease with smallpox, as well as a demonstrated potential for person-to-person transmission and up to 10% lethality in humans (23, 24).

CPXV is endemic in Europe and infects humans via zoonosis with infections among both animals and people on the rise (25). Infections with CPXV can be serious though rarely disseminate or are fatal (3, 26). The VACV has also begun circulating among cattle in Brazil, raising agricultural concerns (27). Thus, there remains an interest in the study of poxvirus therapeutics and vaccines.

Cowpox virus is the likely ancestor of the OPXV genera as it contains all open

Virus	Infections in	Spectrum of hosts	Natural host
Variola (VARV)	human	narrow	human
Vaccinia (VACV)	human, buffalo, cattle, elephant, pig, rabbit, etc.	broad	unknown
VACV-like Brazilian isolates (BRZ-VACV)	human, cattle, rodent	broad	rodent
Buffalopox (BPXV-VACV)	buffalo, cattle, human	broad	
Rabbitpox (RPV-VACV)	rabbits in breeding establishments	broad	
Monkeypox (MPXV)	human, ape, monkey, rodent, prairie dog, etc.	broad	rodent, sciuridae
Cowpox (CPXV)	human, cat, cattle, elephant, rodent, rhinoceros, etc.	broad	rodent
Camelpox* (CMLV)	camel	narrow	unknown
Ectromelia (ECTV)	mouse, laboratory mouse	narrow	vole?
Racoonpox	racoon	broad?	unknown
Volepox	vole, pinon mouse	narrow	vole
Uasin-Gisha pox	horse	medium (?)	unknown
Taterapox	tatera kempi (gerbil)	narrow	gerbil?

*Camelpox viruses show a very close relationship to VARV. Infections with camelpox virus in humans, however, have not been observed [133].

Table 2.2 Orthopoxvirus Host Ranges

Orthopoxviruses are listed along with species who have been reportedly infected, a generalized overview of the host species range, and the natural host, if known. Table reprinted with permission from Pauli, G. et al. 2010 (16).

reading frames found in OPXV species, while each of the other OPXV species contains some subset of those genes. CPXV has a very broad host range although the natural reservoir, suspected to be voles, is poorly documented or understood (28). The primary vector for transmission to people are domestic cats and rodents, although less conventional transmissions such as to monkeys and elephants have been reported (3).

Other members of the OPXV include camelpox virus, ectromelia virus (ECTV), racoonpox virus, skunkpox virus, taterapox virus and volepox virus. Mousepox, caused by ECTV, will be discussed extensively later in this chapter. Camelpox disease is camel-specific, but infections of these animals can cause severe disease, even death, and economic loss to camel owners (29). Racoonpox, skunkpox, and volepox viruses are examples of North American OPXVs, but the first genomes were only published in 2015 and much yet remains to be discovered about the similarities and differences of these viruses in comparison with each other and other OPXV (30, 31). Non-North American OPXV species have greater than 90% sequence identity, but this remains to be well documented for the North American OPXV species (15).

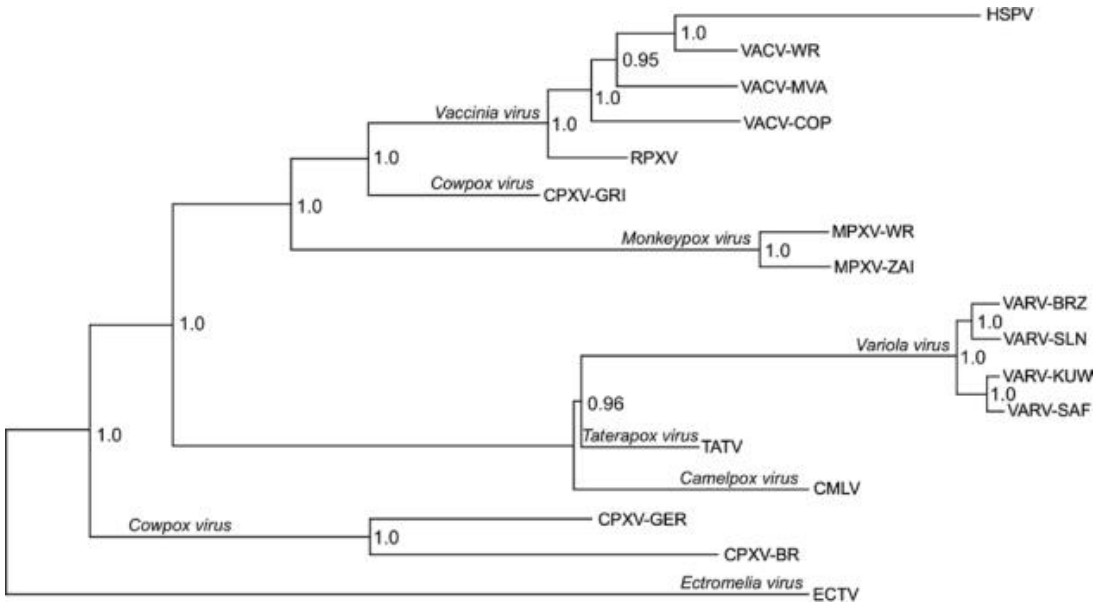

Figure 2.2 Phylogenetic relationship between Orthopoxviruses

A total of 141 genes were codon-aligned from each indicated orthopoxvirus and used for phylogenetic prediction using Bayesian inference by Hendrickson, R. C., et al (4). Each branch displays species names, and strain names are provided at each terminal node. Numbers at nodes provide the clade credibility values (a measure of the confidence of the branching pattern for the indicated clade) for each node. Figure reprinted with permission under the shared creative commons attribution license.

2.1.3 Virus Structure

Poxviruses are brick-shaped viruses larger than most animal viruses. The basic infectious form is the intracellular mature virus (MV), but an extracellular enveloped virus (EV) form is basically an MV wrapped in an additional cell-derived membrane. The basic virus structure as imaged by cry-electron tomography (32) reveals particles roughly 360 x 270 x 250 nm with rounded edges. The outer MV membrane is a single lipid membrane surrounding two lateral bodies of amorphous structure and an hourglass shaped core between them comprised of a proteinaceous wall that encloses a nucleocapsid (Figure 2.3, (32)). Deep-etch EM was used to confirm the single outer membrane, but does not provide clarification on the presence of a core membrane and its structure (33).

The MV contains about 80 viral proteins (34, 35) although the localization and function remains unclear for some. A new analysis software, VirusMapper (36), uses super-resolution microscopy to preform single particle analysis and visualize the localization of viral proteins within virus particles. Of particular interest, the F17 protein which along with H1 and G4 is known to be found in the lateral bodies (37), was visualized within these structures suggesting this technique could be used to identify additional components and their localization in the virus.

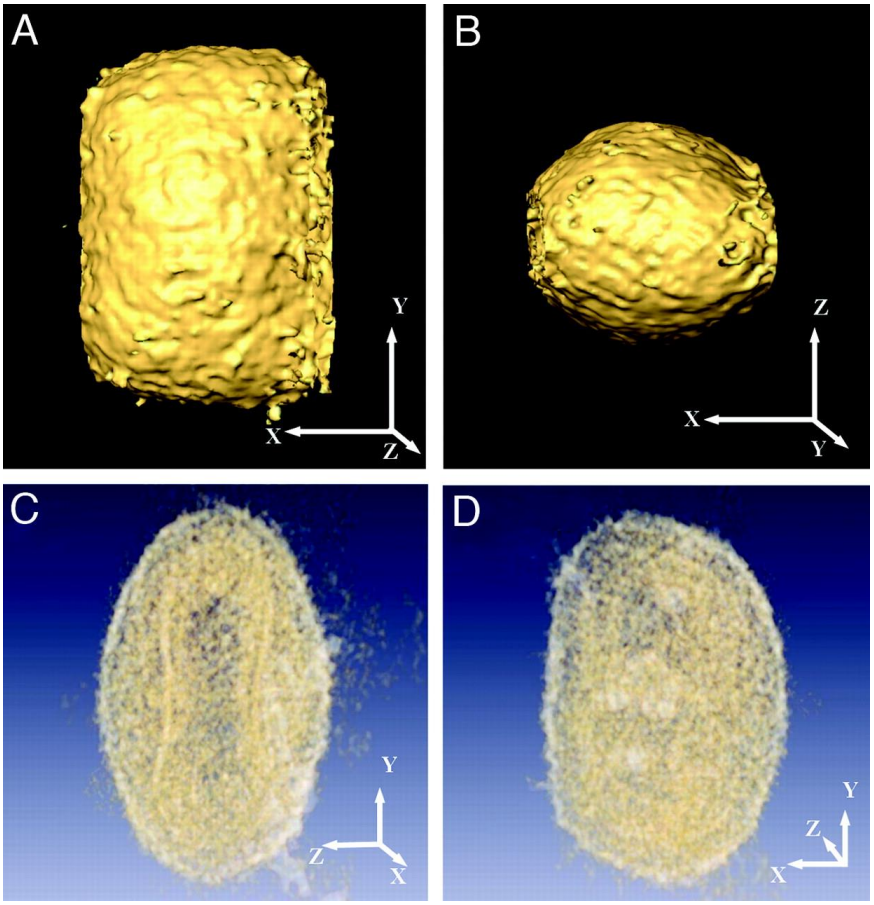

Figure 2.3 Cryo-electron tomography of vaccinia virus

Images were captures by Cyrklaff et al. (32) using cryo-electron tomography of intracellular mature vaccinia virus. Images are denoised and surface-rendered viral image in A and B to demonstrate the shape and size of the virus. In C and D the reconstructed virus is translucent to display the dumbbell-shaped core and internal architecture. Reprinted with permission, copyright (2005) National Academy of Sciences.

2.1.4 Genome Organization and Nomenclature

Poxviruses have linear dsDNA genomes that range in size from 134 kbp to more than 300 kbp (15). By themselves, poxviral genomes are non-infectious, but can be rescued by co-infection with an unrelated poxvirus (38). At the ends of the genome are hairpin loops that contain inverted terminal repeats (ITRs). Within the ITRs are A- and T-rich, incompletely base-paired loops connecting the two DNA strands (39), concatameric resolution sequences (40), short, tandemly repeated sequences (41, 42), and a few open reading frames (ORFs). Directional deep-sequencing has been used to identify replication origins within the ITRs and supports a genome replication model utilizing leading and lagging strand synthesis (43).

Nearly 100 genes are conserved amongst chordopoxviruses, and about half of those are also conserved in entomopoxviruses (Figure 2.4, (44)). Genes are rarely overlapping, but can be found running in opposite directions on each strand and ORFs tend to point towards the nearest genome end (45). Upstream promotors drive transcription at early or post-replicative stages of infection (46, 47). Essential genes tend to be located centrally and perform functions essential for replication such as transcription, genome replication and assembly. Towards the ends of the genome are more variable genes with functions in host defense and interactions (15).

The naming of genes or ORFs is based upon fragments of the genome resulting from HindIII restriction enzyme digestion of the VACV-Copenhagen strain and labeled A-O in decreasing order based upon the molecular weight of the fragment

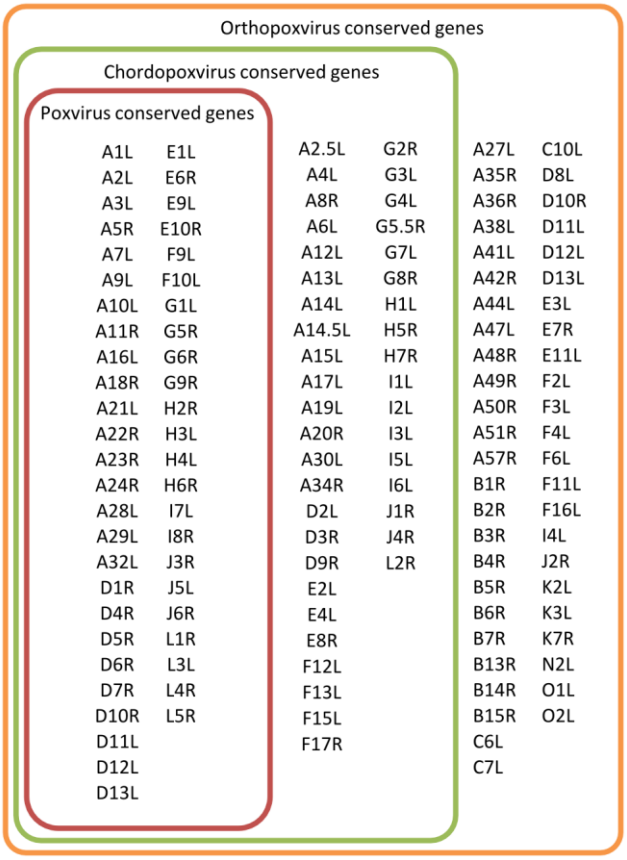

Figure 2.4. Conserved poxviral genes organized by level of conservation

Conserved poxviral genes as organized by Dabrowski, P. W. et al. (25). In the red box are those genes found in all poxviruses and represent the highest level of conservation. In the green box are genes conserved in all chordopoxviruses, and in the orange box are those genes conserved in all orthopoxviruses. Gene names are given using the VACV-Copenhagen nomenclature. Figure reprinted with permission under the Creative Commons Attribution License.

(48). Within each fragment genes are numbered left to right (except for fragment C which is reversed) and ORFs are also given the designation L (left) or R (right), depending on the direction (15). For example, A5R is the 5th ORF in the largest HindIII fragment and transcribed from left to right (R). The protein is referred to as A5.

2.2 Virus Replication

2.2.1 Attachment and Entry

Attachment of viruses occurs at the cell surface, with entry through the plasma membrane or following endocytosis, with the preferred route of entry varying between viral strains and host cell types (15, 49). Vaccinia encodes four proteins involved in binding, A26, A27, D8 and H3. A27 and H3 mediate MV entry to cell surface via heparin sulfate, D8 can bind chondroitin sulfates, and A26 binds to the extracellular matrix protein laminin (50-53). A26 and A27 are tethered to the MV surface by the A17 transmembrane protein (54). A27 has also been implicated in fusion as co-expression of A17 and A27 at the cell surface can induce cell-to-cell fusion (55).

Twelve addition VACV entry proteins; A16, A21, A28, G3, G9, H2, I2, J5, L5, and O3 have been demonstrated to form a complex known as the entry fusion complex (EFC). Two additional proteins, F9 and L1, are EFC-associated. The structure and protein-protein interactions known within this complex remain limited and unclear, and the mechanism of fusion remains unknown (56). Cellular attachment molecules have not been identified during the binding of EVs, however, the outer viral membrane must be removed following fusion as the EFC proteins are located on the MV membrane (15, 57). Entry requires fusion of the viral membrane with either the plasma or endosomal membrane. A25 and A26 have been implicated as determinants during the entry process as they repress fusion with the plasma membrane and in their absence VACV can bypass the low pH requirement (49, 58). Route of entry is also dependent on virus strain and host cell type (49, 59). Different

routes of infection have also been implicated in triggering differential innate sensing and signaling within the host cell to restrict infection. For example, in macrophages VACV-WR endosomal entry induces IFN-β signaling that can result in an anti-viral state (60).

2.2.2 Viral Gene Expression

Viral gene expression begins almost immediately following VACV entry into the cytoplasm and early transcripts can be detected as early as 20 minutes post-infection. Expression is temporally regulated (Figure 2.5) with early genes expressed first, followed by intermediate and late genes following genome replication. Early transcription occurs within activated viral cores as all of the necessary components are packaged into the mature viruses. Cores are transported on microtubules to the sites of transcription (61). Early transcripts encode enzymes and factors that are necessary for genome replication and transcription of the subsequent intermediate genes, such as DNA polymerase E9 and intermediate transcription factors A8 and A23. Additional early transcripts are involved in the moderation of the host immune response.

All viral mRNAs are both capped and polyadenylated (15). The D5 protein is required for genome uncoating, and along with other early protein products, for DNA replication (62). Core uncoating signals the switch to intermediate gene expression and the decapping enzymes D9 and D10 may play a role in the rapid decline of early transcripts (15). In addition, these proteins play a role in the destabilization of host proteins following infection and in control of the unintentional production of

complimentary dsRNA (15, 63). The primarily bi-direction synthesis of early transcripts toward the nearest end of the genome may also be a mechanism for reducing the amount of dsRNA produced during extensive amounts of transcriptional activity (45).

After genome replication, intermediate transcription can occur for enzymes and factors necessary for late gene expression. Late genes are transcribed next, and continue for the remainder of infection, including structural components of viruses and enzymes packaged into infectious particles. These include the multi-subunit DNA-dependent RNA polymerase, RNA polymerase-associated protein of 94kDa (RAP94), VACV early transcription factor (VETF), capping and methylating enzymes, poly(A) polymerase, and topoisomerase, among many others subsequently used for early transcription and subsequent genome replication (15).

2.2.3 Genome Replication and Viral Factories

The poxviral lifecycle occurs entirely in the cytoplasm, however, the process is not nucleus independent (64). Replication foci are known as viral factories and appear within two hours post-infection (hpi) following VACV infection (65). Recent evidence supports a leading-lagging strand synthesis with the origins of replication located in the hairpin loop sequences of VACV (43) and is supported by the necessity of either virally-encoded ligase or host DNA ligase I (66). Following duplication of the viral genome, concatamers are resolved into unit length genomes by the virus-encoded Holliday junction resolvase (67). Three proteins are essential for DNA replication in VACV; DNA polymerase, nucleoside triphosphatase, and DNA

glycosylase, and each is present in all sequenced poxviruses (15).

2.2.4 Mature Virus Morphogenesis

The first distinct structures formed in viral factories are crescents (C) that grow into complete spherical IVs. These spherical membranes are coated with a honeycomb lattice composed of D13 protein trimers (33) and a dense nucleoprotein (Nu) mass is packaged inside the IV before it is completely sealed (68). Seven core proteins are required for the filling of IVs, A15, A30, D2, D3, F10, G7 and J1 (69). The major transmembrane protein component of Cs and IVs are A14 and A17. Each of these proteins can be found in endoplasmic reticulum (ER) and ER-Golgi intermediate complex (ERGIC) membranes, interact either directly or indirectly with one another, and are phosphorylated by the F10 kinase (70). The N-terminal of A17 interacts with the D13 coat and is essential for IV formation (71).

A new group of viral membrane assembly proteins (VMAP) are conserved in all chordopoxviruses and have been identified as essential for poxvirus membrane biogenesis: A6, A11, A30.5, H7 and L2. It is suspected that these proteins interact with cellular and viral proteins while participating in the disruption of ER membranes within factories. These small ER fragments form into Cs and IVs, which is one reason why contiguous membranes between the ER and forming viruses have been so difficult to image (72, 73). The A32 protein, a possible ATPase, is necessary for packaging of the viral genome (74, 75). The I6 protein, a telomerase binding protein, also plays a direct and critical role in the genome encapsidation within the viral particle (76). A second telomere binding protein, I1, binds specifically to viral

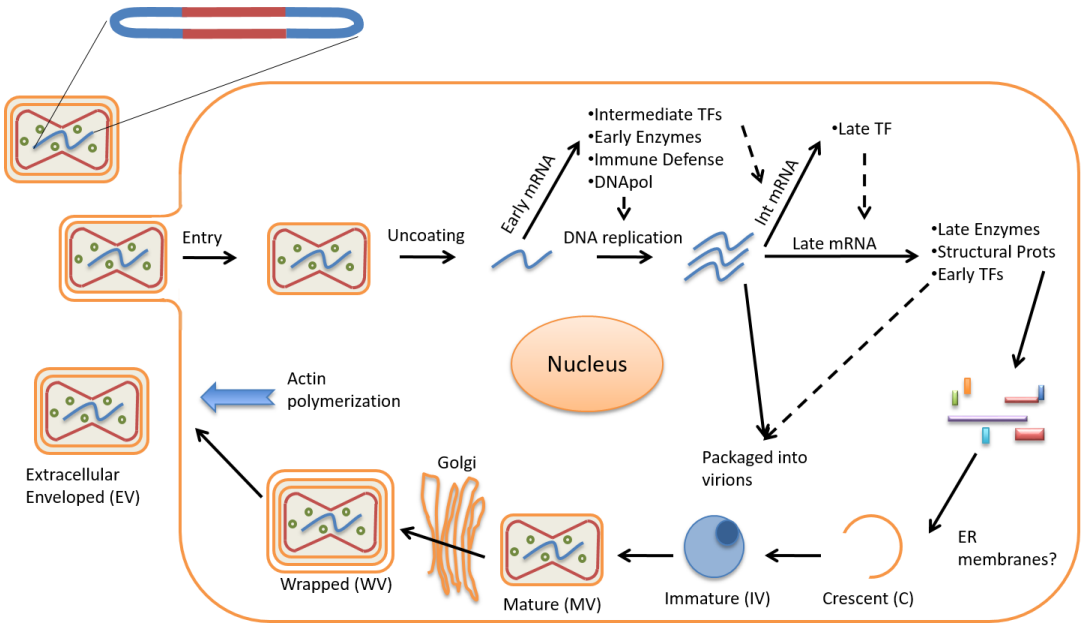

Figure 2.5 Poxviral lifecycle

The poxviral lifecycle occurs entirely in the cytoplasm of infected cells and is carefully regulated to occur in a temporal cascade. Following entry of virus particles cores are uncoated and early transcription occurs. Early genes include the DNA polymerase subunits, immune defense molecules and intermediate transcription factors. Following genome replication intermediate and subsequent late gene expression occurs. Late genes include structural proteins and enzymes packaged into mature viruses. Virus particles are first visualized as crescent (C) shaped membranes that form into complete spherical immature viruses (IVs). Packaging of DNA into IVs is followed by maturation events that result in the characteristic brick-shaped structure of the infectious mature virus (MV). Some MVs can be wrapped in two additional membranes (WVs) and transported via microtubules to the periphery of the cell. WVs can bud to become extracellular enveloped viruses (EVs) or polymerize actin tails to facilitate viral spread.

hairpins, but is not essential for this early stage of morphogenesis (15, 77).

Maturation into the infectious MV requires loss of the D13 scaffold via cleavage of the A17 membrane protein by viral I7 protease (78). In addition, the core proteins A3, A10, A12, L4 and G7 are also proteolytically processed (79). The E10, A2.5 and G4 proteins form a unique cytoplasmic disulfide bond pathway, found in all poxviruses, and necessary for virus maturation. At least 9 viral proteins have intramolecular disulfide bonds formed by the cytoplasmic redox system, including L1, F9 and seven EFC members (15, 80). Some OPXVs have the ability to occlude MVs in a dense protein matrix within the cytoplasm known as A-type inclusion (ATI) bodies. Occlusion requires two proteins: the structural ATI protein, and the A26 protein anchored to A27 in the MV membrane bridging the connection between MVs and ATIs (81).

2.2.5 Extracellular Virus Maturation

A second form of infectious poxvirus, the EV, is formed after wrapping of an MV in two additional membranes to form wrapped virions (WVs), followed by loss of the outermost membrane during exit from the host cell to form extracellular enveloped virions (EVs). There is good evidence that the membranes wrapped around MVs originate from the trans-Golgi network (TGN). Some of the strongest evidence is that labeling of WV membranes demonstrates that they contain glycoprotein and glycolipid sugars added in the late TGN (82) and when EV proteins are individually expressed they can be found within TGN membranes (82-84). The retrograde transport pathway moves proteins from the TGN to the ER. Although B5 can utilize

the secretory pathway for transport into the TGN, F13 localization in the TGN is blocked when retrograde transport is inhibited. When retrograde transport is inhibited, F13 is not found in the TGN and wrapping of MVs is blocked (85, 86). The formation of post-Golgi vesicles incorporating B5 and A36 is induced by F13 in the TGN through activity of a phospholipase motif (83, 84). Once wrapped, viruses contain 9 EV-specific proteins: A33 (87), A34 (88), A36 (89), A56 (90), F12 (91), F13 (92), B5 (93), E2 (94), and K2 (95, 96).

Wrapped viruses move on microtubules away from viral factories. The A27 protein on the MV surface is necessary for microtubule movement of MVs out of viral factories prior to wrapping (97). Interactions between A36 and the F12/E2 complex of EVs and cellular microtubule motor kinesin facilitates transport to the sites of wrapping (98-100). After wrapping, WVs have three outer membranes. Once WVs reach the periphery of the cell the outer viral membrane fuses with the plasma membrane and releases double-membraned EVs. Most EVs remain cell-associated, but some can form actin tails and protrude away from the host, and yet others can detach entirely to facilitate long distance dissemination (101).

2.3 Ectromelia virus and Mousepox Disease

2.3.1 Introduction

Ectromelia virus (ECTV), originally isolated from laboratory mice in 1929 (102), causes a smallpox-like disease known as mousepox (103). Historically, mousepox has caused disastrous outbreaks in laboratory colonies (104-106) demonstrating its virulence in laboratory mice. The isolation of ECTV from laboratory mouse strains during seemingly natural infections (102) demonstrates a matched virus/host model not readily and easily available for other OPXVs that do not naturally infect laboratory mice (Table 2.2). Similarities between mousepox and human smallpox have led to the suggestion that mousepox provides a better model for the evaluation of smallpox antivirals and therapeutics then other poxviral models (107-109) making it an ideal candidate for the study of poxviral pathogenesis.

Although multiple ECTV strains have been isolated, the highly virulent and highly infectious Moscow strain (72) of ECTV (110, 111) is the most commonly studied. The annotated Moscow sequence was first published in 2003 (112) and sequence analysis showed 99.5% nucleotide identity with the NAV strain isolated in the United States nearly 50 years after MOS, demonstrating the similarity among ECTV strains, including the originally isolated Hampstead strain (102).

2.3.2 Susceptible and Resistant Mice

Much of the early characterization of mousepox was performed using outbred mice, resulting in seemingly two forms of disease: a rapidly fatal disease course 6 to 7 days

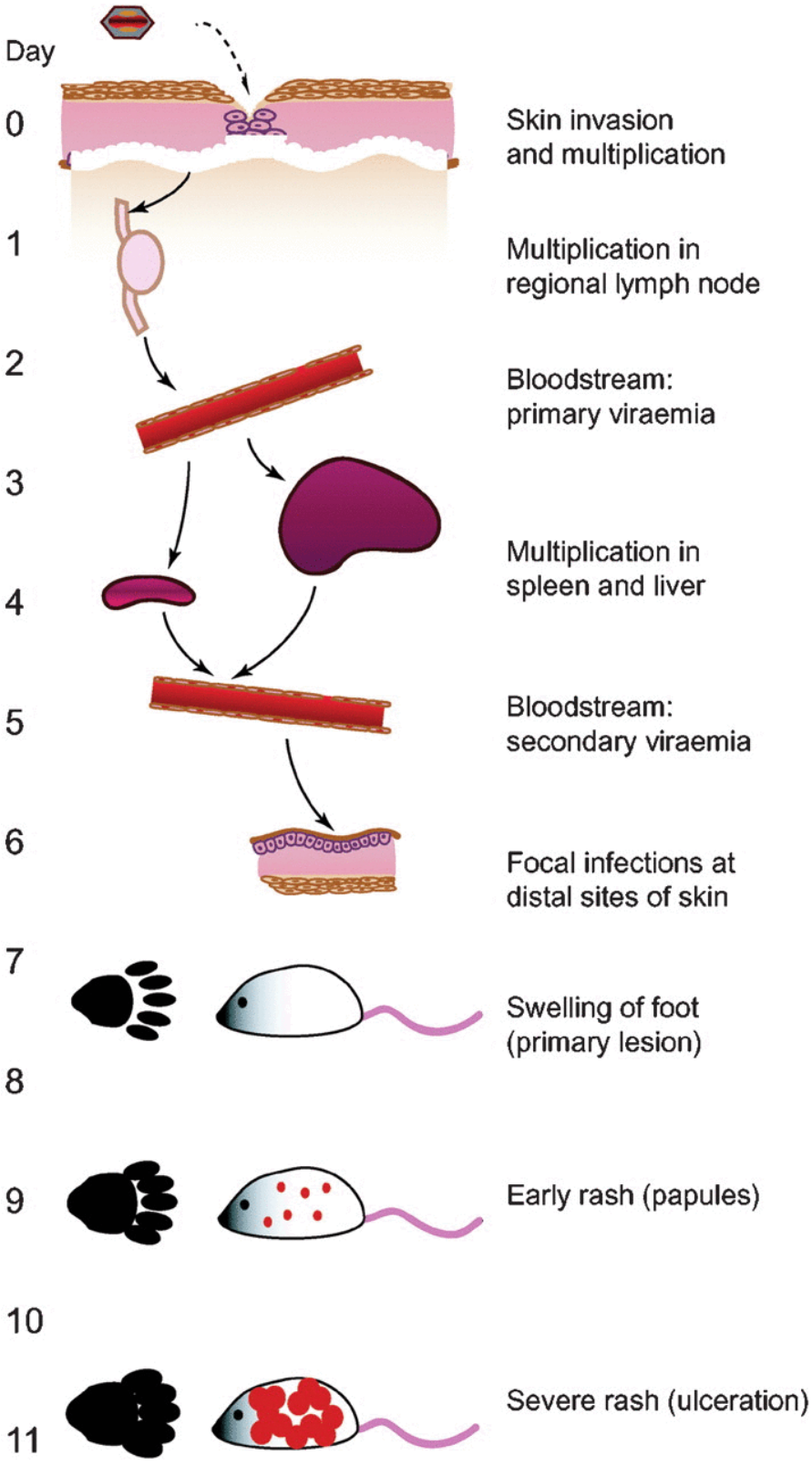
Day
0
Skin invasion and multiplication
1
Multiplication in regional lymph node
2
Bloodstream: primary viraemia
3
Multiplication in spleen and liver
4
5
Bloodstream: secondary viraemia
6
Focal infections at distal sites of skin
7
Swelling of foot (primary lesion)
8
9
Early rash (papules)
10
11
Severe rash (ulceration)

Figure 2.6 Timeline of mousepox disease course

Natural mousepox transmission likely occurs via abrasions in the skin, primarily the foot. Viral replication at the site of infection begins almost immediately and spreads to the regional lymph node within the first 24 hr. Replication continues in the lymph node before the first viremia occurs and the virus enters the blood stream, typically 2-3 dpi. Virus then reaches the liver and spleen where it continues to replicate and cause tissue damage. About a week after infection virus has reached the skin and can begin to form visual lesions as it replicates. The infected foot, the site of the primary lesion, can also become very swollen and susceptible animals typically succumb to disease due to organ failure of the spleen and/or liver at around this time. Animals that survive the first 7-14 days will develop a more pronounced rash and full ulcerations on the skin. After a few weeks inflammation of the foot decreases and scars are left at the site of the primary lesion and pustules from the rash. Reprinted with permission from Microbiology Society (131).

post-infection (DPI) (Figure 2.6) with extensive necrosis of the liver and spleen; and a chronic form presenting with ulcerative lesions on the feet, tail and snout (102, 114). Eventually, these separate disease courses were identified as susceptible and resistant mousepox, respectively, and not representative of separate diseases but rather different outcomes of mousepox. Both disease outcomes occur following high viral titers in the spleen and liver, and death is primarily due to high viral doses in these organs. In contrast, animals that survive eventually developed the whole body rash following control of virus in the spleen and liver (115-117).

Disease patterns were further characterized using inbred mouse strains and found to be greatly influenced by the genotype of the mouse (118). Clinical disease has also been found to be more severe in very young suckling mice and older mice (one-year old) than in adult 8-week-old mice (119), as well as shorter time to death in male mice over female (115) suggesting that immune fitness and hormones may play a role in virulence.

2.3.3 Footpad Model

Epizootic infections of ECTV are seemingly indistinguishable from footpad inoculation or scarification (120) and have led to the suggestion that the natural route of transmission from animal-to-animal occurs through small abrasions of the skin (103, 111). Infection by intradermal injection of a small volume (typically 10-100 µl) into the rear footpad is most commonly considered the best mimic for natural mousepox transmission and has been the most extensively characterized (Figure of footpad infection, (121)).

The following are descriptions of the disease progression following footpad infections in susceptible mouse genotypes, typically resulting in death from acute mousepox 7 to 10 DPI (120, 122).

2.3.4 Primary Lesion

Following infection, the first infected cells are either dermal cells or cells in the Malpighian layer of the epidermis followed by local replication in the epidermis which forms the primary lesion (123). Intradermal innocula have also been shown to enter the lymphatics almost immediately following inoculation (124). The primary lesion that develops at the site of infection consists of localized swelling that rapidly increases in size with pronounced edema due to cutaneous anaphylaxis (123) and is usually punctuated by a minute breach of the skin (120). About 7 DPI swelling of the infected foot becomes visible (Figure 2.6) and virus can be found at high concentrations. Swelling and edema quickly increases reaching a maximum at about day 10. There may be A type inclusions (ATIs) of occluded infectious virions in the epidermal cells or lymphatic infiltrations of the dermis. If the mouse survives, a hard adherent scab will form following ulceration, and drop off to reveal a permanent scar on the foot after 7 to 14 days (122).

2.3.5 Lymphatic Involvement

During the 4-6 day incubation period, virus replicates locally in the development of the primary lesion, as well as within the spleen and liver. Subsequent disease course, including the extent of secondary rash formation, is largely dependent on the degree

of virus replication in these organs. Spread from the primary lesion into the lymphatics often occurs via macrophages causing a sequential infection of local lymph nodes and internal organs known as “primary viremia”. Regional lymph nodes draining the primary lesion become enlarged and necrotic (122), and serve as sites for viral replication, including the presence of numerous ATIs. Necrosis of the lymph nodes can be attributed directly to viral replication, but may also be due to the stress caused by severe mousepox disease (125, 126).

2.3.6 Spleen and Liver

Subsequent lympho-hematogenous spread from lymph nodes into the liver and spleen occurs early, prior to establishment of adaptive immunity, and more slowly in resistant mice than susceptible mice (127, 128), suggesting differences in innate immune responses to infection. Virus reaches the spleen via infected lymphocytes where it replicates and maintains very high titers (up to 10^{10} PFU/g tissue) until death. Infiltrating infected lymphocytes infect splenic follicles that undergo necrosis and result in the characteristic mottled spleen of mousepox. The liver is also infected during acute mousepox, along with pronounced hepatosplenomegaly (118, 129). The phagocytic Kupffer cells of the liver appear to be infected first, followed by the parenchymal cells (130). Viral loads in the liver are typically lower than the spleen, and appearance of the liver is relatively normal, until the day of death when the liver becomes enlarged and studded with white foci representing hepatic necrosis and viral titers increase to rival those in the spleen (129, 131).

2.3.7 Secondary Viremia

Secondary viremia is the result of virus, primarily from the heavily infected spleen and liver tissue, being released into circulation. It can cause infections of the skin and sometimes kidneys, lungs and intestines. Intestines are often engorged and sometimes necrotic (117). Kidneys and bladder can be necrotic and sometimes hemorrhagic in very young mice. Virus is detectable in the blood at titers up to 10^4 PFU/mL on day 8 or 9. Histologically, virus can be detected in low levels within most tissues at this late stage, including: bone marrow, nasal mucosa, ovary, vagina, uterus, etc. (116).

2.3.8 Secondary Rash

Although virus titers in the skin are often elevated, high viral loads of the spleen and liver can cause death prior to visible lesion formation (122). In surviving animals, virus deposited in the skin eventually develops into a multifocal necrotic rash known as the secondary rash, the severity of which is dependent on the degree of viremia (129). The secondary rash appears 2 to 3 days after the primary lesion (9-11 DPI, Figure 2.6) as raised, slightly pale areas. As these areas of proliferation and edema increase in size they may become visible as slightly raised macules. Numerous ATIs are present in epidermal cells and lesions develop epidermal necrosis of the superficial cells. Widespread inflammatory edema and lymphocytic infiltration of the dermis accompanies massive necrosis, and animals will develop papules that close over with scabs during healing. The presence of conjunctivitis commonly accompanies the rash. Animals that die of acute mousepox frequently succumb shortly prior to, or simultaneously to, when the secondary rash visibly develops,

roughly 9 to 11 DPI (122).

2.3.9 Intranasal Innoculation

Intranasal infection of susceptible mice has also been studied as ECTV was historically unintentionally passaged along with influenza virus, developing into a generalized mousepox disease. Low inoculum volumes result in local upper respiratory infections with minimal lung involvement, death results from necrosis of the liver (103), and high viral loads have been reported in the spleen. Larger volumes (greater than 10 µl) can result in congestion of the lungs and lead to pneumonia. BALB/c mice were approximately 100-fold more resistance to the intranasal route than A/NCr mice that present an LD_{50} of 0.3 PFU (117).

2.4 Host Immune Responses and Poxviral Evasion Mechanisms

The large size of poxviruses allows for the inclusion of many different genes that encode for proteins capable of interacting with and modulating the immune response (Figure 2.7). Due to selection pressure, by diverse host immune responses, these genes are more often mutated between species and can be highly specific in target or function. In some cases, proteins can also be multifunctional and/or capable of regulating the host immune response at multiple stages. Together with the complexity of the host immune response, this can be a challenging puzzle to break apart and understand, but it is critical for medical and research professionals that the role of defense proteins from both host and pathogen are well understood.

The mousepox infection model provides a naturally matched virus-host model for the study of the host immune response and viral defense mechanisms, which compete against each other. It has been clearly demonstrated that resistance to mousepox requires a strong polarized type 1 immune response. Thus the NK cells, CTLs, and IFN-gamma responses are especially important for survival, although not the only components of the immune system modulated by the virus, suggesting that the immune response and modulation by the virus is highly complex. Reviewed below is a selection of some of the important viral-host interactions during poxvirus infection with some important ECTV proteins important during mousepox disease highlighted.

2.4.1 Immune Sensing Mechanisms

Host cell Pattern Recognition Receptors (PRRs) are innate sensing molecules that

recognize Pathogen Associated Molecular Patterns (PAMPs) such as double-stranded RNA (dsRNA), lipopolysaccharides and nucleic acid variants, among others. The first PRRs discovered were membrane-associated toll-like receptors (TLRs) on both cell surfaces and endosomal membranes. There are also cytosolic RNA sensors like RIG-I-like receptors (RLRs), including retinoic acid inducible gene I (RIG-I) and melanoma differentiation antigen 5 (MDA5); as well as cytosolic DNA sensors such as absent in melanoma 2 (AIM2), cyclic GMP-AMP synthase (cGAS) stimulator of interferon (IFN) genes (STING), DNA dependent protein kinase (DNA-PK), and DNA-dependent activator of IFN-regulatory factors/Z-DNA-binding protein 1 (DAI) (132).

Similar to PRRs, host cell inflammasomes are multimeric cytosolic sensors of infection that recognize conserved molecular components. Some inflammasomes are composed of nucleotide-binding domain, leucine-rich repeat and pyrin domain containing protein (NLRP) and contain caspase 1. Proteolytic activation via caspase 1 results in active IL-1β and IL-18, pro-inflammatory cytokines with antiviral properties. (133, 134).

2.4.2 Evasion of Innate Sensing and Activation of NF-κB

To counteract host cell PRR sensing and subsequent events poxviruses possess their own set of intrinsic immunomodulatory proteins capable of blocking host cell immune sensing events at multiple stages. First, poxviruses can block the binding of PAMPs to the sensing receptors. The C-terminus of E3 contains a Z-DNA-binding domain with unknown function, but both domains of E3 contribute to virulence (135,

136). DNA-PK, a PRR for IFN-regulatory factors (IRF) 3-dependent innate immunity, is bound by C16 and can block sensing of DNA in the cytoplasm (137).

A second strategy of poxviruses to evade the host immune response is to inhibit downstream signaling pathways of PRRs, and VACV has evolved many mechanisms for blocking these pathways. VACV A46 is capable of binding multiple Toll/IL-1R (TIR) domain-containing adaptor molecules including myeloid differentiation primary response gene 88 (MyD88), MyD88 adaptor-like (MAL), TIR-domain-containing adaptor-inducting IFN-β (TRIF) and TRIF-related adaptor molecule (TRAM) all of which associate with the cytoplasmic tails of TLRs (138, 139). This inhibitory capacity allows blocking of multiple IFN-β inducing pathways. The A52 protein acts by binding and inhibiting IL-1R-associated kinase 2 (IRAK2) and tumor necrosis factor (TNF) receptor-associated factor 6 (TRAF6) (138, 140) just downstream of A46 targets.

The structure of A52 has been revealed as a B-cell lymphoma 2 (Bcl-2) –like fold (141) containing protein, a structure conserved among multiple other VACV proteins that inhibit the host innate immune response and/or apoptosis, including: A46, A49, A52, B14, C1, C6, C16, F1, K7, N1, and N2 (142-145). The K7 protein binds IRAK and TRAF6 preventing nuclear factor kappa-B (NF-κB)(146) and the DEAD-box RNA helicase 3 (DDX3) preventing IRF3 activation via the kinases TANK-binding kinase 1 (TBK1) and IKKε (147), kinases that act at the convergence of several IRF3 activation pathways. VACV C6 also interacts with scaffold adaptor proteins for TBK1/ IKKε to inhibit IRF3 and IRF7 activation (148). Lastly, the protein N2 inhibits IRF3 after phosphorylation and transport to the nucleus, although

the mechanism remains unknown (149).

The NF-κB pathway in host cells can also be activated by IL-1- and TNF-mediated signaling which converges at the inhibitor of κB kinase (IKK) complex. Viral proteins that inhibit the IKK complex directly include N1 acting at the dimer interface (150), B14 binding IKKβ and blocking phosphorylation of the inhibitor of κB (IκBα) (151), and C4 whose mechanism is unknown (152). A49 has been shown to stabilize IκBα through molecular mimicry preventing its ubiquitination and degradation in the proteasome thus trapping NF-κB in the cytoplasm (153). The K1 protein may have a similar function although the mechanism remains unclear (154), and M2 reduces extracellular signal-regulated kinase 2 (ERK2) phosphorylation and p65 translocation (155, 156).

NF-κB is a potent mediator of anti-viral immunity and so it is not surprising that ECTV, like other poxviruses, encode many proteins to help modulate the activity of this cellular response. ECTV002 inactivates NF-κB subunit p105 (157, 158) and reduces expression of proinflammatory cytokines *in vivo* leading to attenuation in BALB/c mice. Interestingly, C57BL/6 mice deficient in IRF7 but not MyD88 or TLR9 also are attenuated when infected with this mutant virus (158) suggesting that a cross-talk between T1-IFN (Type 1 interferon) and NFkB signaling pathways contribute to resistance to mousepox (158). ECTV150 is a BTB/kelch protein that inhibits NF-κB signaling through inhibition of p65 translocation (159). The VACV K1 protein has also been shown to inhibit NF-κB by preventing IκBα degradation (154) and the ECTV homolog is 97% similar, suggesting it may have the same function.

Cooperatively these mechanisms provide a profound block on IFN-β production by poxvirus-infected cells through the blockage of IRF3 and NF-κB activation. However, the production of IFNs by neighboring infected or uninfected cells can still induce an anti-viral state that can inhibit poxviruses.

Infected cells, such as CD11b+ inflammatory monocytes in the draining LN, produce T1-IFNs and ISGs dependent upon STING, indicating the need for cytosolic PRR recognition of PAMPs for T1-IFN production following ECTV infection (158, 160). However, other PRRs such as TLR9 (but not other TLRs), its adapter MyD88, and downstream components IRF7 and NFκB, when deleted in B6 resistant mice result in mousepox susceptibility (158, 161, 162). Two separate PRR pathways act to indirectly (TLR9-MyD88-IRF7) and directly (STING-IRF7/NFkB) induce T1-IFN expression by inflammatory and infected monocytes, respectively, and thus control and protection against mousepox (163).

2.4.3 Interferon Production and Interferon Stimulated Genes

Each of these PRR receptor families induces signaling cascades culminating in the activation of transcription factors such as NF-κB, IRF3 and IRF7, and activator protein 1 (AP1) that lead to the production of inflammatory cytokines and type 1 IFNs (T1-IFN), IFN-α and IFN-β (164). In contrast, IFN-γ, the only T2-IFN, is produced by activated natural killer (NK) cells and activated T cells (165).

Receptor binding of T1-IFNs to the IFN α/β receptor (IFNAR) results in initiation of the Janus kinase (JAK)/signal transducer and activator of transcription

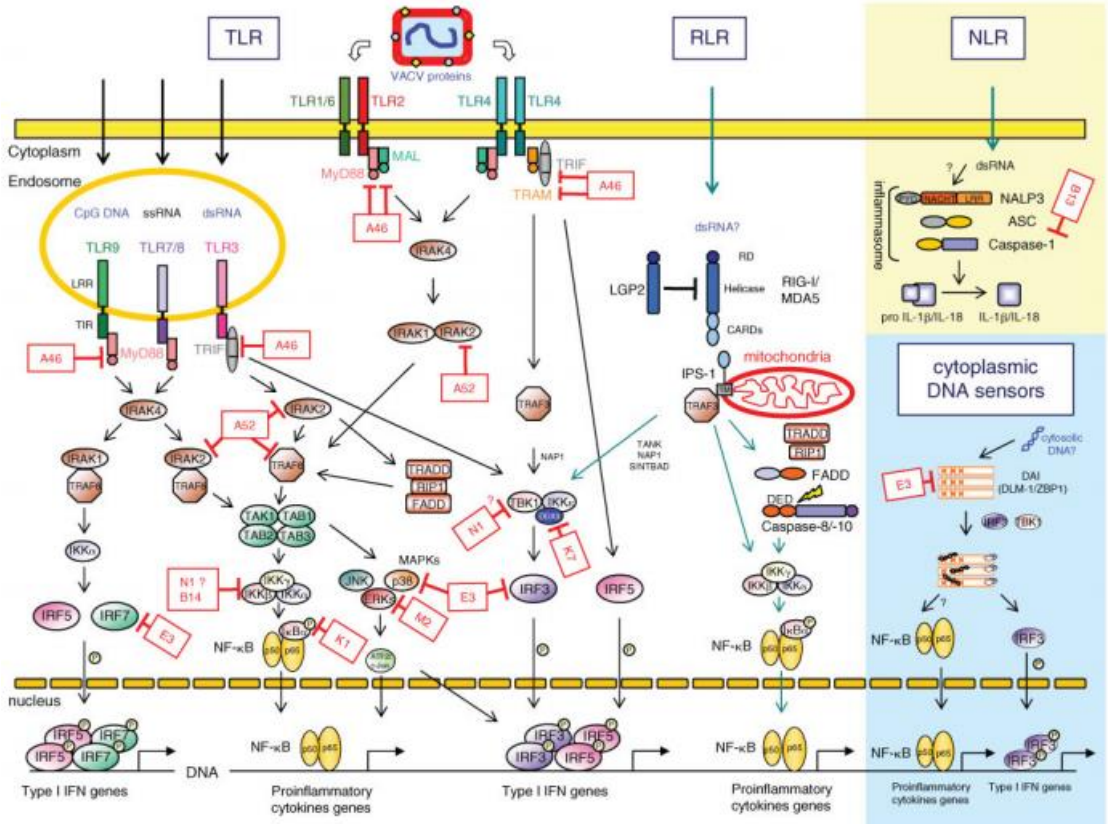

Figure 2.7 Vaccinia virus immune modulatory proteins interact with host signalling cascades.

This comprehensive figure compiled by Perdiguero, B. and Esteban, M. (166) shows the complicated interplay between host defense molecules and viral immune modulators. At the top are pattern recognition receptors TLR, RLR, NLR, and cytoplasmic sensors, which when stimulated by their associated PAMPS initate downstream signalling cascades. Viral immune modulator proteins are shown in red boxes at the points where they can interact along these cascades. Key transcription factors such as NF-κB, IRF3 and IRF7 are activated by these signaling cascades and translocate into the nucleus to stimulate production of T1-IFNs and pro-inflammatory cytokines.

(STAT) pathway and transcription of hundreds of IFN-stimulated genes (ISGs) (165). Some ISGs, protein kinase R (PKR), 2′-5′-oligoadenylate synthase (OAS), ISG15 and Mx proteins can confer an antiviral state. For example, activation of OAS by dsRNA leads to the activation of RNAse L, which is capable of degrading viral and cellular mRNAs (167). When activated by dsRNA, PKR autophosphorylates and can phosphorylate eukaryotic translation initiation factor (eIF2α) resulting in the cessation of protein translation. Other ISGs include PRRs (such as RIG-I) and IFN-response signaling factors (such as IRFs and STAT1) that assist in the detection and amplification of the IFN-response in infected and neighboring cells (168). Together, ISGs are important for the amplification and regulation of the IFN response and other mechanisms that interfere with the viral life cycle.

2.4.4 Inhibition of Interferon Stimulated Genes

Poxviruses employ a variety of strategies to inhibit the anti-viral effects of IFNs. The previous sections described methods employed by poxviruses to reduce the production of T1-IFNs through the blockage of innate sensing, but poxviruses also block IFNs from reaching their receptors, blocking IFN-induced signal transduction, dephosphorylating signaling molecules, and inhibiting the expression and action of IFN-response genes.

Lateral bodies may serve as immediate delivery packets for viral defense molecules as they break away from the cores early during infection. Known proteins include F17, which dissociates in the reducing environment of the cytoplasm, and the proteins vH1 and G4 are released. Although the function of G4 remains to be

determined, vH1 dephosphorylates STAT1 and STAT2 thus inhibiting signaling from all IFN receptors (37, 169).

The shutdown of host protein synthesis by decapping enzymes D9 and D10 is both fast and highly efficient and contributes to the reduced production of ISGs (170, 171). These enzymes also reduce the accumulation of dsRNA and thus reduce sensing via the ISGs PKR and OAS (63, 172). The previously mentioned E3 protein binds dsRNA preventing sensing by PRR but also PKR and OAS. In addition, the K3 protein, which has amino acid similarity to eIF2α, functions as a non-phosphorylatable substrate for PKR and competitor with eIF2α (173).

2.4.5 Interferon Decoy Receptors

The production of decoy receptors also provides an effective strategy used by poxviruses to block IFNs. T1-IFNs can be inhibited by the early protein, B18, both on the cell surface and in solution (174, 175). B18 binds T1-IFNs from a wide range of species (176), however, it only inhibits IFN-α efficiently. Inhibition of IFN-β by poxviruses relies primarily on intracellular mechanisms such as disruption of innate sensing and downstream signaling molecules (177). A soluble T2-IFN decoy receptor is encoded by the poxvirus B8R gene and binds IFN-γ outside of cells. Interestingly, B8 protein can dimerize unlike cellular IFN-γ receptor, but it lacks the transmembrane and cytoplasmic domains (178, 179). Like B18, the B8 protein has a broad host range (180). A variety of poxviruses also express decoy receptors targeting IL-18 (181), and TNF (182) receptors.

The importance of interferons for recovery from mousepox has long been

known (183). T1-IFNs and ISGs appear first in the draining LN then in the liver coincident with viral spread (184), indicating that these factors are produced in infected tissues and not present due to systemic distribution. When infected, ECTV spreads faster to the spleen and liver in 129 mice deficient in cellular IFNAR1, demonstrating that early T1-IFN and ISG production is important for viral control and subsequent survival (158, 163). When anti-T1-IFN antibodies were given following footpad infection to resistant C57BL/6 mice it was found that depleting IFN-alpha had no effect on organ titers, but IFN-beta was important for viral clearance in the liver and not the spleen. Either treatment resulted in only 25% mortality (185). High levels of IFN-α2 binding has been detected on the surface of ECTV-infected cells (186) and an inhibitor of IFN-α activity can be found in cellular supernatants (187).

ECTV166 is a secreted T1-IFN decoy receptor and deletion of ECTV166 from ECTV attenuates mousepox in BALB/c mice. Death of RAG-1 deficient mice (which lack adaptive immunity) following footpad infection by an ECTV166 deletion virus indicates a role for the adaptive response in the protection of T1-IFNs (188). Furthermore, ECTV166 depletion by antibody after infection results in restoration of T1-IFN signaling in livers and allows survival in susceptible mice (184). Thus, ECTV must effectively control T1-IFN responses for lympho-hematogenous spread and to protect the liver, the likely cause of death from mousepox. Interestingly, the ECTV vT1-IFN receptor has been shown to inhibit both human and mouse IFN-α, but only human IFN-β (187, 188).

Unlike the modest role of T1-IFNs during recovery of C57BL/6 mice from mousepox, treatment with anti-IFN-gamma antibody resulted in enhanced spread and

replication especially in the liver, spleen, ovaries and lungs (185). Part of the activity of IFN-γ is mediated through nitric oxide production, a critical component in the inherent resistance to mousepox (189). As IFN-γ is a critical component in the activity and promotion of a type 1 immune response these data serve to underscore its importance during control of ECTV infection. Efforts by the virus to this effect include expression of an IFN-γ decoy receptor (ECTV158) that when deleted from the virus during infection allows for more IFN-γ production by the infected animal. Susceptible BALB/c mice infected with the mutant virus were shown to be able to control replication and survive the infection (190), however the extent of this attenuation remains somewhat controversial (191, 192). An increase in the percentage of IFN-γ producing CD8+ T cells in the draining LN and spleens of resistant C57BL/6 mice early after infection further supports the importance of an early IFN-gamma response (193).

2.4.6 IL-1 Family Cytokine Responses

The innate inflammatory response against viral infection is amplified by cytokines such as TNF-α, IL-1 and IL-18. In addition, these cytokines can directly induce apoptosis of infected cells via TNF-α and influence the developing adaptive immune response. OPXVs have evolved multiple strategies for the inhibition of these key cytokines including additional decoy receptors, precursor processing inhibitors, and downstream signaling inhibitors.

The IL-1 protein is synthesized as pro-IL-1β following NF-κB activation and cleaved into effective IL-1β by caspase 1. In addition to the NF-κB inhibition

strategies already discussed, VACV is capable of blocking caspase 1, and IL-1 maturation, by inhibiting the activation of inflammasomes. The F1 protein also interacts with NLRP inflammasomes and reduces active IL-1β and IL-18 production (134). Two forms of IL-1, α and β, generally overlap in function as they each interact with the same cellular receptors. Ectromelia-infected cells secrete a vIL1β protein receptor (homologous with B15 in VACV (175)) with similarity to the extracellular domain of the type II TNFR. This mock receptor inhibits binding of mouse and human IL1β to the cellular receptor. Unlike cellular receptors, vIL1β shows no binding activity with IL1α (194, 195). Details on the contribution of vIL1β to pathogenicity during mousepox has not been demonstrated, but deletion from VACV does result in increased morbidity intranasally (175) and decreased pathogenicity following intracranial infection (196).

IL-1 and IL-18 (discussed below) require cleavage of premature cytoplasmic forms by caspase 1 to become mature and active in modulating the immune response. ECTV-encoded serine protease inhibitor (serpin) SPI-2 (homologous with B13 in VACV) has been shown to inhibit caspase 1 and 8 and thus TNF-mediated apoptosis, which also utilizes caspase 1 (197). Although not demonstrated in ECTV, the cytokine response modifier A (CrmA) CPXV homolog can block the processing and release of both IL-1β and IL-18 in CPXV or VACV (195, 198-200). The role of SPI-2 in pathogenesis during mousepox infection remains to be determined.

IL-18 is a member of the IL-1 family of cytokines, expressed in the epidermis, and has potent pro-inflammatory potential through its induction of other cytokines. IL-18 is also an activator of NK cells. ECTV expresses an IL-18 BP (p13) with high

similarity to IL-18 BPs of other poxviruses, and that has been shown to reduce NK-cell activity and IFN-γ levels after infection (201, 202). Mousepox resistant C57BL/6 mice altered to become deficient for IL-18 or IL-12p40, both important for IFN-γ production, had reduced CD8+ T cells at the site of infection and increased splenic T regulatory cells following ECTV infection. When both IL-18 and IL-12p40 were depleted, C57BL/6 mice became susceptible to mousepox via reduced NK and CTL responses (203).

2.4.7 Tumor Necrosis Factor α

TNF-α is another important early cytokine mediator of the immune response that acts via the type I (p55) or type II (p75) TNF receptor (TNFR) thought to be produced predominantly by macrophages and activated T cells. It can induce an antiviral state in uninfected neighboring cells, selective cytolysis of infected cells, apoptosis, and recruit lymphocytes to the site of infection (204). Production of TNF is also inhibited as it is an NF-κB target gene. When resistant mice deficient in both TNFRs are infected they become susceptible to lethal infection by ECTV and it was determined that both receptors are necessary for resistance (205).

Orthopoxviruses encode four vTNFR decoy receptors: CrmA, CrmB, CrmC and CrmD. Ectromelia virus encodes only one full length vTNFR, CrmD (195, 206) and a second, truncated vTNFR, CrmE (207). Although uncharacterized, CrmC is also fragmented in ECTV, and the CrmB appears to be missing although ORF 008 may be related (42% similarity) (112). Interestingly, an additional secreted member of the TNFR superfamily, a CD30 homolog, was shown to reduce Th1-mediated

inflammation *in vivo* (208), but was determined not to be a major virulence factor during mousepox (209).

2.4.8 Other Important Cytokines

The expression of cytokines can influence the type of adaptive immune response generated against infection and can have drastic effects on the outcome of disease. Some cytokines like IL-4 or IL-6, part of a type 2 immune response, reduce the cellular immune response, reduce anti-viral cytokine expression, and can increase the virulence of VACV (210, 211). Others like IL-2 and IFN-γ, characteristic of a type 1 immune response, can reduce the virulence of VACV by stimulating the activation and proliferation of NK cells and T cells (212, 213). IL-6 along with IL-17 has been shown to inhibit the protective effects of CTLs during viral infection (211). In susceptible BALB/c mice IL-6 dependent activation of STAT3 does not occur, as it does in resistant C57Bl/6 mice that rapidly activate both STAT1 and STAT3. These evidence suggest that IL-6 is necessary for the survival of mousepox (214).

2.4.9 Chemokine Responses

Chemokines are a class of chemoattractant cytokines that recruit leukocytes to sites of cellular stress, such as viral infections (145). Circulating leukocytes detect chemokine gradients on endothelial surfaces used to direct them to the site of infection. There are a variety of different chemokines produced by different cell types and with different chemokine receptor specificities that fine tune the inflammation response. Chemokines are classed by the position of conserved cysteine residues: C, CC or

CXC. VACV has evolved several methods to inhibit the production or function of chemokines including inhibition of their expression due to NF-κB and IRF3 activation. VACV also expresses chemokine-binding proteins (vCKBP) including CC chemokine inhibitor (vCCI) that binds a range CC chemokines with high affinity and is secreted by infected cells early during infection (215). A similar protein, A41, also binds chemokines (CCL21, CCL25, CCL26 and CCL28) although with lower affinity and it does not inhibit chemokine receptor binding. However, heparin binding competes with A41 binding, suggesting that its mechanism of action is via disruption of the chemokine concentration gradient on endothelial cells (216).

The most abundant secreted protein of ECTV is the vCKBP, vCCI, with no sequence similarity to cellular chemokine receptors, although it is well conserved amongst poxviruses (195, 217). Activity in mousepox has not yet been evaluated, but during rabbitpox or myxoma virus infection lack of vCCI results in reduced leukocyte infiltration at the site of infection (218, 219) and has been structurally demonstrated to bind CCL2, CCL3 and CCL5 (220).

In addition to the highly conserved vCKBP, the ECTV-Nav E163, a VACV A41 homolog, protein has been shown to bind the glycosaminoglycans on chemokines, including CXCL10 and CXCL12α with high affinity and inhibit the chemokine-induced leukocyte migration to the sites of infection via disruption of the chemokine gradient (221).

2.4.10 Complement Control

When on the host cell surface, EV protein A56 (EMICE, the ECTV homolog (222))

can bind the virally encoded complement control protein vC3, a protein capable of inhibiting the complement cascade by binding host C3a and C3b (223). It is possible A56 could have a similar role on the EV surface. The virus also incorporates the host proteins CD46, CD55, CD59, CD71, CD81 and MHC class I molecules into EVs. Both CD55 and CD59 are complement control proteins and when incorporated into VACV EVs reduces the efficacy of human complement control (224).

Recovery from mousepox requires the complement control system. When C3, a central component of the complement cascade, was absent resistant C57BL/6 mice had increased viral dissemination and mortality. Sera deficient in components of either the classical or alternative pathways had reduced capacity to neutralize virus particles suggesting both pathways play a role in viral pathogenecity (225).

2.4.11 Regulation of Apoptosis

Apoptosis is the controlled cell death induced by the sequential cleavage of caspase proteases and is a powerful mechanism for the elimination of virally-infected cells. The process is controlled by a balance of pro-apoptotic and anti-apoptotic members of the cellular Bcl-2 family of proteins. Pro-apoptotic proteins, such as Bid or Bad, bind effector proteins Bak and Bax on the outer membrane of the mitochondiria and induce the release of cytochrome *c* into the cytoplasm and the formation of the caspase activation platform or apoptosome. As caspase 1 is one of the modulators of the apoptotic response, production of SPI-2 inhibits apoptosis in addition to its role inhibiting pro-IL-1β cleavage (197). The SPI-2 protein (also known as CrmA) can also inhibit multiple caspases including caspase 8, 10 and granzyme B (226). Another

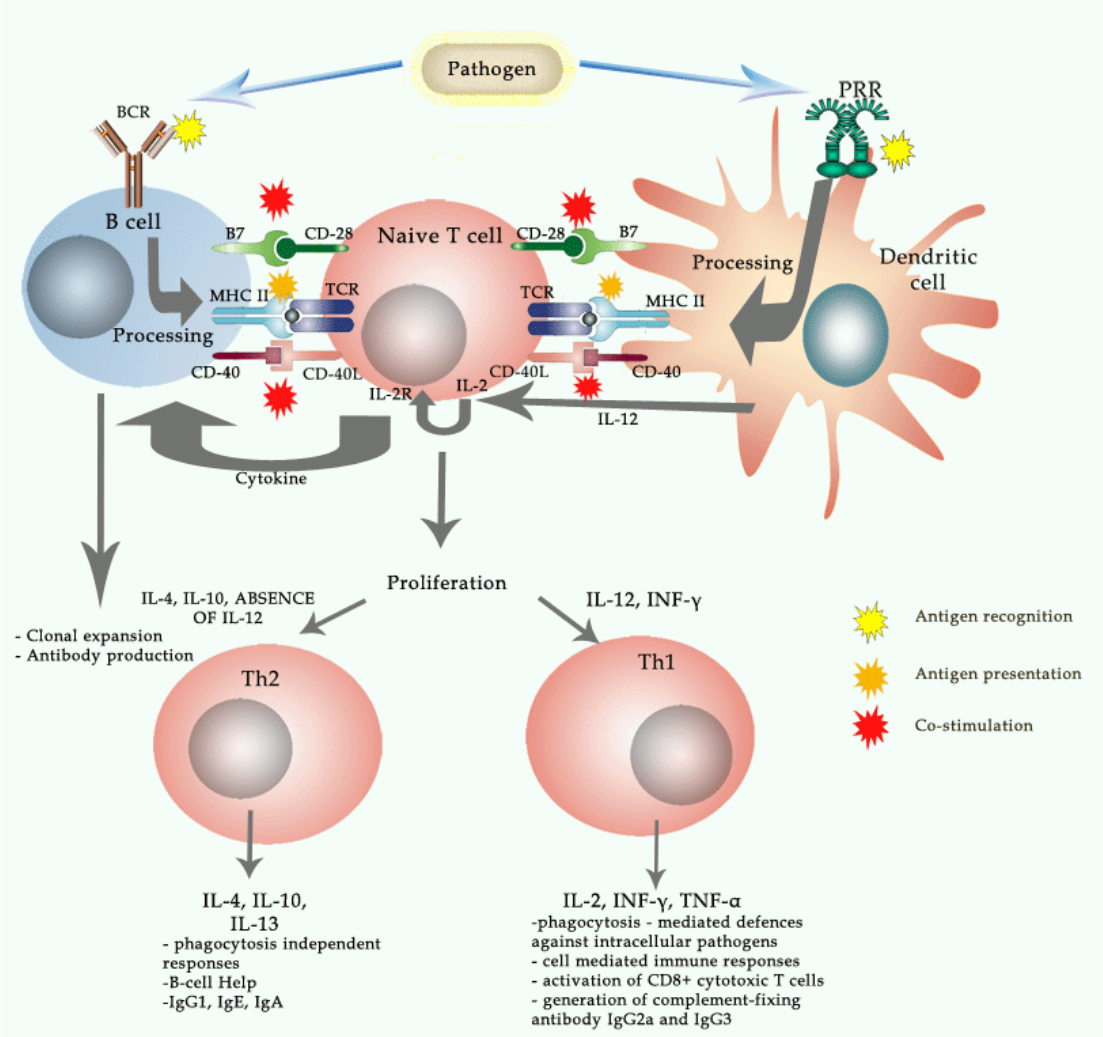

Figure 2.8 Schematic representation of immune response against pathogens

The adaptive arm of the immune response is a complex network of signals and responses. Simply, pathogens can be picked up and processed by antigen presenting cells, like the dendritic cell depicted here, for presentation to naïve T cells. B cells can also recognize pathogens via their B cell receptor (BCR) and with the help of T cells become activated, expand, and adapt as they produce antibodies. T cells, once they have recognized their associated antigen, can differentiate into type 1 (Th1) or type 2

(Th2) helper cells, driving an antibody and B cell driven response (Th2) or cytolytic T cell and cell-mediated response (Th1). This response is driven in part through the production of distinct cytokines: IL-4, and IL-10 are primarily Th2 drivers and will produce IL-4, IL-10 and IL-13; IL-12 and IFN-γ are primarily Th1 driver and will produce IL-2, IFN-γ, and TNF-α. Images source: http://2008.igem.org/Team:Slovenia/Background/Immune_response

inhibitor, SPI-1, blocks apoptosis via a caspase-independent pathway by inhibiting cathepsin G (227, 228).

Poxviral proteins F1 and N1 both adopt a BCL-2-like fold (229, 230). F1 binds the NLRP-1 protein thus inhibiting the inflammatory response and apoptosis, as NLRP-1 is an upstream activator of caspase 1 (134). The N1 protein binds pro-apoptotic Bcl-2 proteins Bid and Bad to inhibit apoptosis (150).

2.4.12 Natural Killer cells

Natural killer (NK) cells are a specialized subtype of granular lymphocytes with high cytolytic activity against virus-infected and tumor cells. As an important component of the innate immune response, they form a primary defense against viral infections before the adaptive arm of the immune response fully develops. NK cell activation is dependent on cytokines such as IFN-α, IFN-β, IL-12 and IL-18, but cytolytic activity is regulated by a variety of activating and inhibitory receptors on the surface of target cells (231). Most NK inhibitory signals recognize MHC class I molecules ensuring tolerance against self-antigens. Activating receptors are often natural cytotoxicity receptors such as NKp46, NKp44, NKp30 as well as CD16 and NKG2D (232).

It is well known that NK cells are important immune components in response to poxviruses as they are essential for C57BL/6 resistance against mousepox. When NK cells are depleted it also increases susceptibility to VACV (233, 234). Infection with VACV increases susceptibility to NK lysis (235) following downregulation of MHC class I (236), but cytotoxicity can be attributed directly to downregulation of HLA-E or C-type lectin related protein b (Clr-b) (237, 238). The extent of this MHC

class I downregulation is quite variable between poxviruses (239). Protein CPXV012 impairs ER peptide loading and dissociated of MHC class I from transporter associated with antigen processing (TAP) protein (240). Protein CPXV203 sequesters MHC class I molecules in the ER using its C-terminal KDEL-like sequences (241). The VACV A56 protein has also be identified as a novel viral ligand for activating receptors NKp30 and NKp46 (242). Some orthopoxviruses, including CPXV and MPXV, encode a protein that resembles an MHC class I molecule (OMCP) that can block the recognition of host ligands and inhibit NKG2D-dependent NK lysis (243).

NK cells were first identified as important for ECTV susceptibility via genetic analysis (244), (next section). However, studying the role of NK cells by antibody depletion or genetic mutations is complicated as these approaches can have off target effects on NKT cells when using NK1.1 antibody (245), CD8+ T cells when using anti-asialo GM1 (183, 246), or granule exocytosis in *bg/bg* mutant mice (183). When C57BL/6 mice are infected with ECTV, NK cells but not NKT cells, are crucial for the recovery from mousepox. NK cells have been shown to proliferate, accumulate, and are activated in the spleen and liver of virus-infected mice (247). Protection in C57BL/6 mice via NK cell activity is suggested to occur through two mechanisms; first, the reduction of lympho-hematogenous spread of virus from LN to spleen is reduced through NK cell perforin cytotoxicity and IFNγ production (248), and secondly, by amplification in the infected liver and direct protection via the same mechanisms (247).

2.4.13 Adaptive Responses

Following the non-specific innate immune response there is a delayed, target-specific immune response known as the adaptive arm of immunity (Figure 2.8). Adaptive responses are not only antigen specific, but they can adapt, improve, and provide lasting, long-term immunity to protect against re-infection. To assist in this specialized response, innate factors can influence the adaptive responses for optimized effect. With the help of activated CD4+ T helper cells, B cells produces virus-specific antibodies capable of neutralizing extracellular viruses, and CD8+ cytotoxic T cells (CTLs) are capable of direct virus-infected cell killing. Both arms of adaptive immunity are induced by VACV infection with CD4+ T cell-dependent antibody responses being most important for viral clearance and CTLs controlling disease severity and mediating protective memory upon reinfection (249-251). Key cytokines like TNF-α, IL-1β, IL-4, and IFN-γ control adaptive responses in addition to their roles during inflammation. Thus, the methods of controlling these cytokines also influence adaptive immune responses.

2.4.14 Antigen Presentation and T Cell Help

In order to develop a target-specific response, adaptive immune cells must encounter pathogen-specific sequences known as antigens in a stimulatory environment. Antigen presenting cells (APCs) such as dendritic cells (DCs) collect pathogenic material by phagocytosis for display to B cells and T cells via MHC molecules. CD4+ T cells recognize peptides bound to MHC class II molecules of professional APCs via their T cell receptor (TCR). Once activated CD4+ T cells will proliferate and expand.

Depending on the cytokine environment they are in, CD4+ T helper (Th) cells will differentiate into Th1 cells (primarily stimulated by IFN-γ and IL-12), or Th2 cells (stimulated by IL-4 and IL-10). Th1 cells will drive a primarily cellular adaptive immune response through the production of IL-2, IFN- γ and TNF-α, utilizing CD8+ cytolytic T cells (CTLs). Th2 will drive a humoral response of B cells and antibody through the production of IL-4, IL-10 and IL-13. Th cells can also differentiate into effector, memory or regulatory Th cells (252). The different types of activated CD4+ T cells have a variety of roles within the host immune response, including: the priming of CD8+ T cells, B cells, cytokine production and direct cytolytic activity (253).

The priming of B cells and CD8+ T cells in response to viral infections typically requires CD4+ Th cell help to direct and maximize the response (254). Following VACV infection the degree of CD4+ Th cell help-dependence is also dependent on the route of infection and dependence is increased at lower viral doses (255). Infected antigen presenting cells can also directly present antigen via MHC class I molecules to CD8+ T cells, and indeed this direct presentation has been shown to be a major source of CTL activation by VACV-infected cells (256, 257). Some leukocytes can be directly infected by poxviruses during infection, including B and T lymphocytes, NK cells, dendritic cells and monocytes/macrophages (143). This infection can contribute to the direct presentation of viral antigens to CTLs by APCs, despite the fact that infection does not induce maturation in dendritic cells (258), and the counteractive downregulation of MHC molecules by viral factors in infected cells.

In addition to the helper roles of CD4+ T cells during T cell priming and B

cell memory, CD4+ T cells can also have direct influences on the adaptive immune response through the production of cytokines (like IFN-γ) and via target cell lysis (253). As poxviruses, and VACV in particular, are of interest as vaccine vectors the role of Th cells in the development of protective immunity has been an area of intense interest. Extensive work has been conducted to identify the epitopes utilized during the immune response and at least 246 distinct epitopes restricted by MHC class I and 61 restricted by class II have been identified. However, only nine different antibody epitopes have been mapped (249). Achieving a better understanding of these epitopes can help us to understand how the immune response is directed against poxviruses and vaccine vectors and, hopefully, help to improve their efficacy (259).

2.4.15 Role of CD4+ T Cells During Disease

T cells have been well established as essential for the control of ECTV infection, even in animals who would be otherwise resistant. When C57BL/6 mice were treated with antithymocyte serum they succumb to mousepox infection (260), and adoptive transfer of effector splenocytes can decrease viral loads in the absence of antithymocyte serum (261).

CD4+ T cells have a variety of roles within the host immune response including the priming of CD8+ T cells, B cells, cytokine production and direct cytolytic activity (253). For these reasons it can be challenging to determine the exact role of CD8+ versus CD4+ T cells and other immune cells that rely heavily on each other for their activities. Nonetheless, the role of CD4+ T cells is essential for control of ECTV infection and has been well established (246). When CD4+ T cells are

absent during primary infection, mousepox disease lasts for extended periods of time (246). Although somewhat controversial, it appears that CD8+ T cell priming and CTL response are largely independent of CD4+ T cell help or CD40-CD40L interactions (262-264). However, the helper function of CD4+ T cells is still required for priming of B cells by CD40-CD154 costimulation (265), and a similar delay in death is observed in the absence of B cells or antibody (20-90 DPI) as in the absence of CD4+ T cells (163, 266). There are some studies suggesting that CD4+ T may have an additional cytolytic role during infection. CD4+ T cells expressing granzyme B have been found in the popliteal LN and liver, and when CD4+ T cells are deficient in Prf animals had reduced viral control (267).

2.4.16 CD8+ T cells and the Cellular Response

CD8+ T cells are stimulated through recognition of foreign antigen presented on the surface of infected cells via MHC class I molecule interactions with the TCR. MHC class I molecules are found on essentially all nucleated cells in the body allowing CD8+ T cells to recognize many different infected cell types. Following stimulation by antigen, T cells can be activated by co-stimulation via CD4+ Th cell-dependent or Th–independent mechanisms, such as self-help (268), to become CTLs. CTLs can then recognize target cells using their TCR and kill via granule-mediated cytolysis or Fas-Fas ligand (FasL) stimulation of apoptosis. Once activated, T cells undergo clonal expansion with the help of IL-2, a driver of the cellular immune response. Some CD8+ T cells can also differentiate into memory cells that persist after infection and protect against reinfection (252).

Production of pox-specific CTLs peaks 5-6 dpi and have been shown to be crucial in the specific defense against poxviruses (269). However, pox-specific CTLs are not essential for surviving VACV infection (196). Instead, it appears that CD4+ T cell-dependent antibody responses play the greatest role in clearance following acute infection. However, CD8+ T cells may play a more important role in the absence of an antibody response (251). When humans are vaccinated with VACV they develop poxvirus-specific CTL responses and both CD4+ and CD8+ T cell specific memory is maintained as memory cells (269).

CD8+ T cells are stimulated by viral peptides loaded onto MHC class I molecules and can become effector CTL cells capable of direct cytolytic killing. CD8+ T cell responses in resistant B6 mice are very strong with as many as 60-80% of total CD8+ T cells being specific for ECTV at day 5 in the popliteal LN and day 7 in the spleen (263, 270) Of these, up to 10% are specific to the immunodominant K^b epitope of ECTV158, the secreted IFN-γ binding protein (270, 271). When CD8+ T cells are depleted in C57BL/6 mice prior to footpad infection the animals become highly susceptible to mousepox, demonstrating the importance of CD8+ T cells for resistance (246). If the CD8+ T cell response is delayed, as it is in CD28-deficient C57BL/6 mice, animals have poorer control of virus spread and the disease becomes lethal in a higher proportion of mice (270). Thus, early and strong CD8+ T cells response are required for effective control of ECTV infection. These responses are independent of CD4+ T cell help or CD40-CD40L interactions (262, 263). In addition to their role in cytotoxicity, CD8+ T cells may play a role in protection against mousepox due to memory T cells. Memory CD8+ T cells can protect against

mousepox by Prf-mediated killing of infected cells within the draining LN, independent of IFN-gamma (272).

2.4.17 B Cells and Antibodies

The cellular response driven by CTLs is only one arm of the adaptive immune system. B cells, and the antibodies they produce, are the key components of the humoral response. Typically, these two competing immune responses work to complement each other. Factors such as pro-inflammatory cytokine IFN-γ stimulates T cells and the cellular arm, while anti-inflammatory IL-10 and IL-4 stimulate B cells and the humoral arm. There is evidence that B cells and antibody are required for viral clearance (249).

As previously discussed, there are two infectious forms of VACV, the MV and EV. Each displays a unique population of proteins on their surface membranes requiring the immune response to generate responses to both forms. Antibodies are critical for protection against poxvirus infection in humans and primates (273), and as EVs are the major circulating form, it is not surprising that EV-targeting antibodies protect better against a lethal challenge in mice and rabbits than MV-targeting antibodies (274, 275). In humans the only neutralizing EV-specific antibodies are against the B5 protein, but anti-A27, L1, H3 and D8 antibodies against MV proteins have been observed (276, 277). Neutralization via anti-B5 antibodies appears to be facilitated by complement (278, 279). This suggests that the outer EV membrane acts as a shield to hide the highly antigenic MV membrane proteins during vulnerable exposure while circulating (280). The glycosylation of surface EV proteins, but not

MV proteins, may provide some protection by stimulating host humoral responses (281).

As the protective properties of smallpox vaccination have been suggested to be due to antibody alone (282) the importance of antibodies in the protection against mousepox is of great interest. As previously described, when B cells or antibody production are inhibited, death is delayed suggesting that the role of antibody for clearance of ECTV is essential and occurs after the cytolytic response (266). The interaction of CD40 on B cells and CD154 on CD4+ T helper cells is essential for efficient antibody production. In C57BL/6 mice CD-40 deficient mice CTL responses are equivalent to wildtype C57BL/6 mice at 7 DPI, but antibody response are inefficient and death occurs 20-90 DPI. Adoptive transfer of CD40-sufficient B cells can restore resistance to mousepox (263). It is likely that cytotoxic CD8+ T cells serve as a first defense against the virus, but antibodies are essential in the prevention of death and clearance of the infection (163)

Fenner demonstrated (103, 129, 283) that anti-HA antibody titers decline faster than immunity against mousepox, and that anti-VACV serum is only partially protective against mousepox. These findings suggest that antibody specificity may be complex and that it may not be the only correlate of protection. Anti-VACV antibodies, capable of recognizing ECTV MVs (as opposed to EVs), are capable of protecting or curing mousepox (284) which may provide one explanation for this difference in antibody specificity.

2.4.18 Viral Pathogenesis

The route of virus infection can be critical as it alters how the virus is introduced to the host and how the picture of disease being observed. For example, peripheral routes of infection, specifically intradermal and subcutaneous, increase immunodominance following VACV infection (285, 286) versus the systemic infection following intranasal infection (287). Additionally, some VACV strains and isolates demonstrate reduced immunodominance of antigens and this correlates with reduced viral spread and robust priming, especially in the spleen (288).

The removal or inactivation of the immunomodulatory proteins that have been discussed in this chapter often attenuate the infection. This can mean increased inflammation and immune cell infiltrates to the site of infection, and/or decreased viral titers at the site of infection and key organs. Sometimes this attenuation can vary between routes of infection. More information is needed to understand why these differences occur.

One model that has been developed for the study of poxviruses in a natural host, and discussed in detail during this review, is mousepox. The potential of this animal infection model to help researchers break apart and understand the components of the immune response, viral immunomodulators that contribute to disease, and the mechanisms by which they do so, make it an ideal model for the characterization of poxviral diseases and viral virulence factors. Furthermore, the existence of genetically resistant and susceptible strains of mice has allowed researchers to examine the roles of genetic determinants of disease.

2.4.19 Genetics of Resistance to Lethal Mousepox

Mouse models have been used to demonstrate the importance of host genes in determining the severity to multiple viral infections and that this resistance is usually under polygenic determinants (289). As previously mentioned, delayed spread of ECTV to the spleen and liver in resistant C57BL/6 mice indicates a genetic role to the resistance of some mouse strains to mousepox. Two major components have been identified; T1-IFNs and NK cells.

In general, mouse strains resistant to lethal mousepox disease display a polarized type 1 cytokine response, and a potent cell-mediated immune response. A predominant type 2 response, or a lack of sufficient type 1 response, is characteristic of susceptible strains (131, 191). Genetic crosses have been useful in the search of the specific genetic components that dictate such responses. It appears that many of the genetic factors identified limit the early viral spread rather than viral replication within organs.

The resistant to mousepox 1 (*rmp-1*) gene on chromosome 6 was identified by crossing susceptible DBA/2 mice with resistant C57BL/6 mice and identifying a large locus, *Prp*, that confers a C57BL/6-like response to infection, thus indicating involvement in resistance to mousepox (244). The NK cell gene complex (NKC) (290) is adjacent to this locus and contains a variety of NK cell receptors (116, 118, 233). The *Klrd1* gene, encoding CD94, is not expressed by NK cells in susceptible DBA/2 mice. In NK cells, CD94 forms heterodimeric NK inhibitory receptors with NKG2A and activating receptors with NKG2C and NKG2E (291). The activating CD94-NKG2E receptor has been shown to recognize the MHC class Ib molecule Qa-

1^b on ECTV-infected cells (292), thus providing a mechanism for the enhanced NK cell activity that promotes resistance in C57BL/6 mice. Interestingly, most Qa-1^b-deficient mice have increased early viral spread from the draining lymph node to the liver and spleen (163) demonstrating the importance of restricting early viral spread for survival. Interestingly, the CD94-NKG2A inhibitory receptor dimer has been demonstrated to optimize the CD8+ T cell response and is necessary for resistance to Ectromelia as it prevents over activation and exhaustion of T cells (293).

Additional genes have also been identified. *Rmp-2* on chromosome 2 maps near the complement C5 gene and has been found to protect female mice better than male (294) *Rmp-3* on chromosome 17 is also gender/gonad-dependent and has been linked to the MHC complex (294). It may even encode the Qa-1^b gene identified as interacting with the presumptive *rmp*-1 gene, CD94 (163). Lastly, *rmp-4* on chromosome 1 is found in an area with a variety of genes that could be involved in NK cell responses including; the genes for lymphotactin/XCL1, the NK and T-cell receptor 2B4, and the E-, L-, and P-selectin genes (295).

Chapter 3: Characterization of a large, proteolytically processed cowpox virus membrane glycoprotein conserved in most chordopoxviruses[1]

3.1 Summary

Most poxvirus proteins are either highly conserved and essential for basic steps in replication or less conserved and involved in host interactions. Homologs of the CPXV219 protein, encoded by cowpox virus, are present in nearly all chordopoxvirus genera and some species have multiple copies. The CPXV219 homologs have estimated masses of greater than 200 kDa, making them the largest known poxvirus proteins. We showed that CPXV219 was expressed early in infection and cleaved into N- and C-terminal fragments that remained associated. The protein has a signal peptide and transited the secretory pathway where extensive glycosylation and proteolytic cleavage occurred. CPXV219 was located by immunofluorescence microscopy in association with the endoplasmic reticulum, Golgi apparatus and plasma membrane. In non-permeabilized cells, CPXV219 was accessible to external antibody and biotinylation. Mutants that did not express CPXV219 replicated normally in cell culture and retained virulence in a mouse respiratory infection model.

---

[1] Adapted from: **Reynolds, S. E. and Moss, B**. Characterization of a large, proteolytically processed cowpox virus membrane glycoprotein conserved in most chordopoxviruses. Virology. 2015 Sep;483:209-17 Copyright © Elsevier

3.2 Introduction

Poxviruses are large DNA viruses that reproduce in the cytoplasm of infected cells and have been widely studied because of their impact on human health, zoonotic spread, historic role as the first live virus vaccine, modern development as recombinant vaccine vectors, and use as model systems to investigate virus replication and host interactions (296, 297). Of the 200 or more proteins encoded by poxviruses, nearly 100 are conserved in all members of the chordopoxvirus subfamily and about half of those are also conserved in entomopoxviruses (44). The majority of the highly conserved proteins have essential roles in virus replication, whereas most of the less well conserved proteins of chordopoxviruses are concerned with modulating host interactions (298). The goal of the present study was to characterize an unusual protein that is widely conserved among the chordopoxvirus genera except for members of the parapoxvirus genus, suggesting an evolutionarily conserved but not strictly essential function. Curiously, vaccinia virus is the sole member of the orthopoxvirus genus that lacks an open reading frame (ORF) encoding this protein. With predicted molecular weights of more than 200 kDa, these conserved proteins are larger than any other known poxvirus proteins. Here we characterize the cowpox virus (CPXV) homolog encoded by open reading frame CPXV219 (UniProt Q8QMM9). CPXV is of particular interest because it may have been the original smallpox vaccine, is the cause of an increasing number of zoonoses, contains the largest and most complete genome and has the broadest host range of all known

orthopoxviruses (5, 25). CPXV219 was expressed early during infection, trafficked through the secretory pathway, was N-glycosylated and cleaved into two major fragments and exposed on the plasma membrane. Additional studies indicated that the CPXV219 gene was dispensable for growth in tissue culture and unnecessary for virulence in mice.

3.2 Results

3.2.1 CPXV219 is conserved in most chordopoxviruses

The CPXV219 ORF of the Brighton red strain of CPXV is located near the right end of the genome and is predicted to encode a 1919 amino acid protein with a N-terminal signal peptide (SP), a near C-terminal transmembrane (TM) domain, two additional hydrophobic domains, and sites of N-linked glycosylation (**Fig. 3.1A–C**). With the exception of VACV, all sequenced orthopoxviruses have similar length homologs. In VACV strain WR, the absence of DNA adjacent to the expected site of the CPXV219 homolog suggests the occurrence of a large deletion. The amino acid sequence identities of CPXV219 homologs of the orthopoxviruses ectromelia virus, variola virus, monkeypox virus and horsepox virus compared to CPXV are 93%, 93%, 85% and 86%. Except for parapoxviruses, at least one strain of all other chordopoxvirus genera encodes a CPXV219 homolog with sequence identity of 30–45% relative to CPXV219. The highest sequence conservation of CPXV219 homologs is in the C-terminal region and some sheeppox strains have a N-terminal deletion. Avipoxvirus strains contain 5–6 duplicated full-length homologs in the center of the genome and crocodilepox virus has 3 copies near the left end of the genome. No homologs have

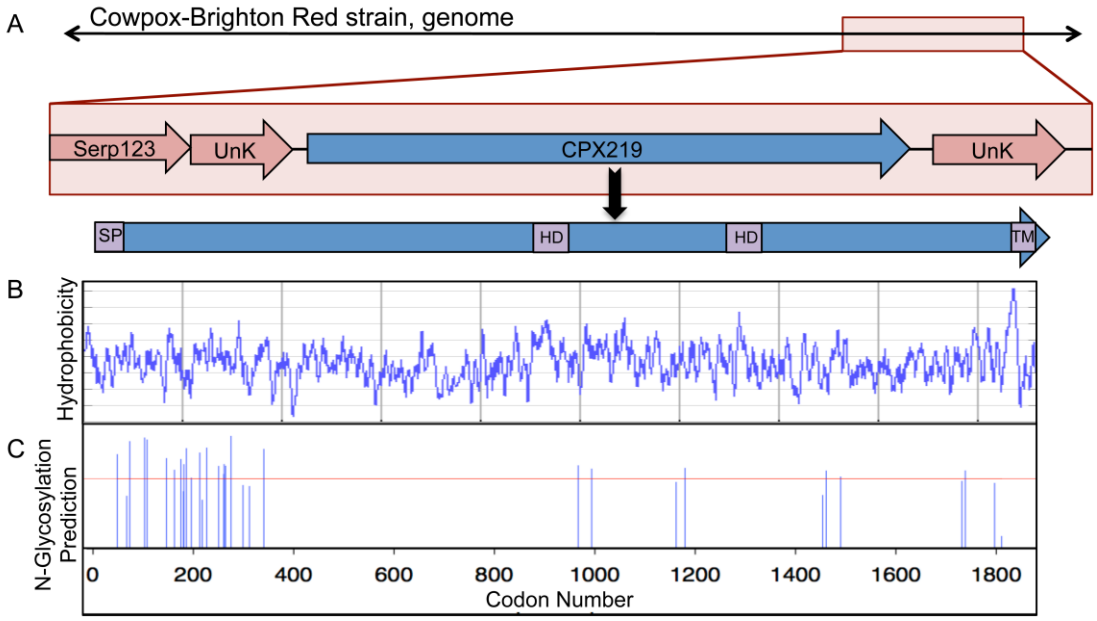

Figure. 3.1 Predicted features of CPXV219

(A) Diagram of CPXV219 ORF. Top shows the position of CPXV219 (blue) flanked by ORFs of unknown function (pink) near the right end of the CPXV genome. CPXV Serp123 corresponds to VACV C12L. Within the gene is a 20 amino acid N-terminal signal peptide (SP) predicted by the SignalP program (http://www.cbs.dtu.dk/services/SignalP/), a strongly predicted C-terminal transmembrane (TM) domain and hydrophobic domains (HD) that were more weakly predicted TMs by the DAS TM prediction server (http://www.sbc.su.se/ miklos/DAS/). (B) Hydrophobicity plot of CPXV219 predicted by the Protscale program using a window of 9 (http://web.expasy.org/cgi-bin/protscale/protscale.pl Kyle & Doolittle). (C) N-glycosylation sites predicted by the NetNGlyc program (http://www.cbs.dtu.dk/services/NetNGlyc/).

been recognized in entomopoxviruses, non-poxvirus species or prokaryotic or eukaryotic organisms.

3.2.2 CPXV219 is non-essential for replication

The absence of a CPXV219 homolog in VACV suggested that the protein is not essential for replication and a recent study determined that CPXV219 could be deleted from CPXV, though the growth properties of the mutant were not described (299). To more fully analyze the requirement of the 219 protein for CPXV replication, homologous recombination was used to make a deletion mutant (CPXV 219delGFP) by replacing the entire approximately 6000 bp ORF in CPXV with one encoding the green fluorescent protein regulated by a VACV promoter in the same orientation as CPXV219. Recombinant virus plaques were identified by fluorescence microscopy and clonally purified by repeated plaque isolation. In addition, the GFP of CPXV 219delGFP was replaced with the original CPXV219 gene in order to make the control virus CPXV 219Rev and with one containing stop codons near the N-terminus to make the mutant CPXV 219Stop. PCR and DNA sequencing confirmed the genomic modifications (data not shown). In addition, we confirmed that the stop codons arrested translation by constructing and testing a recombinant CPXV that had the same stop codons in the CPXV219 gene with a C-terminal epitope tag (shown in **Fig. 3.3D**). The CPXV 219delGFP and CPXV 219Stop viruses replicated under one step growth conditions and formed plaques as well as the parent and CPXV 219Rev control viruses in BS-C-1 cells (**Fig. 3.2A, B**) or HeLa, RK13, BHK21 and MRC5 cell lines (data not shown), demonstrating that the 219 protein was not required for

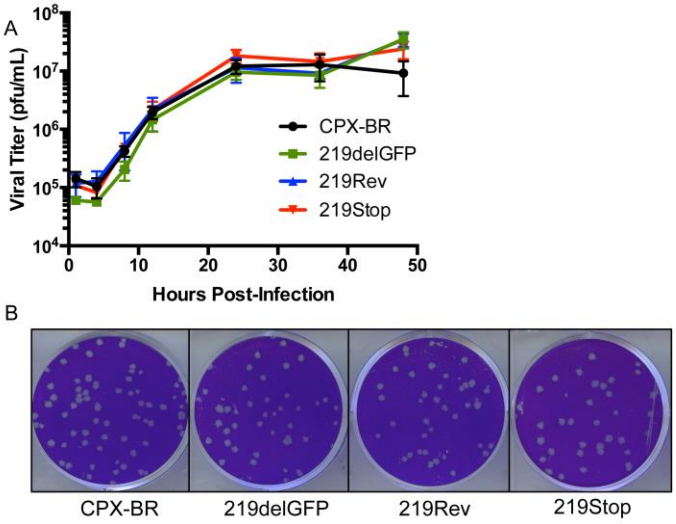

Figure 3.2 CPXV219 is not essential for virus replication

(A) One step growth curve. HeLa cells were infected with 3 PFU/cell of the parent CPXV strain Brighton (CPXBR) and CPXV 219delGFP, 219Rev and 219Stop and the cells plus media were collected at the indicated times. The cells were lysed by repeated freeze-thawing and the virus titers were determined by plaque assay on BS-C-1 cells. (B) Plaque formation. BS-C-1 cells were infected with the indicted viruses, overlaid with semisolid medium and stained with crystal violet after 72 h.

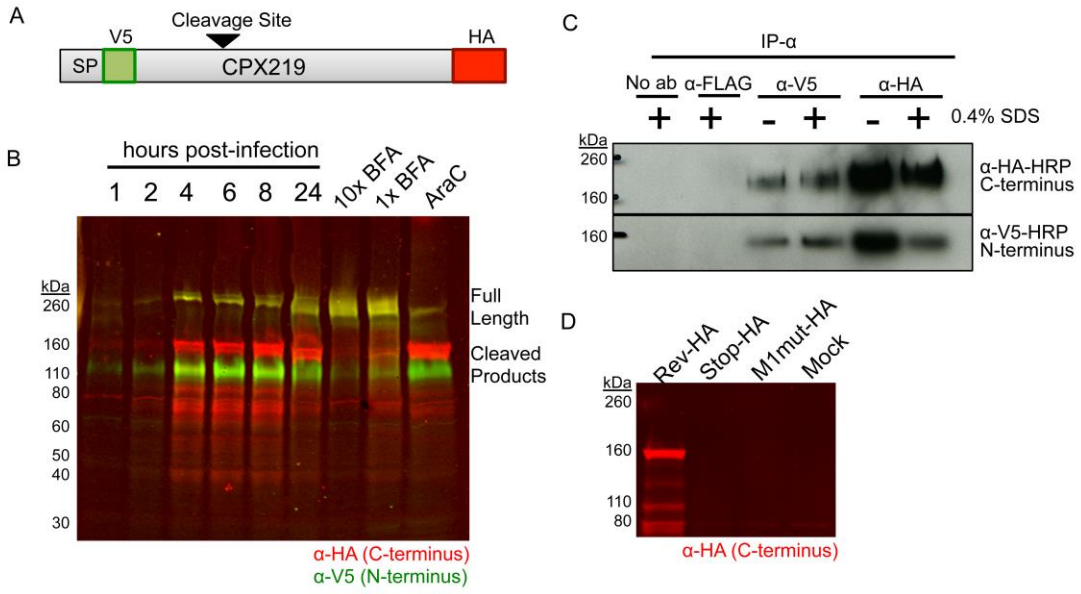

Figure 3.3 Expression of CPXV219

(A) Diagram of the CPXV219 protein containing a V5 epitope tag immediately after the predicted SP and an HA epitope tag just before the termination codon expressed by CPXV V5-219-HA. The arrow indicates the predicted cleavage site. (B) Western blots. HeLa cells were infected with 3 PFU per cell and whole cell lysates were collected at the indicated hours. In parallel, cells were pretreated and infected with 5 mg/ml (1X) or 50 mg/ml (10X) of BFA or 40 mg/ml AraC for 24 h. The infected cells were lysed with β-mercaptoethanol and SDS and the proteins were resolved by SDS-PAGE. The proteins were transferred to a membrane, probed with antibodies to the V5 (green) and HA (red) epitopes and visualized by infrared fluorescent imaging. Yellow indicates coincidence of V5 and HA antibodies. (C) Association of N- and C-terminal fragments. HeLa cells were infected with 5 PFU per cell of CPXV V5-219-HA for 24 h, harvested in non-denaturing lysis buffer, and incubated with anti-V5 or anti-HA MAb in the presence or absence of 0.4% SDS. Antibody complexes were

bound to magnetic protein G Dynabeads and then analyzed by SDS-PAGE and Western blotting. (D) Absence of internal initiation. BS-C-1 cells were infected with 5 PFU per cell of CPXV 219RevHA, CPXV 219Stop-HA and CPXV M1mut-HA. After 24 h, whole cell lysates were analyzed by SDS-PAGE and Western blotting using antibody to the HA epitope tag, and visualized by infrared fluorescence. The positions of marker proteins are shown on the left of each panel.

CPXV replication in cell culture.

3.2.3 CPXV219 is expressed early in infection as full-length and N- and C-terminal fragments

Initial Western blotting experiments employing a recombinant CPXV with a FLAG tag at the C-terminus of CPXV219 revealed a minor band with an apparent mass greater than the 260 kDa marker, a major band of about 160 kDa and additional more rapidly migrating products (data not shown). To further investigate synthesis and apparent processing of CPXV219, we constructed a recombinant CPXV containing specific epitope tags at both the N- and C-termini. Because of the large size of the ORF, a stepwise green-to-white and white-to-green fluorescence screen was used to first replace the C-terminus with GFP and then replace the GFP with the C-terminus of CPXV219 containing an HA tag just before the termination codon to form CPXV 219-HA. A similar two-step procedure was used to replace the N-terminus of 219-HA with GFP and then with the N-terminus of CPXV219 containing a V5 tag downstream of the predicted SP to form CPXV V5-219-HA. In this manner, we obtained a recombinant virus with a specific tag at each end of CPXV219 (**Fig. 3.3A**). The addition of the epitope tags did not affect plaque formation or growth kinetics (not shown). To analyze protein synthesis, HeLa cells were infected with CPXV V5-219-HA, collected at sequential times and lysed directly in buffer containing SDS and β-mercaptoethanol. The proteins were resolved by SDS-polyacrylamide gel electrophoresis (SDS-PAGE), transferred to nitrocellulose filters and probed with antibodies to the epitope tags followed by infrared dyes, which allowed the two tags

to be visualized in the same gel. The major CPXV219 bands were prominent at 4 h, increased at 6 h and unchanged at 8 h suggesting an early promoter (**Fig. 3.3B**), which was consistent with the putative promoter sequence preceding the ORF (not shown). Expression of CPXV219 in the presence of cytosine arabinoside (AraC), an inhibitor of DNA replication that prevents intermediate and late gene expression, confirmed regulation by an early promoter (**Fig. 3.3B**). Antibodies to both N- and C-terminal tags recognized the slowest migrating band with an estimated mass of 260 kDa (which appeared yellow due to the overlap of red and green), indicating that it was the full-length protein. This protein was present in increased amounts, relative to the smaller ones, at 24 h. Antibody to the N-terminal tag recognized a 110-kDa band in addition to the full-length protein, whereas antibody to the C-terminal tag recognized a prominent 160-kDa band as well as smaller bands ranging from 80 to 40 kDa in mass (**Fig. 3.3B**).

3.2.4 Association of the N- and C-terminal fragments of CPXV219

Western blotting indicated that most of the CPXV219 is present as N- and C-terminal fragments. Although the fragments separated under denaturing and reducing conditions, there was a possibility that they remain associated in infected cells. To investigate whether the fragments associate with each other, we carried out immunoprecipitation (IP) experiments. HeLa cells were infected with the CPXV V5-219-HA and solubilized with 1% NP-40. The lysates were incubated with antibody to the V5 or HA tags in the presence or absence of 0.4% SDS to allow separation of loosely bound proteins, followed by the addition of protein G dynabeads. After

washing, the proteins were eluted from the beads and analyzed by SDS-PAGE and Western blotting **(Fig. 3.3C**). When anti-V5 MAb was used to capture the CPXV219 protein, irrespective of SDS, the N-terminal V5 and C-terminal HA fragments were detected by Western blotting indicating their association. Similarly, when anti-HA MAb was used to capture the CPXV219 protein, both fragments were detected by Western blotting. Control experiments showed absence of pulldown with irrelevant anti-FLAG MAb. Intracellular co-localization shown below by confocal microscopy also supported the association of the N- and C-terminal fragments.

3.2.5 Proteolytic processing of CPXV219

We considered several possibilities for the appearance of multiple forms of CPXV219: proteolytic cleavage, internal transcription initiation and internal translation initiation. Additional CPXV mutants were constructed to rule out a possibility that the 160-kDa and smaller C-terminal fragments arise from internal transcription or translation start sites. Starting with the virus containing CPXV219 that had GFP replacing the N-terminus and HA at the C-terminus (used for making CPXV V5-219-HA), we swapped GFP with either (i) the N-terminus of CPXV219 in which the first methionine was mutated from ATG to AGT (CPXV 219M1mut-HA) or (ii) in which the codons at position 5 and 10 were mutated to stop sequences (CPXV 219Stop-HA) or (iii) the original N-terminus was restored (CPXV 219Rev-HA). The recombinant viruses with HA-tags at the C-termini were clonally purified and characterized by PCR and DNA sequencing of the relevant portion of the genome. HeLa cells were infected with the recombinant viruses and the lysates were

analyzed by SDS-PAGE and Western blotting with antibody to the C-terminal HA tag (**Fig. 3.3D**). No C-terminally labeled bands were detected from cells infected with CPXV 219StopHA or CPXV 219-M1mut providing evidence against internal initiation and supporting the model in which CPXV219 is produced as a long polypeptide and subsequently cleaved. Cleavage of CPXV219 could be carried out by viral or cellular proteinases. The two predicted viral proteinases are homologs of VACV I7 (71, 300) and G1 (301, 302), which are expressed post-replicatively. Although not characterized in CPXV, the putative promoter sequences suggested that they are also expressed post-replicatively. Since cleavage of CPXV219 occurred in the presence of a DNA replication inhibitor (**Fig. 3.3B**), it seemed unlikely that either the I7 or G1 homologs were involved. In view of the predicted signal peptide and C-terminal TM domain, we considered that proteinase cleavage might occur by a cellular enzyme during transit through the secretory system. The drug brefeldin A (BFA) inhibits protein transport from the endoplasmic reticulum to the Golgi apparatus indirectly by preventing formation of COPI mediated transport vesicles (303, 304). When CPXV V5-219-HA infected cells were treated with BFA, there was an accumulation of the 260-kDa band and reductions of the smaller 160- and 110-kDa bands, suggesting that cleavage occurs in the Golgi or a post-Golgi compartment during transport of CPXV219 through the secretory pathway (**Fig. 3.3B**).

3.2.6 CPXV219 undergoes SP cleavage

In a prior construct, we placed the V5 tag after the putative SP to ensure that it would be retained in the mature protein. To confirm SP cleavage actually occurs, we

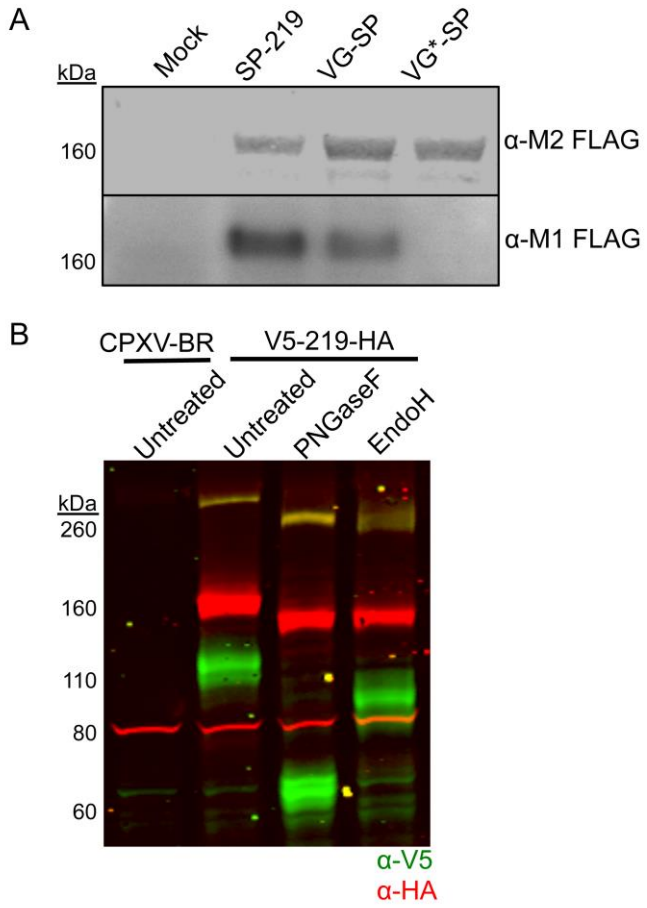

Figure 3.4 Signal peptide cleavage and glycosylation of CPXV219

(A) Western blots. HeLa cells were infected with 10 PFU per cell of viruses expressing CPXV219 proteins that contain a single FLAG epitope tag following the putative CPXV219 SP (SP-219), the VSV-G SP (VG-SP) replacing the CPXV 219 SP, or non-cleavable VSV G SP (VG*-SP) replacing the CPX V219 SP. After 18 h, whole cell lysates were treated with β- mercaptoethanol and SDS and analyzed by SDS-PAGE and Western blotting. Separate membranes were blotted with anti-FLAG clone M2 or anti-FLAG antibody clone M1 and visualized by infrared fluorescence (upper) and chemiluminescence (lower). (B) Glycosylation. HeLa cells were infected

with 3 PFU per cell of CPXV V5-219-HA or parental CPXV-BR. After 18 h, the cells were harvested, lysed with 50 mM Tris pH 7.0, 150 mM NaCl, and 0.5% NP-40 detergent and nuclei removed by centrifugation. The clarified lysates were incubated with PNGaseF, EndoH, or left untreated and analyzed by SDS-PAGE and Western blotting. Antibodies to V5 (green) and HA (red) were visualized by infrared fluorescence. Yellow result from coincidence of red and green. The positions of marker proteins are shown on the left of each panel.

followed a previously described strategy (305) that takes advantage of two MAbs that react with the 19 amino acid FLAG tag: one (M1) reacts with the FLAG epitope only when it is located N-terminally, whereas the other (M2) reacts with internal as well as N-terminal FLAG epitope. Thus, reactivity with M1 MAb could occur only after SP cleavage. Three recombinant viruses were constructed with FLAG tags at the N-terminus (**Fig. 3.4A**). One construct (CPXV SP-FLAG-219) contained the predicted SP sequence of CPXV219 immediately preceding the FLAG epitope tag; a positive control (CPXV VGSP-FLAG-219) was created by replacing the predicted CPXV219 SP sequence with the known SP sequence of the G protein of vesicular stomatitis virus (VSV) followed by the FLAG epitope tag; a negative control (CPXV VG-SP*-FLAG-219) was generated using a VSV-G SP sequence with two amino acids mutated that impair cleavage (306). Cells were infected with the three viruses and the lysates were analyzed by SDS-PAGE and Western blotting. Using the M2 antibody, we showed that the three proteins were expressed and contained the FLAG epitope (**Fig. 3.4A**). However, only the SP-FLAG- 219 and VGSP-FLAG-219 were detected by the M1 MAb that is specific for N-terminal FLAG, which could only arise by SP cleavage at the ER (**Fig. 3.4A**). The negative control VG-SP*-FLAG-219 was not detected with M1 MAb (**Fig. 3.4A**). These results confirmed the prediction of signal peptide cleavage at the N-terminus of CPXV219.

3.2.7 CPXV219 is N-glycosylated in the ER and traffics to the Golgi apparatus

The finding of SP cleavage as well as the effect of BFA on cleavage of CPXV219 suggested that the protein traffics through the secretory pathway. Glycosylation could

account for apparent mass of 4260 kDa determined by SDS-PAGE, whereas the ORF sequence predicts a mass of 215 kDa. Bioinformatics predicted numerous N-glycosylation sites clustered mainly between codons 69 and 364 and additional sites between codons 997 and 1776 (**Fig. 3.1A**). To test these predictions, lysates of cells infected with CPXV V5-219-HA were digested with peptide N-glycosidase F (PNGaseF), which cleaves between the innermost GlcNAc and asparagine residues of N-linked glycoproteins and endoglycosidase H (EndoH), which also cleaves asparagine-linked oligosaccharides but not after further processing in the Golgi apparatus. Thus, EndoH-resistance can occur after transit to the Golgi apparatus. Undigested and digested proteins were analyzed by SDS-PAGE and Western blotting with antibodies to V5 and HA. As predicted, the N-terminal segment of CPXV219 exhibited a large mobility shift, equivalent to 45-kDa, upon PNGase digestion whereas the C-terminal segment was reduced by only about 10-kDa (**Fig. 3.4B**). The combined mass of the PNGase-digested N- and C-terminal fragments was similar to that predicted for the full-length CPXV219, indicating that there is one or a few closely spaced cleavage sites at about 600 amino acids from the start codon. Mobility shifts of full-length, N-terminal and C-terminal fragments also occurred after EndoH digestion (**Fig. 3.4B**). However, EndoH digestion did not decrease the mobility of the N-terminal fragment as much as PNGase suggesting partial resistance due to carbohydrate processing in the Golgi apparatus.

3.2.8 Cellular localization of CPXV219

Fluorescent probes conjugated to anti-V5 and anti-HA antibodies were used to

localize V5-CPXV219-HA and its cleavage products by confocal microscopy. Extensive co-localization of the probes within the cell and at the plasma membrane supported the association of the N- and C-terminal fragments (**Fig. 3.5A**). Another recombinant CPXV with C-terminal triple-FLAG (219-3xFLAG), which allowed sensitive detection with anti-FLAG M2 MAb, was used for intracellular localization. Polyclonal antibodies to cell proteins were also used for co-localization. Cells in which CPXV219 co-localized with cellular calnexin, ERGIC-53 and GM130 targeting the ER, ER-Golgi intermediate compartment and cis-Golgi apparatus, respectively, are shown in **Fig. 3.5B**. The plasma membrane also appeared to be stained with FLAG antibody (**Fig. 3.5B**). Taken together these results suggested that CPXV219 traverses the entire secretory pathway rather than halting in one compartment. Additional experiments were carried out to confirm the plasma membrane localization of the CPXV219 and determine whether the protein is accessible from outside the cell. In order to gain high sensitivity, the cells were infected with CPXV 219-3xFLAG virus (**Fig. 3.4)**. Signal peptide cleavage and glycosylation of CPXV219. (A) Western blots. HeLa cells were infected with 10 PFU per cell of viruses expressing CPXV219 proteins that contain a single FLAG epitope tag following the putative CPXV219 SP (SP-219), the VSV-G SP (VG-SP) replacing the CPXV 219 SP, or non-cleavable VSV G SP (VG*-SP) replacing the CPX V219 SP. After 18 h, whole cell lysates were treated with β- mercaptoethanol and SDS and analyzed by SDS-PAGE and Western blotting. Separate membranes were blotted with anti-FLAG clone M2 or anti-FLAG antibody clone M1 and visualized by infrared fluorescence

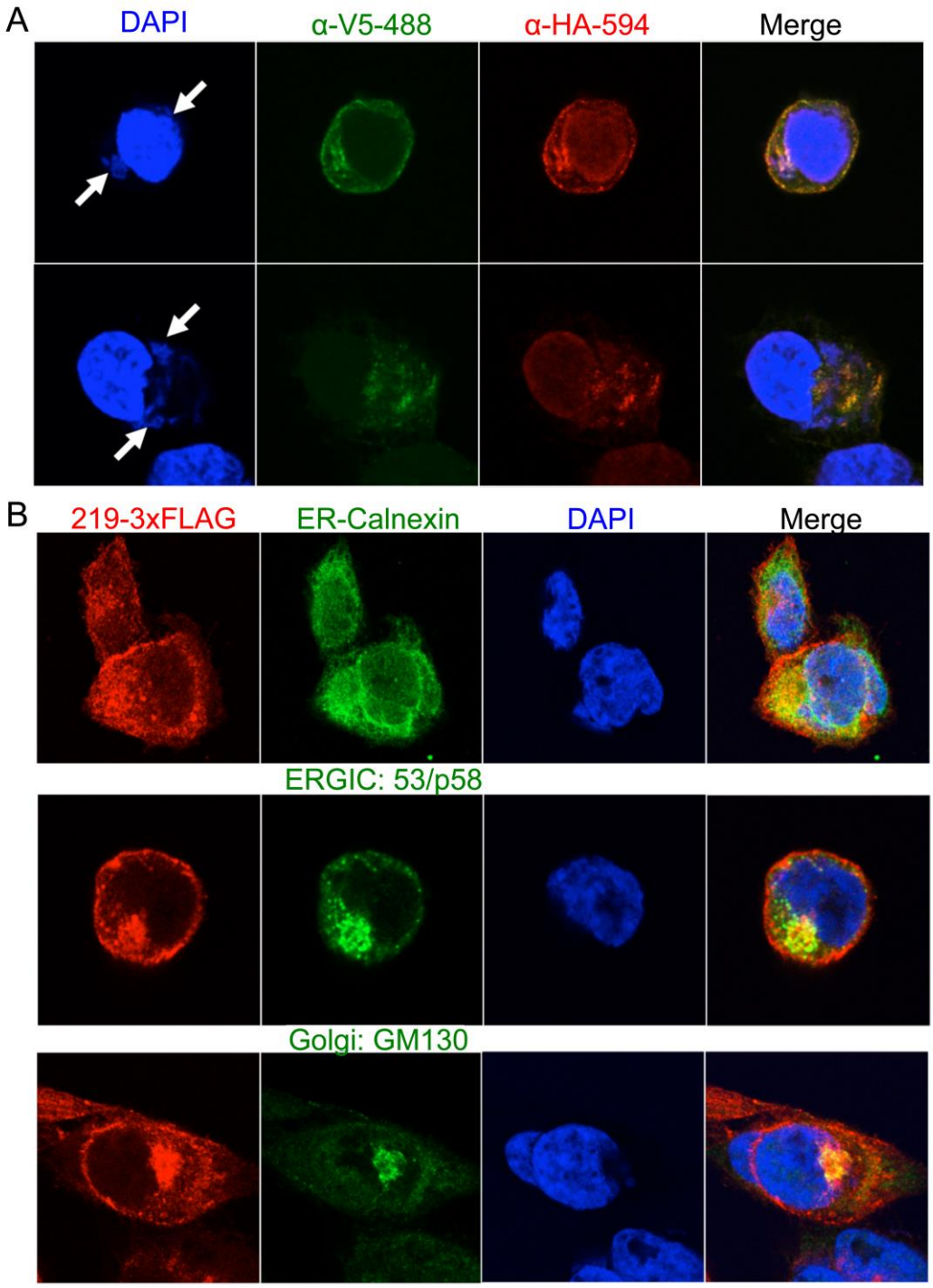

Figure 3.5 Cellular localization of CPXV219

(A) HeLa cells were infected with 5 PFU per cell of CPXV V5-219-HA for 8 h. The cells were fixed and permeabilized and stained with monoclonal fluorescent

conjugated antibodies to the V5 and HA epitope tags. The cells were also stained with DAPI to visualize nuclei and virus factories (arrows). (B) HeLa cells were infected with 3 PFU per cell of CPXV 219-3XFLAG for 8 h and then fixed and permeabilized. Cells were stained with antibodies against the C-terminal FLAG of CPXV219 (red) and either calnexin (green), ERGIC 53/p53 (green) or GM130 (green), which localize in the ER, ERGIC and Golgi network, respectively. DNA in nuclei and virus factories are stained with DAPI (blue). Yellow represents the colocalization of green and red. Representative images are shown.

(upper) and chemiluminescence (lower). (B) Glycosylation. HeLa cells were infected with 3 PFU per cell of CPXV V5-219-HA or parental CPXV-BR. After 18 h, the cells were harvested, lysed with 50 mM Tris pH 7.0, 150 mM NaCl, and 0.5% NP-40 detergent and nuclei removed by centrifugation. The clarified lysates were incubated with PNGaseF, EndoH, or left untreated and analyzed by SDS-PAGE and Western blotting. Antibodies to V5 (green) and HA (red) were visualized by infrared fluorescence. Yellow results from coincidence of red and green. The positions of marker proteins are shown on the left of each panel and stained with anti-FLAG M2 antibody with and without Triton X-100 permeabilization. As a positive control, infected cells were stained with a MAb that binds to the VACV B5 homolog on the surface of unpermeabilized cells. Antibody to L1 a mostly intracellular virion component was used as a negative control. Staining of CPXV219-FLAG in unpermeabilized cells produced a distinct ring that delineated the outside of the cell with the same pattern as B5, but not seen with L1 (**Fig. 3.6A**). After permeabilization, CPXV219-FLAG, B5, and L1 were all stained. The extracellular staining of the C-terminal tag of CPXV219-FLAG demonstrated that the 40 amino acids following the TM domain are extracellular. The relatively weak signal obtained with the N-terminal V5 tag precluded attempts to demonstrate extracellular localization of the N-terminal V5 tag (data not shown). To support the immunofluorescence data, we used a nonmembrane permeable biotin (NHS-SS-Biotin) to label extracellular proteins on live cells infected with CPXV V5-219-HA. Lysates were prepared and incubated with beads attached to NeutrAvidin to purify biotinylated proteins. After washing the beads, the bound proteins were eluted and resolved by SDS-PAGE. The C-terminal

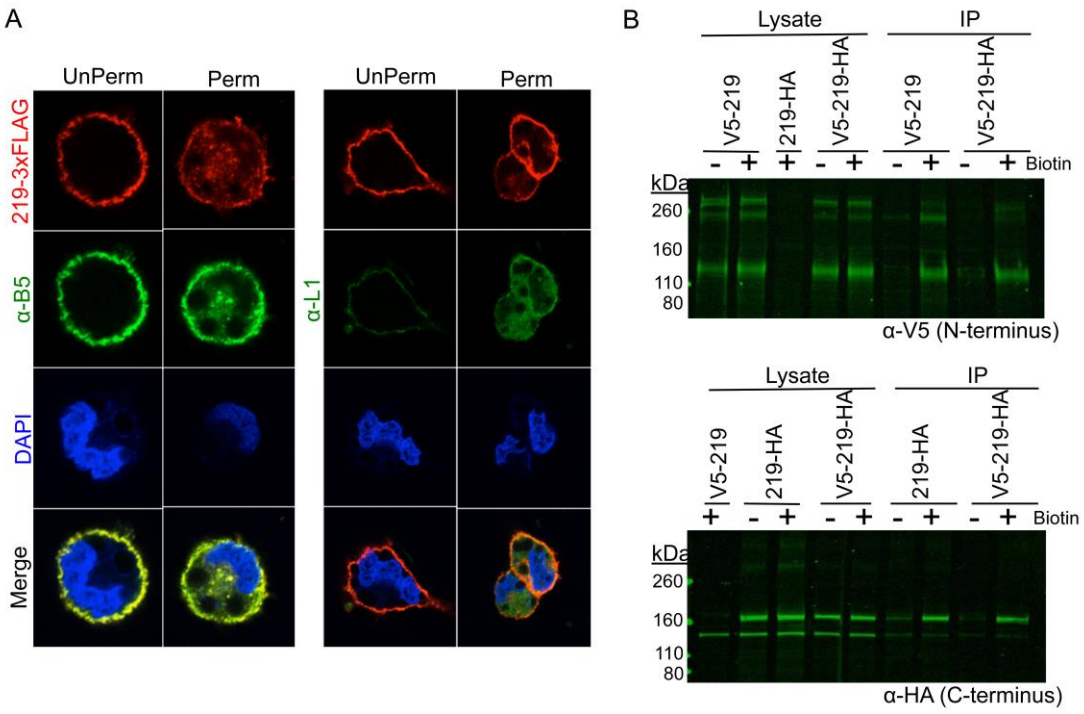

Figure 3.6 Localization of CPXV219 on the cell surface

(A) HeLa cells were infected with 3 PFU per cell of CPXV 219-3XFLAG and stained with FLAG M2 MAb (red) and polyclonal anti-B5 (green) or anti-L1 (green) antibody either prior to treatment (UnPerm) or following fixation in 4% paraformaldehyde and permeabilization with Triton X-100 (Perm). DNA was stained with DAPI (blue). (B,C) Infections were carried out for 18 h with 10 PFU/cell of viruses with epitope tags at the N- or C-termini and then incubated with (+) or without (-) a non-membrane permeable biotin (NHS-SS-Biotin), washed to remove excess biotin, and harvested. Lysates were incubated with neutravidin beads and the bound proteins were eluted and analyzed by SDS-PAGE and Western blotting with anti-V5 (α-V5) or anti-HA (α-HA) MAb. The positions of marker proteins are shown on the left.

fragment of the biotinylated protein was detected using anti-HA and the N-terminal fragment with anti-V5 (**Fig. 3.6B**), whereas the proteins were not detected in the control without biotinylation. These results demonstrate that the N- and C-terminal fragments of CPXV219 remain associated at the cell surface.

3.2.9 CPXV219 does not contribute to virulence in mice

Although CPXV mutants with total or partial deletion of CPXV219 replicated well in cell culture, we considered the possibility that the protein might be more important during animal infection. CPXV 219Stop, without epitope tags or reporter genes, and CPXV 219Rev were used to infect BALB/c mice via the intranasal (IN) route with doses of 10^4 –10^6 PFU. At the low dose of 10^4 PFU, there was minor weight loss and 100% survival of mice infected with the mutant and revertant viruses (**Fig. 3.7A, B**). At 10^5 PFU, there was slightly greater weight loss and lower survival with the revertant virus compared to the mutant virus, whereas at 10^6 PFU the weight loss was similar for both and few mice survived (**Fig. 3.7A, B**). The calculated LD50 values of 1.0×10^5 and 2.1×10^5 for CPXV 219Rev and CPXV 219Stop, respectively, suggested at most a minor effect of CPXV219 expression on virulence in BALB/c mice. We also compared the virulence of CPXV 219Stop and CPXV 219Rev in CAST/Eij mice, which are more susceptible to CPXV and other orthopoxvirus infections than BALB/c mice (307, 308). Because of their sensitivity to CPXV, the CAST/Eij mice were infected IN with CPXV 219Rev and CPXV 219Stop at 1, 10, or 100 PFU. Weight loss and time to death were monitored. All of the low dose 1 PFU animals

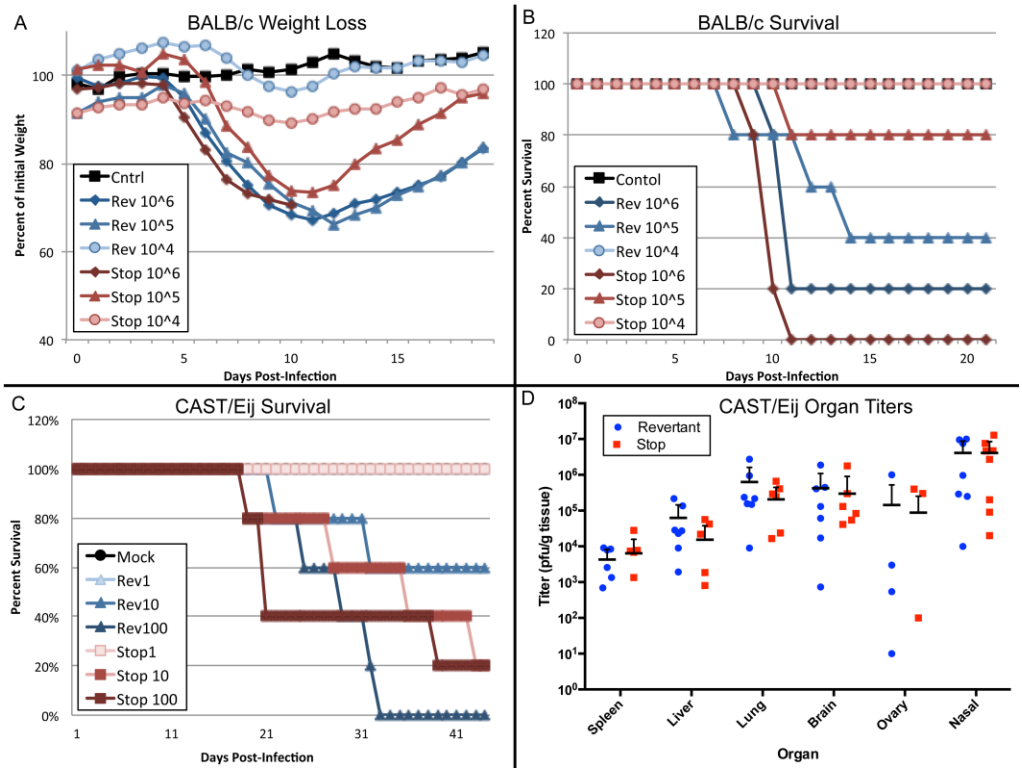

Figure 3.7 Comparison of CPXV 219rev and CPXV 219Stop in mouse infection models

(A) Infection of BALB/c mice. CPXV 219rev and CPXV 219Stop were administered at doses of 10^4, 10^5 and 10^6 PFU intranasally to groups of 5 BALB/c mice and the animals were weighed daily. (B) Percent survival of BALB/c mice from panel A. (C) Survival of CAST/EiJ mice. CPXV 219Rev and CPXV 219Stop were administered at doses of 10^1, 10^2 and 10^3 PFU intranasally to groups of 5 CAST/EiJ mice and the animals were weighed daily. Percent survival was plotted. (D) Organ titers of mice from panel C. At time of death organs of CAST/EiJ mice were collected, weighed, and frozen. Organs were then homogenized and titered on BS-C-1 cells. The PFU/g was calculated for spleen, liver, lungs, and brain and the total PFU/organ for the ovaries and nasal turbinates.

survived. At 10 PFU, 60% of the mice infected with CPXV 219Rev survived and 20% of those infected with CPXV 219Stop survived. At the high dose of 100 PFU, none of the mice infected with CPXV 219Rev survived, and 20% of those infected with CPXV 219Stop survived (**Fig. 3.7C**). Weight loss for all groups was minimal even up to death and none reached the 70% level that would trigger termination. LD50 values of 15 and 5 PFU were calculated for CPXV 219Rev and CPXV 219Stop, respectively. Similar results were obtained in a second study (not shown). At the times of death, organs were harvested and titered by plaque assay on BS-C-1 cells (**Fig. 3.7D**). The organs contained similar titers of CPXV 219Rev and CPXV 219Stop and differences were not significant. We concluded that CPXV219 does not appear to contribute greatly to virulence during an IN infection of either BALB/c or more sensitive CAST/Eij mice.

3.3 Discussion

Our study of the CPXV219 protein was motivated by the very large size of the ORF and its conservation in most but not all chordopoxvirues. Indeed, members of some genera have multiple copies suggesting an important role. CPXV219 was synthesized within the first 4 h of infection and in the presence of an inhibitor of DNA replication, indicating an early stage promoter. By constructing a recombinant virus with epitope tags at both ends, we detected the full-length protein, which migrated with an apparent mass of > 260 kDa, and more abundant 110 kDa N-terminal and 160 kDa C-terminal fragments by Western blotting under denaturing conditions.

Immunoprecipitation experiments, however, indicated that the fragments remained associated prior to denaturation in vitro. The possibility that the C-terminal fragment arose from internal initiation was ruled out by its failure to form either when stop codons were introduced near the N-terminus or by removing the start codon. An increase in amount of full-size protein occurred when BFA was added, suggesting that proteolytic cleavage occurred during transit through the Golgi apparatus. Further studies demonstrated cleavage of a signal peptide and transit through the secretory pathway. Extensive N-glycosylation, also occurred during trafficking; approximately 45- and 10-kDa reductions in the masses of the N- and C-terminal fragments occurred following PNGase digestion. If we estimate that each N-glycosylation contributes 2.2 kDa to protein mass, then approximately 20 of the 21 predicted sites in the N-terminal fragment were glycosylated and 4 or 5 of the 10 predicted sites in the C-terminus were glycosylated. The acquisition of endoH-resistance, particularly of the N-terminal fragment, was further evidence of Golgi or post-Golgi transport. The CPXV219 protein was visualized throughout the secretory pathway including the plasma membrane and was detected in unpermeabilized cells by labeling with fluorescent antibody to a C-terminal epitope tag and confocal microscopy. Based on the available data, we suggest the topological model in **Fig. 3.8**. In step I, CPXV219 is co-translationally inserted into the ER with cleavage of the signal peptide and glycosylation. In step II, the protein is transported to the Golgi network where modification of carbohydrate and proteolytic cleavage occur. In step III, the two fragments while still associated are transported to the plasma membrane. The C-

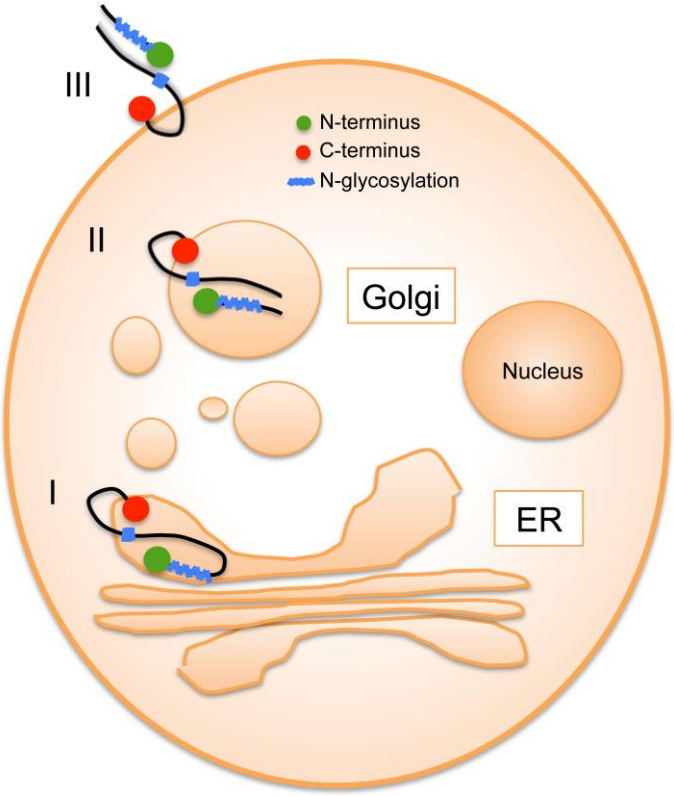

Figure 3.8 Topological model of CPXV219

I, the CPXV protein is co-translationally synthesized at the ER, with removal of the signal peptide, and glycosylated. II, the protein is transported to the Golgi network where the carbohydrate is modified and cleavage occurs to form two major fragments. III, the two fragments while still associated are transported to the plasma membrane where the segments that were in the ER are now extracellular. The linear model of CPXV219 shows placement of the signal peptide (SP), epitope tags (V5 and HA), cleavage site, N-glycosylated region, C-terminal transmembrane domain (TM) and internal hydrophobic domain (HD) that may serve as a second TM.

terminus was considered to be outside of the plasma membrane because the epitope tag was accessible to antibody in unpermeabilized cells. The site of CPXV219 cleavage at approximately amino acid 600 of the full-length protein must have been in the ER based on the inhibition by BFA and at least part of the region between amino acid 1000 and 1800 must also have been in the ER since that is where the potential N-glycosylation sites are located. Assuming that the predicted TM near the C-terminus is utilized, then CPXV219 must traverse the membrane twice. There are two additional hydrophobic regions estimated between amino acids 925 to 938 and 1317 to 1325, one of which must traverse the membrane. Based on the location of the potential N-glycosylation sites, we predict that the more distal hydrophobic site was used. This would mean that a loop between amino acids 1325 and 1856 is cytoplasmic. The entire N-terminal fragment must have been in the ER based on the cleaved signal peptide, the extent of N-glycosylation and the absence of additional hydrophobic domains. Since fluorescence microscopy showed the N-terminal fragment colocalizing with the C-terminal fragment within the cytoplasm and at the plasma membrane and co-immunoprecipitating with the C-terminal fragment, we also placed it on the cell surface in our model. However, further experimentation is needed to directly confirm the predicted topology. In a recent study Alzhanova et al. (308) analyzed the monkeypox virus (MPXV) homolog of CPXV219. Their study and ours were consistent in providing evidence for proteolytic cleavage of the full length protein and cell surface expression of the C-terminal fragment, despite methodological differences. In contrast to our approach, which involved construction of recombinant CPXV containing epitope tags at both the N- and C-termini,

Alzhanova et al. (309) relied on transient expression by plasmids in uninfected cells or by adenovirus vectors. Because the majority of their studies were carried out with only a C-terminal epitope tag, they did not demonstrate the formation of a stable N-terminal fragment. The inhibition of cleavage by BFA suggested the action of a Golgi or post-Golgi proteinase. The approximately 65- and 150-kDa sizes of the deglycosylated CPXV219 fragments suggested that the major cleavage site or sites are about 600 amino acids from the N-terminus. The Arg-X-X-Arg and Arg-Arg sequences between amino acids 589 and 596 are candidate furin cleavage sites. A conserved run of Ser residues is just downstream of the putative cleavage sites and additional Ser residues are about 30 amino acids further downstream. A region rich in prolines (35%) and arginines (15%) with 14 PXXP sequences occurs between amino acids 706 and 778 of CPXV219 and is conserved in other orthopoxvirus homologs. Such proline-rich regions are found in SH3 domains and may be involved in protein–protein interactions (310). Despite the conservation of CPXV219 homologs in most poxviruses, we found that introduction of stop codons near the N-terminus or deletion of the entire ORF had no effect on replication in tissue culture cells. This suggested that CPXV219 likely had a role in countering host defenses. However, the CPXV219 null mutant was not attenuated in either BALB/c mice or the more sensitive CAST mice (308). We considered that other CPXV genes might make the role of CPXV219 partially redundant or that the activity of CPXV219 is fine-tuned for its natural rodent host and is non-functional in mice. Both ideas are consistent with the recent report by Alzhanova et al. (309). While searching for a MPXV gene product that renders T-cells non-responsive they identified MPX197, a homolog of CPXV219. In a rhesus

macaque model, deletion of the MPX197 resulted in increased survival, reduced viral load, and increased levels of both CD4+ and CD8+ pox-specific T cells. The MPXV, VARV and CPXV homologs each inhibit human and monkey T cells but are less active on mouse T cells, providing a possible explanation for our finding that a CPXV219 null mutant did not affect the disease course of CPXV in mice. In addition, CPXV encodes two inhibitors of MHC class I presentation (241, 311, 312) that could compensate for the absence of CPXV219. In the future, we plan to investigate the role of the ectromelia homolog in the mouse, its natural host.

3.4 Materials and Methods

3.4.1 Cells

BS-C-1 cells were propagated in minimum essential medium with Earle's salts supplemented with 10% fetal bovine serum, 100 U/mL of penicillin, and 100 mg/ml of streptomycin (Quality Biologicals, Gaithersburg, MD). HeLa cells were propagated in Dulbecco's modified Eagle's medium supplemented with 10% fetal bovine serum and antibiotics as described above.

3.4.2 Recombinant CPXV219 viruses

DNA sequences were generated using overlapping PCR for the purpose of homologous recombination in the generation of mutant viruses. The flanking regions of the C-terminus of CPXV219 were amplified from CPXV-BR genomic DNA using SR42 (5′ -AAG ATG CTA AAA ATA AGA AAA GGA CAT ATA-3′), SR96* (5′ -CCA TTT ATA GCA TAG AAA AAA ACA AAA TGA AAT ATT CAC GTA TTC

ATT AGA ATC GTC ATG-3′), SR3n (5′ -ATG CAC GAG CTG TAC AAG TAA TAA TAA AAA AAT AGT TTA ACT CTT TTT AGA ACC AGT TTG-3′) and SR4 (5′ -GTT TAT ATC ACA GCA TTC TAC AAA CAG TCT AAA C-3′). In a second PCR the overlapping tails of the above primers (underlined) were used to flank GFP under the control of a VACV p11 promoter amplified using SR94 (5′ -TTT CAT TTT GTT TTT TTC TAT GCT ATA AAT GGT G-3′) and SR20 (5′ -TTA CTT GTA CAG CTC GTC CAT GCC GAG AGT GAT CCC-3′). The resulting PCR product containing an independently regulated GFP flanked by the regions up- and downstream of the 219 C-terminus was gel purified and transfected (lipofectamine 2000, Invitrogen) into cells infected with CPXV-BR. Recombinant viruses that express GFP were detected by fluorescence microscopy and isolated by three rounds of plaque purification beneath a 5% methylcellulose overlay. The correct site and sequence of the CPXV219-CtdelGFP recombinant was confirmed by PCR.

C-terminally tagged CPXV219 was generated using the same homologous recombination method described above but replacing GFP with the wild-type C-terminal CPXV219 sequence and an HA tag (N-YPYDVPDYA-C) immediately prior to the stop codon. The primers SR105 (5′ -AGC GTA GTC TGG GAC GTC GTA TGG GTA GTA CCG ATT ATC CAT AAT TTC CAT AGA TAC TG-3′) and SR106 (5′ -CGA CGT CCC AGA CTA CGC TTA ATA AAA AAA TAG TTT AAC TCT TTT TAG AAC CAG TTT GG-3′) were used in overlapping PCR to generate the recombination fragment. Non-fluorescent plaques were purified in tissue culture and generation of CPXV 219-CtHA was confirmed by PCR and sequencing.

The same technique was also used to generate the N-terminal V5 tag (N-

GKPIPNPLLGLDST-C) of the doubly tagged mutants of CPXV219. The primers SR1 (5′ -AAC ATG AGT ATT CTA GGT GTC TCT ATT GAA TG-3′), SR93 (5′ -CAC CAT TTA TAG CAT AGA AAA AAA CAA AAT GAA AGG TTG CCG GTC ATA AAC AAA CC-3′), SR95 (5′ -CAT GCA CGA GCT GTA CAA GTA ATA TAA TTG TAA ACT AAC TAC AAA TTC TGC ATG TGA TG-3′) and SR55 (5′ -GCA TAA GTT ACC TCT TTA ACA CTA GAA AGC TTT TGG-3′) were used, along with the previously described GFP amplification, to create the GFP deletion construct CPXV219-NtdelGFP. Primers SR138 (5′ -GGT CGA GTC GAG GCC GAG GAG GGG GTT GGG GAT GGG CTT GCC ACA CCA CGA ACA TGT CGC-3′) and SR139 (5′ -CGG CCT CGA CTC GAC CTA TGA AAC ATG TGT AAG AAA ATC TGC ATT G-3′) were used to generate the N-terminal recombination product in which the V5 tag was inserted directly following the signal peptide cleavage site. Plaques were purified and confirmed by PCR and sequencing. Mutants used to confirm the signal peptide were similarly generated from the CPXV 219-NtdelGFP in which a single FLAG tag (N-DYKDDDDK-C) was inserted immediately following the wild-type CPXV219 signal peptide (N-MNLQRLSLAIYLTATCSWC-C), a known signal peptide (SP) sequence from the VSV-G protein (VG-SP: N-MKCLLYLAFLFIGVNC-C), or the known SP with a single mutation (bold) disrupting cleavage (VG-SP*: N-MKCLLYLAFLFIGVN**R**-C) as shown in Husain et al. (305).

Viruses were propagated in BS-C-1 cells and released through 3 repeated freeze/thaw cycles. Samples were sonicated prior to each use and viral titers were determined in duplicate using BS-C- 1 cells.

3.4.3 Antibodies

The HA epitope tag was detected with anti-HA clone HA-7 Mab (Sigma), anti-HA rabbit Pab (Invitrogen) or horseradish peroxidase (HRP)-conjugated rabbit anti-HA polyclonal antibody (PAb) (Thermo). The V5 epitope tag was detected with anti-V5 SV5- Pk1 MAb (Thermo) or with HRP conjugated anti-V5 rabbit PAb (Bethyl). Directly conjugated anti-HA mouse IgG1, clone 16B12 (Life Technologies) and anti-V5 FITC clone SV5-Pk1 (Thermo) were used for confocal microscopy. The FLAG epitope tag was detected with either anti-FLAG M2 MAb or anti-FLAG M1 MAb (Sigma) specific for FLAG at the free N-terminus. Anti-calnexin, anti-ERGIC-53/p53 and GM130 (C-terminal) rabbit PAbs were obtained from Sigma. The anti-B5 rat MAb 19C2 (82) and anti-L1 rabbit PAb (313) were described previously.

3.4.4 Western blotting

Cells were harvested and lysed in 2 x SDS sample buffer added directly to the cell monolayer. Cell lysates were disrupted in a cup sonicator and heated to 95 °C for 10 min. Equal volumes of lysates were analyzed by SDS-PAGE using a 4–12% Tris–glycine gel and 1 x Tris–glycine SDS running buffer (Invitrogen) at 125V for 2 h. Samples were transferred via a semi-dry transfer (Invitrogen) and nitrocellulose membranes were blocked in 5% milk in Tris-buffered saline with 0.1% Tween-20. Antibodies were incubated at a 1:1000 dilution in 5% milk overnight. Proteins used for Western blots were detected using anti-mouse and/or anti-rabbit secondary antibodies conjugated to IRdye 680 or 800 and visualized using a LI-COR Odessey

infrared imager (LI-COR Biosciences, Lincoln, NE). For visualization of the anti-FLAG M1 antibody, goat anti-mouse HRP secondary (KCL, diluted 1:10,000) was visualized using chemiluminescence (ECL, Thermo).

3.4.5 Glycosidase treatment of cell lysate

HeLa cells (2.5×10^5) were washed in phosphate-buffered saline (PBS) and lysed in 75 ml of 50 mM Tris pH 7.0, 150 mM NaCl, and 0.5% NP-40 detergent on ice for 20 min. Nuclei were removed by low-speed centrifugation (400 x g, 5 min, 4 °C). The supernatants were adjusted to contain 0.5% SDS and 1% β-mercaptoethanol and heated at 95 °C for 10 min. PNGaseF (1500 U) or EndoH (1500 U; New England Biolabs) was added and incubated overnight at 37 °C. Samples were analyzed by SDS-PAGE and Western blotting.

3.4.6 Confocal microscopy

HeLa cells were grown on coverslips (12 Circle #1, Thermo) to approximately 80% confluency in 24-well plates and infected with CPXV219 mutants at multiplicity of 3 PFU/cell for the indicated amount of time at 37 °C. Cells were washed briefly in PBS and fixed in 4% paraformaldehyde in PBS. Cells were permeabilized in 0.1% Triton X-100 for 10 min and blocked in 10% fetal bovine serum in PBS for at least 1 h at room temperature. Antibody was incubated overnight at a 1:250 dilution in blocking buffer at 4 °C, washed in PBS, and incubated with secondary (Life Technologies, Alexa-fluor mouse-488, rabbit-594) at a 1:250 dilution in blocking buffer for 4–18 h. Cell nuclei were stained with 4′ , 6-diamidino-2-phenylindole, dihydrochloride

(DAPI, Invitrogen) 1:1000 in H_2O for 30 min, washed in PBS, mounted to glass slides with a drop of prolong gold anti-fade mounting media (Invitrogen) and viewed with a confocal microscope.

3.4.7 IP analysis

HeLa cells were infected at a multiplicity of 5 PFU per cell for 24 h and harvested in lysis buffer containing 1% NP-40, 50 mM Tris– HCl, 150 mM NaCl, 100 ml EDTA and complete protease inhibitor (Roche) and allowed to proceed at 4 °C for 30 min. The lysates were cleared by centrifugation at 1600 rpm for 15 min at 4 °C. IP was carried out overnight using 2–4 mg of either anti-V5 or anti-HA MAb in the presence or absence of 0.4% SDS using 15–25 ml of magnetic protein G Dynabeads (Invitrogen). After incubation, the beads were washed in PBS containing 0.5% Tween-20 and resuspended in 2x SDS sample buffer (0.125 M Tris–HCl, pH 6.8, 4% SDS, 0.005% Bromophenol Blue, and 20% glycerol) with 5% β-mercaptoethanol (Sigma), heated to 95 °C for 10 min, and analyzed by Tris–glycine SDS-PAGE.

3.4.8 Biotinylation of extracellular proteins

HeLa cells were infected with epitope-tagged CPXV at a multiplicity of 10 PFU per cell for 18 h, washed in PBS, labeled with 0.5 mg/ ml of a non-membrane permeable biotin (NHS-SS-Biotin, Thermo), washed to remove excess biotin, quenched by 10 min wash in 2.5% fetal bovine serum in EMEM, and incubated in lysis buffer containing 10 mM Tris–HCl, 10 mM NaCl, 5 mM MgCl, 1% Triton X-100, 0.5% sodium deoxycholate, and 0.5% NP-40 at 4 °C for 30 min. Lysates were incubated

with 15–25 ml of Neutravidin agarose beads (Thermo) and washed. The beads were treated with 2 x SDS sample buffer with 5% β-mercaptoethanol (Sigma), heated to 95 °C for 10 min, and analyzed by Tris–glycine SDS-PAGE and Western blotting.

3.4.9 Intranasal infection model

All experimental procedures involving mice were approved by the National Institutes of Allergy and Infectious Disease Animal Care and Use Committee and carried out in a humane manner. Female BALB/c and CAST/EiJ mice were purchased from Taconic Biosciences and Jackson Laboratory, respectively. Animals were kept in a clean environment in sterile microisolator cages. Groups of 5 BALB/c or CAST/Eij mice were anesthetized with isofluorane and inoculated in a single nostril with a 10 ml suspension of sucrose-cushion purified virus. The infection inoculum was titered by plaque assay to confirm dosages. Mice were weighed daily following infection and euthanized if reached 70% of their initial body weight in accordance with NIAID Animal Care and Use protocols. All experiments were performed in an animal biosafety level 2 (ABSL2) suite with approval of the NIAID Animal Care and Use Committee.

Chapter 4: A homolog of the variola virus B22 membrane protein contributes to ectromelia virus pathogenicity in the mouse footpad model[2]

4.1 Summary

Most poxviruses encode one or more homologs of a 200,000-kDa membrane protein originally identified in variola virus. We investigated the importance of the ectromelia virus (ECTV) homolog C15 in a natural infection model. In cultured mouse cells, the replication of a mutant virus with stop codons near the N-terminus (ECTV-C15Stop) was indistinguishable from a control virus (ECTV-C15Rev). However, for all doses injected into the footpads of BALB/c mice, there was less mortality with the mutant. At 1,000 PFU all mice survived ECTV-C15Stop infection, whereas none survived ECTV-C15Rev. Similar virus loads were present at the site of infection with mutant or control virus whereas there was less ECTV-C15Stop in popliteal and inguinal lymph nodes, spleen and liver indicating decreased virus spread and replication. Decreased spread was evidently not due to an intrinsic viral function of C15 as the survival of infected mice was dependent on host CD4+ and CD8+ T cells.

---

[2] Adapted in part from: **Reynolds, S. E., Earl, P.L., Moore, I., Moss, B**. A homolog of the variola virus B22 membrane protein contributes to ectromelia virus pathogenicity in the mouse footpad model. Manuscript submitted for publication

4.2 Introduction

Poxviruses are large double-stranded DNA viruses that infect a wide variety of hosts. Within the chordopoxvirus subfamily are two obligate human pathogens (296): molluscom contagiosum virus, which causes a localized skin disease in young children and more extensive lesions in immunodeficient individuals, and variola virus (VARV), the causative agent of smallpox and member of the genus orthopoxviridae (OPXV). Other OPXVs can infect humans including the smallpox vaccine vaccinia virus (VACV), cowpox virus (CPXV), and monkeypox virus (MPXV). Host range can be broad as in the case of CPXV, which infects voles, mice, cats, elephants and humans, to the very limited ranges of VARV, camelpox virus and ectromelia virus (ECTV), an OPXV that infects only mice (16, 296).

ECTV, the causative agent of mousepox, is unique among OPXVs because it is the only virus extensively studied in a natural host: the laboratory mouse (102, 131, 283). Mousepox has emerged as a valuable model for the study of OPXV pathogenicity as it causes a well-characterized smallpox-like disease (108, 109). Mouse genetic components that influence the immune response and susceptibility to mousepox have been identified and an early and strong type 1 immune response is key for survival (131, 191).

Poxvirus genomes are organized with conserved, essential genes located centrally while more variable genes, often involved in host range determination and virus-host interactions, are located near the ends (297). Many of these viral immune modulators have been studied during VACV infection revealing a wealth of

information about their roles (145); however, the matched ECTV/mouse model provides the opportunity to study these proteins in the context of a natural infection. One putative immune modulator is the VARV B22 protein and its homologs found in representatives of most poxviruses (the one exception being parapoxviruses) and all OPXV except VACV. The presence of homologs in salmon gill poxvirus, the deepest member of the chordopoxvirus subfamily indicates that the gene was acquired early in poxvirus evolution (12). The presence of multiple copies in some poxviruses and extensive sequence divergence between genera are consistent with a long evolutionary history and host adaptation. The B22 family is also notable for comprising the largest size poxvirus proteins. The gene encoding the CPXV homolog of the B22 protein (CPXV219) is located near the right end of the genome and encodes a protein of 1,919 amino acids. The protein is expressed early in infection, has a signal peptide and transits the secretory pathway where extensive glycosylation and proteolytic cleavage occur prior to insertion into the plasma membrane (314). The MPXV homolog (MPXV197) has similar properties (309). The roles of CPX219 and MPXV197 have been studied in mice and rhesus macaques, respectively. In mice, the absence of CPXV219 does not influence CPXV pathogenesis even in those that are more susceptible to OPXV infections than standard inbred laboratory strains (314). Although MPXV primarily infects African rodents, the absence of MPXV197 results in a milder disease with accelerated T cell responses and less T cell dysregulation than in wildtype MPXV infection of rhesus macaques (309). When examined *ex vivo* B22 homologs show a species-specific ability to inhibit T cell activation as measured by cytokine production (309). CPXV219 inhibits activation of

human but not mouse T cells (309); the latter is consistent with our finding that deletion of the gene does not affect CPXV virulence in mice (314).

The species-specificity of B22 homologs makes the mousepox model attractive for examining their role during poxviral disease in a natural host. C15, the ECTV homolog of B22 has an amino acid identity of 92, 91 and 83% with the corresponding CPXV, VARV and MPXV proteins, respectively. An ECTV mutant that does not express the C15 open reading frame was constructed and found to reduce mortality in mice susceptible to mousepox. At high doses of the C15 deletion mutant, the viral load in critical organs including the liver and spleen were reduced compared to wild type virus. Depletion studies showed that T cells were critically important for resistance of mice to the C15 mutant. The different effects in mice of deletion of B22 homologs from CPXV and ECTV highlight the importance of choosing the appropriate model to examine the role of viral immune modulators during disease.

4.3 Results

4.3.1 Construction and replication of ECTV C15 mutants

To facilitate the generation of C15 mutant viruses, we first used homologous recombination to replace the DNA encoding the N-terminal region of C15 in ECTV strain Moscow with the open reading frame for enhanced green fluorescent protein (GFP). The recombinant virus was isolated from plaques exhibiting green fluorescence and then used in a second round of recombination in which GFP was replaced with wild type C15 DNA to produce the revertant C15Rev virus used as a

control or C15 DNA with two stop codons near the N terminus to produce C15Stop virus. Plaques containing recombinant viruses were identified by absence of green fluorescence, clonally purified and verified by PCR and DNA sequencing. Stop codons in the same position were previously shown to prevent expression of CPX219 (314). When sucrose cushion purified virus stocks were analyzed for particle to plaque forming unit (PFU) ratio with the virus counter (ViroCyt) or for genome to PFU ratio by droplet digital PCR there was no difference between mutant and revertant viruses (data not shown).

To assess the impact of the C15 mutation on virus replication in tissue culture, mouse L929 cells were infected at a multiplicity of 3 PFU per cell. Samples were collected at various times post infection and virus titers determined by plaque assay on BS-C-1 cells. There were no observed differences in the rates or yields of virus replication in mouse L929 cells (**Fig. 4.1**) or of the plaque sizes on monkey BS-C-1 cells (data not shown).

4.3.2 Mortality following footpad infection of BALB/c mice

Footpad inoculation causes severe disease in susceptible mice and is considered to be the route of ECTV infection that most closely mimics natural spread (121). To determine whether C15 expression influences the pathogenicity of ECTV, we infected BALB/c mice in the hind footpad with C15Rev or C15Stop at doses ranging

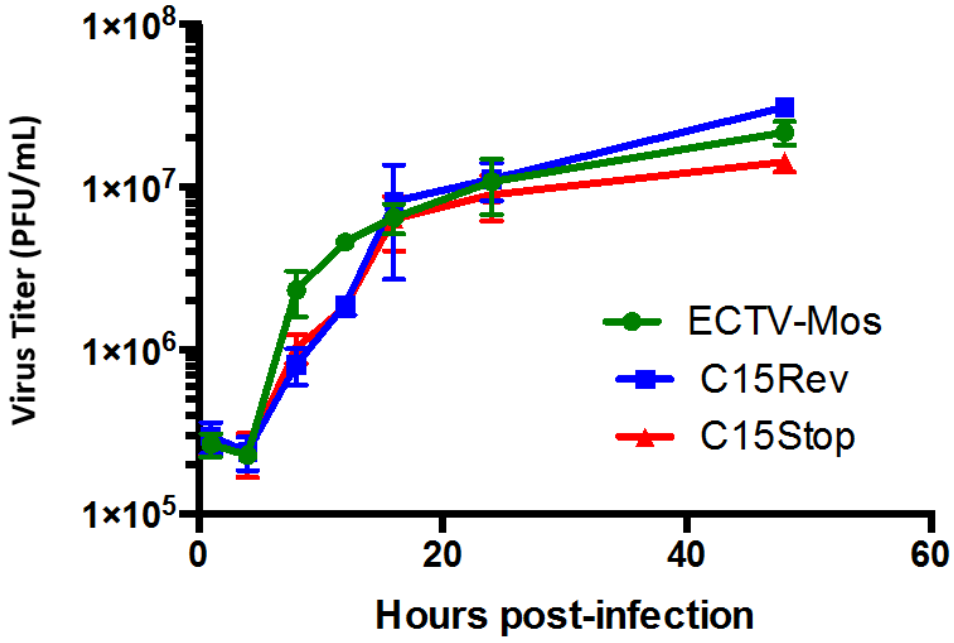

Figure 4.1 C15 expression was not required for replication of ECTV in tissue culture Mouse L929 cells were infected with 3 PFU per cell of ECTV-Mos, C15Rev or C15Stop. Cells and growth media were harvested at various times post infection and virus titers were determined by plaque assays on BS-C-1 cells. Infections were done in triplicate and standard deviations shown by error bars.

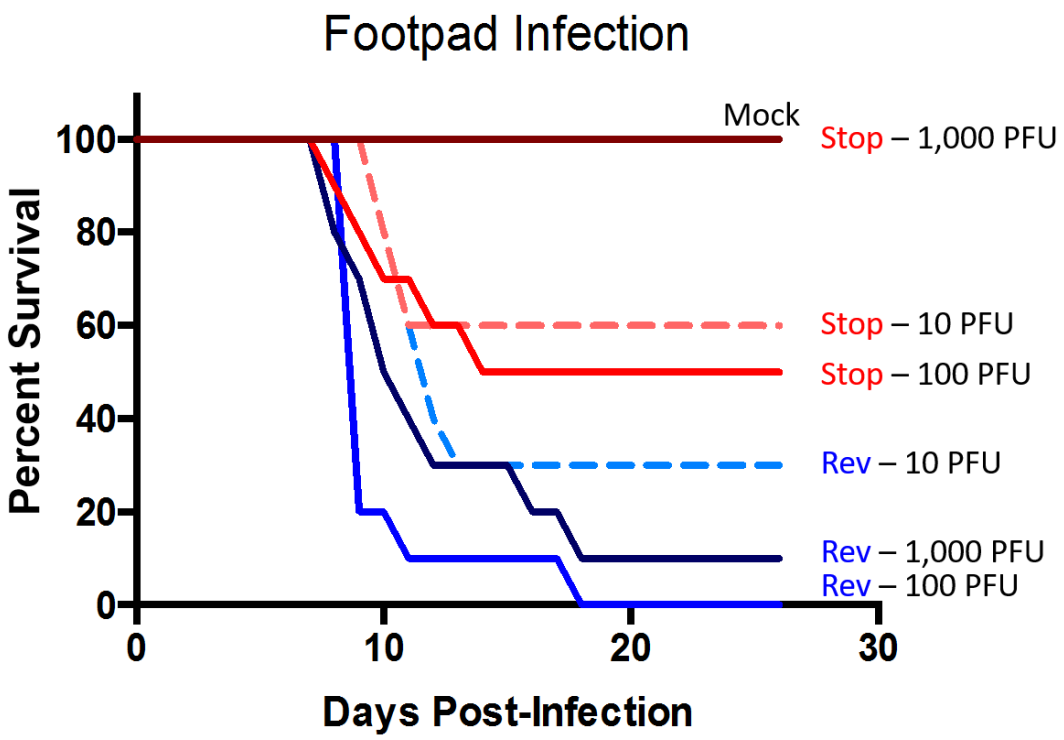

Figure 4.2 Absence of C15 reduces mortality after ECTV footpad infection

Female 8-week old Balb/c mice were injected in the left hind footpad with 10 µl of C15Rev or C15Stop virus at doses of 10, 100 or 1,000 PFU per mouse. Shown are the combined results of two independent experiments each with five animals per dose. Endpoint was determined by natural death, or in 3 cases by the veterinarian's determination of moribund state, followed by euthanasia.

from 10 to 1,000 PFU per mouse. Following footpad infection, death occurred primarily between days 9 and 12 with a few animals succumbing to the disease as late as day 18. No matter the viral dosage, infection with C15Stop resulted in less death than infection with C15Rev (**Fig. 4.2**). Paradoxically, mice died after 10 or 100 PFU of C15Stop but not 1,000 PFU. This result was consistent over multiple experiments and the absence of mortality was observed even at 20,000 PFU/mouse (data not shown).

Animals were scored based on their movement and the conditions of the coat, eyes and limb and the highest total scores at any time (**Fig. 4.3A**). Some animals died early with low scores while others survived longer and attained higher scores. The high scores of animals that were infected with 1,000 PFU/mouse of C15Stop virus and survived were similar to those of animals that were infected with C15Rev and succumbed.

Swelling of the infected foot occurred in most mice between days 5 and 7 and increased for several more days in surviving animals (**Fig. 4.3B**). On day 10, the swelling was significantly greater in the mice infected with C15Stop than with C15Rev. At later times, there were too few surviving animals infected with C15Rev for meaningful comparison.

4.3.3 Decreased virus dissemination in mice infected with C15Stop

To determine the basis for the greater mortality in mice infected with C15Rev than with C15Stop we examined organs known to be key in the spread and pathogenesis of ECTV: the foot (site of infection), popliteal and inguinal lymph nodes, spleen and

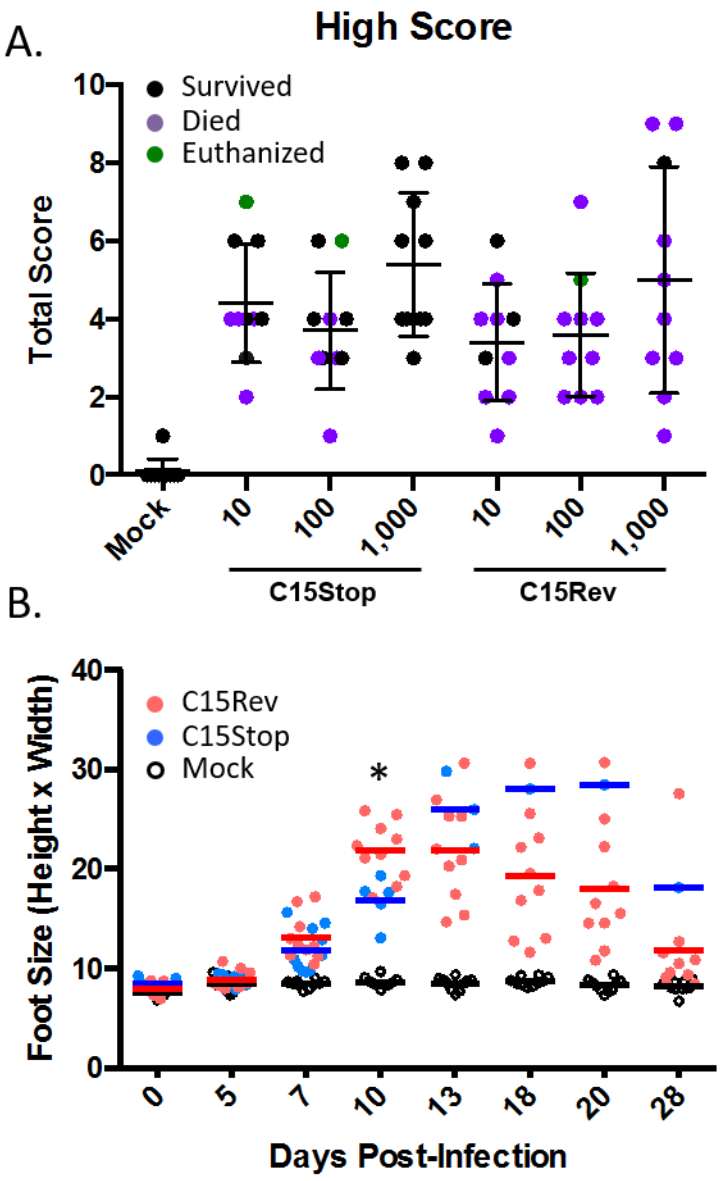

Figure 4.3 Effect of virus dose on disease symptoms

(A) Animals from Fig. 2 were scored for disease symptoms daily following infection. Movement and condition of the coat, eyes and limb all contributed to the score. The highest total score achieved at any time during disease course by each animal was plotted with those animals who survived shown in black, animals that died in purple,

and those euthanized in green. The bars represent the median and one standard deviation above and below. (B) For all animals in Fig. 2 footpad swelling was determined twice weekly by measuring the width and height of swelling and the size was calculated by multiplying these values. On day 13 only three C15Rev animals remained, and on day 18 only one C15Rev animal remained. All five C15Stop animals survived. The bars represent the median values. On day 10 swelling was significantly (Mann-Whitney, *p = 0.0127) greater in the C15Stop animals.

liver. Twenty animals were infected with 1,000 PFU of C15Rev or C15Stop and 5 were sacrificed at each of 2, 4, 6 and 8 days post-infection. Organs were homogenized and virus titers determined. The titers in the foot increased from day 2 to day 8 but were similar to each other in mice infected with C15Rev and C15Stop indicating that differences in mortality were not due to differences in replication at the site of infection (**Fig. 4.4A**). The popliteal lymph node was the closest organ to the site of infection that was analyzed. At day 2 only one C15Stop infected animal had a measurable virus titer in the popliteal node, whereas all mice infected with C15Rev had detectable titers. Furthermore, on days 6 and 8 the virus titers of C15Stop animals in the popliteal lymph node were less than C15Rev by approximately one log ($p < 0.01$, $p < 0.05$, respectively) (**Fig. 4.4B**). Infection of the inguinal lymph node was delayed compared to the popliteal but the pattern was similar: virus titers were detectable in two of five C15Rev infected animals on day 4 but not in C15Stop animals, followed by less in the C15Stop animals on days 6 and 8 ($p < 0.01$). Two animals infected with C15Stop still had no detectable virus in the inguinal lymph nodes on days 6 and 8, whereas C15Rev-infected animals had titers as high as 10^6 PFU/organ on day 8 (**Fig 4.4C**).

High virus loads in the spleen and liver are associated with death due to ECTV (115, 116). Following infection we detected virus in the spleen of C15Rev- and C15Stop-infected animals in similar amounts on day 4; however, on days 6 and 8 there was less virus in the spleens of C15Stop-infected animals ($p < 0.05$, $p < 0.01$, respectively) (**Fig. 4.4D**). In the liver the difference between the virus titers of animals infected with C15Stop and C15Rev was between four and five logs on day 8

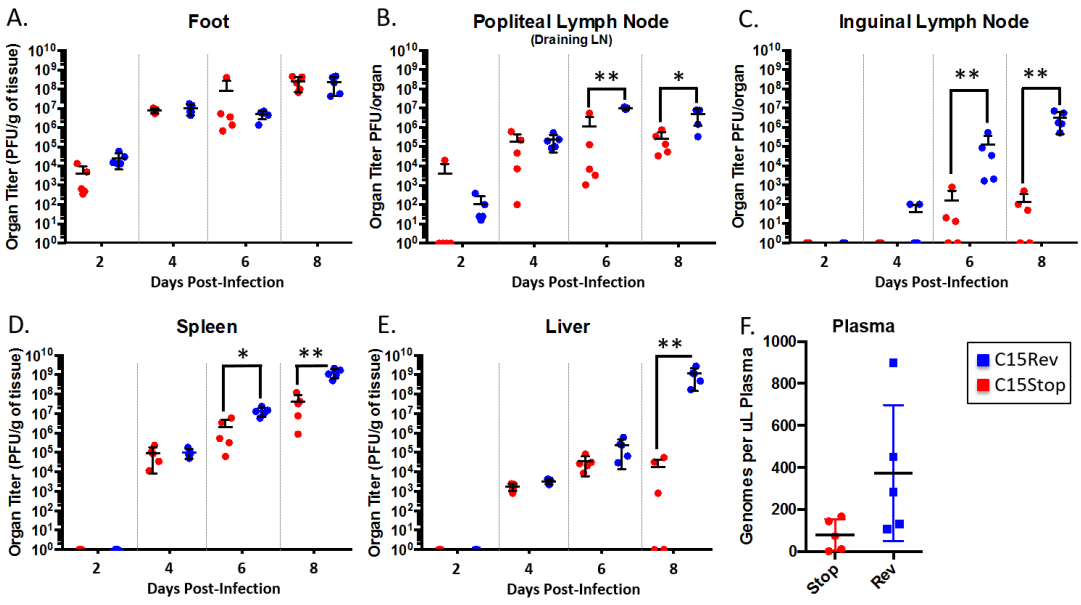

Figure 4.4 Absence of C15 reduces virus load

Female 8-week old Balb/c mice were infected in the footpad with 1,000 PFU of C15Rev or C15Stop and organs were collected on days 2, 4, 6 and 8. Organs were homogenized and virus was titered on BS-C-1 cells. Foot, spleen and liver are shown as PFU/gram of tissue and lymph nodes as PFU/organ. Significant differences by Mann-Whitney are shown, $p < 0.05$ (*) or $p < 0.01$ (**). Plasma from infected animals was collected, DNA was purified and genome copy number was determined through the use of digital droplet PCR. Genomes are reported in copy number per µl of plasma. ($p = 0.0952$)

($p < 0.01$) (**Fig 4.4E**). The number of viral genomes in the plasma was determined by digital PCR. There was a trend for more viral genomes in animals infected with C15Rev than C15Stop ($p = 0.095$) (**Fig 4.4F**). The differences in virus loads in organs of animals infected with C15Stop and C15Rev indicated better control of the spread and/or replication of ECTV in the absence of the C15 protein.

The high virus dose of 1,000 PFU showed the greatest difference in mortality between C15Rev and C15Stop, but also an unusual phenomenon whereby animals infected with lower doses of C15Stop had greater mortality than with higher doses (**Fig 4.2**). To investigate this further we determined virus titers on day 8 from animals that received 10, 100 or 1,000 PFU. Although the virus titers from the foot increased significantly with virus dose, they were similar for mice infected with C15Rev and C15Stop (**Fig 4.5A**). In contrast, the titers in the inguinal and popliteal lymph nodes decreased with increasing dose of C15Stop but were similar or increased with C15Rev (**Fig. 4.5B, C**). A trend to lower virus loads with increasing dose of C15Stop also occurred in the liver although the titers in the spleen were more constant (**Fig. 4.5D, E**). As in the lymph nodes, the amounts of virus in the spleens and livers of mice infected with C15Rev increased with dose (**Fig. 4.5D, E**). Overall, the results indicated that the decreased mortalities at high virus inocula were associated with decreased spread of C15Stop to the lymph nodes and internal organs.

4.3.4 Histological analysis of organs

Organs of mice infected with 1,000 PFU of C15Rev or C15Stop were examined histologically by staining with haemotoxylin eosin (H&E) and antibody to VACV,

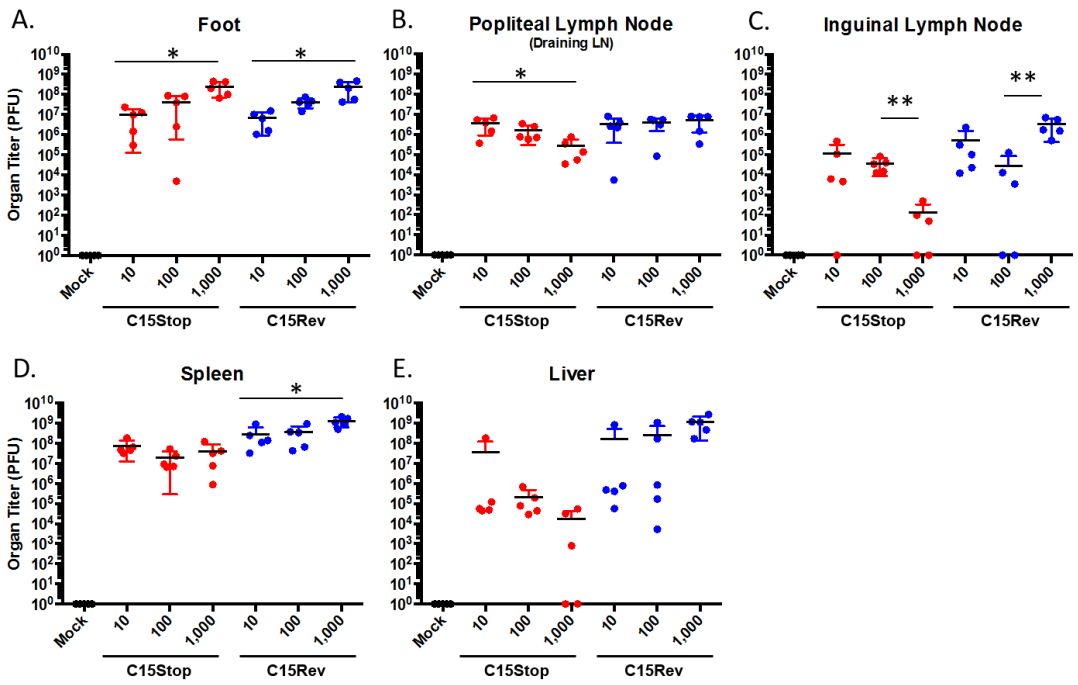

Figure 4.5 Effect on inoculum size on virus load in organs

Female 8-week old Balb/c mice were infected in the footpad with 10, 100 or 1,000 PFU of C15Rev or C15Stop and organs were collected on day 8. Organs were homogenized and virus titered on BS-C-1 cells. Foot, spleen and liver are shown as PFU/gram of tissue. Lymph nodes are PFU/organ. Statistics were performed using the Kruskal-Wallis (nonparametric) method with Dunn's multiple comparison correction. *=$p<0.05$ **=$p<0.01$.

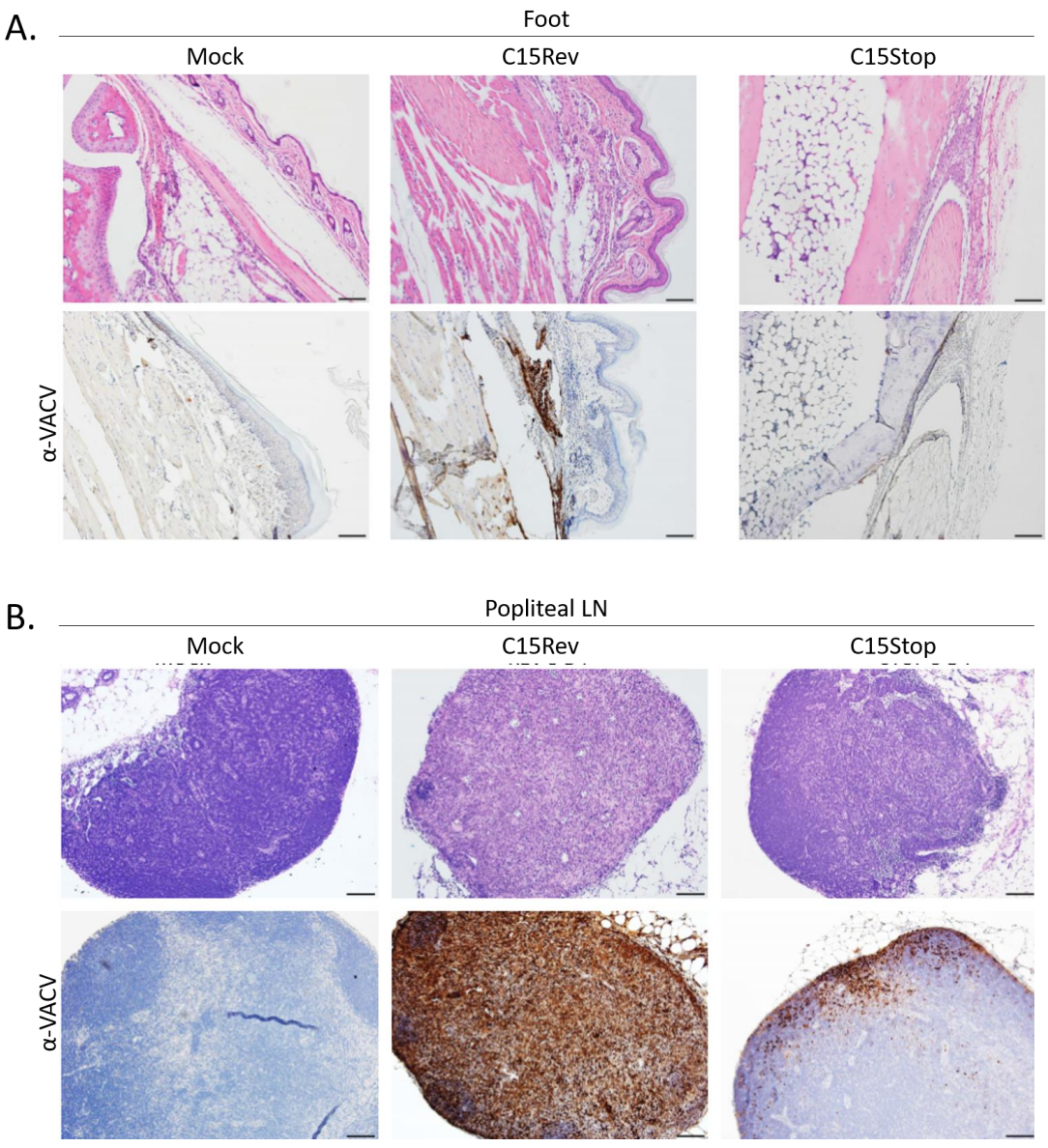
A.
Foot
Mock
C15Rev
C15Stop
α-VACV
B.
Popliteal LN
Mock
C15Rev
C15Stop
α-VACV

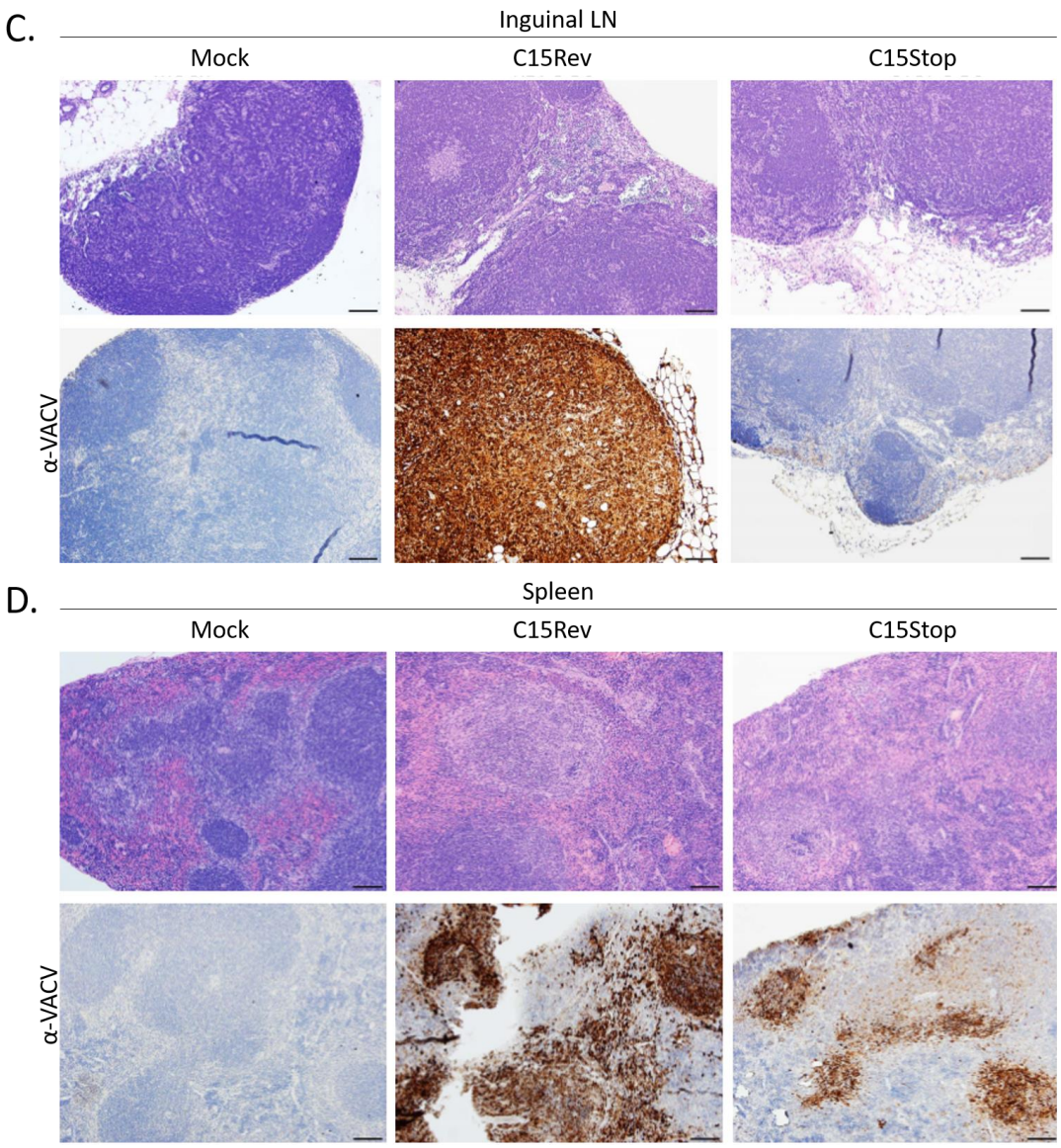

Figure 4.6 Histological analysis of organs

Photomicrographs display images of haemotoxylin and eosin (H&E) staining on top rows and immunohistochemistry utilizing anti-VACV antibody that recognizes ECTV on bottom rows. The foot (A) and popliteal LN (B) are shown 4 DPI, and the inguinal LN (C) and spleen (D) are shown 6 DPI. BALB/c mice infected via the footpad with

C15Rev, C15Stop or uninfected (mock) were sacrificed and organs were collected at various DPI. Representative images are shown here. (A) The foot tissue appears normal but the C15Rev infected animals had increased virus within the tissue. (B) The popliteal LN has severe inflammation and necrosis in the C15Rev infected animals, but not C15stop, and increased virus throughout the LN of C15Rev infected animals. In the (C) inguinal LN 6 DPI there was little inflammation or necrosis of the LN, but increased viral staining in the C15Rev infected animals. (D) The spleen appears inflamed in all infected animals, however, the viral replication foci are larger and more numerous in the C15Rev infected animals at both 4 (not shown) and 6 DPI.

which cross-reacts with ECTV. The sections in **Fig. 4.6** show popliteal lymph nodes and the infected foot on day 4 and inguinal lymph node and spleen on day 6. At each time the infection by C15Rev was more advanced than that of C15Stop consistent with the data on virus loads.

4.3.5 Cytokine levels in blood following infection

The type of immunological response mounted against ECTV infection can have a strong impact on the likelihood of survival. NK cells and CTLs have been implicated as essential for survival along with a strong and early production of IFN-γ, IL-2 (315), IL-12 (316) and TNF-α (315); all components of a type 1 immune response. Characteristics of a type 2 immune response such as IL-4 (317), IL-5, IL-6 (214), and IL-13 (317) are more commonly observed in mice that succumb to mousepox infection. Granulocyte colony-stimulating factor (G-CSF) is important for neutrophil production (318) and increased in susceptible CAST/EiJ mice following MPXV infection, as were IL-6, CXCL1 (KC) and CXCL10 (IP-10) (319).

The levels of 25 cytokines and chemokines in plasma from BALB/c were compared after footpad infection with 1,000 PFU of C15Stop or C15Rev. For most of the cytokines the levels were similar in mice infected with the two viruses. Equal or higher amounts of IFN-γ, IL-12p40, IL-6, G-CSF, CXCL1 and CXCL10 were detected in the plasma of C15Rev infected mice, however, only the increase in CXCL10 had high statistical significance (**Fig. 4.7**). Higher amounts of IL-2 and IL-5 were found in C15Stop infected animals, but only the increase in IL-5 was significant. It is possible that these differences are a result rather than the cause of the

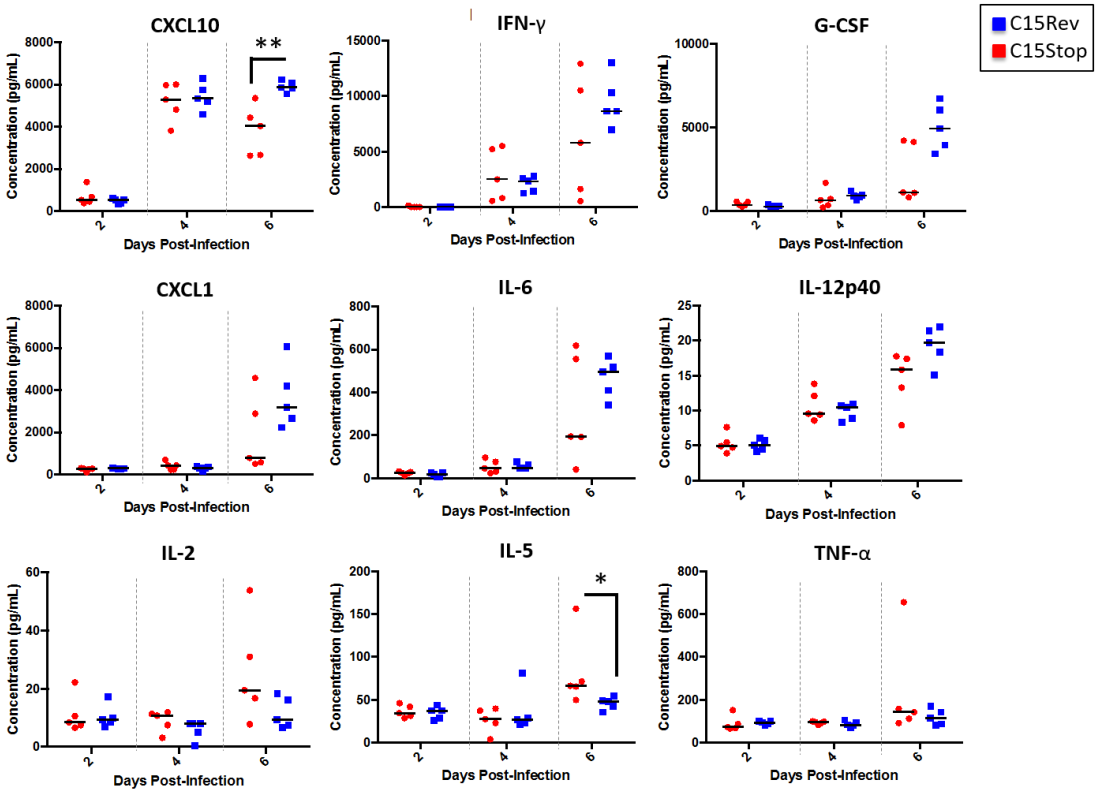

Figure 4.7 Changes in blood cytokines in the absence of C15

Plasma from 1,000 PFU footpad infected animals from Fig. 5 was used to examine blood cytokine levels for a panel of 25 cytokines. CXCL10 was present at significantly lower levels at day 6 following C15Stop infection (Mann-Whitney $p < 0.01$). IL-5 was significantly increased in C15Stop infected animals (Mann-Whitney $p < 0.05$). Other key cytokines of the immune response were generally at equivalent or reduced levels in the absence of C15, including IFN-γ, GCS-F, CXCL1, IL-4 and IL-12p40. IL-2 may be slightly increased in the absence of C15. Bars indicate median values.

greater virus loads in mice infected with C15Rev than C15Stop.

4.3.6 T cells are required for survival of mice following infection with C15Stop

There are two general possibilities to account for the attenuation of C15Stop virus. One is that C15 directly enhances dissemination of ECTV and the other is that C15 inhibits the host response to ECTV. If the former were true, then C15Stop might still be attenuated even if CD4+ or CD8+ T cells were depleted. Depletion was achieved with CD4- and CD8-specific mouse MAbs administered by intraperitoneal injection several days prior to infection. A non-targeting antibody of the same isotype was used as a control. At the time of infection, the extent of depletion of CD4 and CD8 cells was demonstrated in an independent experiment to be over 99% (data not shown). The footpads of 5 mice were inoculated with 1,000 PFU of C15Rev or C15Stop virus in each of two separate experiments. 70% of mice that received the control MAb succumbed to C15Rev, but only one animal infected with C15Stop died very late after infection on day 23 (**Fig 4.8**). In contrast, depletion of either or both CD4+ and CD8+ T cells accelerated the death of both C15Stop and C15Rev virus (**Fig. 4.8**). Thus, the decreased virulence of C15Stop was dependent on a functioning immune system.

4.3.7 Mortality following intranasal infection

To examine if the absence of C15 influences pathogenicity following different routes of infection we infected BALB/c mice intranasally with C15Rev or C15Stop (**Figure 4.9)**. Ten animals were observed over two independent experiments for changes in disease course, time to death, and overall survival. At the highest dose of 100 PFU

per animal we observed very little difference with 70% and 80% mortality in C15Stop and C15Rev, respectively. At lower doses there was distinctly less mortality following infection with C15Stop having 20% mortality at both doses, and C15Rev causing 60% and 80% mortality at 1 and 10 PFU, respectively. At 10 PFU this difference was significant (Mantle-Cox $p = 0.2222$). The LD_{50} of C15Rev was determined to be less than 1 PFU, for C15Stop it was 15.8 PFU. These results suggest that C15 influences pathogenesis in multiple routes of infection, reducing the lethality at low doses following intranasal infection, similar to the results seen following footpad infection. The recovery observed at very high doses following footpad infection was not observed following intranasal infection.

4.3.8 Intracellular cytokine staining of IFN-γ in splenocytes

In an attempt to evaluate the overall population of T cells and IFN-γ producing NK cells spleens of infected animals were collected at 3, 5, and 7 DPI. Spleens were homogenized and the red blood cells were digested away. A population of cells were labeled by antibodies against cell-type identifying surface receptors CD3 (lymphocytes), CD19 (B cells), CD4 (T cells), CD8 (T cells), and CD49 (NK cells). **Figure 4.10A** shows the total number of viable cells from each condition. Note the inflammation as represented by an increase in cell number as compared to mock at day 3. By 7 DPI the C15Rev infected spleens are particularly unhealthy and have reduced numbers of viable cells.

In **Figures 4.10B, C, and E** the percentage of CD8+ T cells, NK cells and CD4+ T cells are shown. CD8+ T cell levels remain between 25-35% of CD3+ cells

throughout the duration of the experiment. NK cells peak at approximately 10% at 5 DPI and are roughly equivalent following infection with both viruses. On 3 and 7 DPI there is roughly 6% NK cells in the C15Stop infected spleens, and only 4% in the C15Rev infected. Like the CD8+ T cell levels, CD4+ T cells remain around 60% of CD3+ cells throughout the experiment.

Another population of splenocytes isolated were stimulated through direct infection with C15Stop virus. The C15Stop virus was used in the stimulation of all conditions to prevent the action of the C15 protein from preventing the activation of immune cells. Following overnight stimulation cells were again labeled for cell surface receptors and following fixation and permeabalization, for IFN-γ. In **Figure 4.10D** the levels of IFN-γ of NK cells is shown with the peak also occurring 5 DPI.In the C15Stop infected animals a little over 1.5% of NK cells were stimulated to produce IFN-γ, but in the C15Rev this was only about 1%. In **Figure 4.10F** we see a less pronounced effect on IFN-γ of CD8+ T cells. Although there is a difference of roughly 0.3% and 0.15% between C15Stop and C15Rev, respectively, these are barely over the background of 0.1% IFN-γ producing cells from mock infected animals. Detection increases to about 0.6% by 7 DPI but there is less difference between viruses.

Together these data do not demonstrate a large change in the population of immune cell subsets of infected spleens, or the ability of these immune cells to be stimulated *ex vivo* by ECTV in the presence of absence of C15.

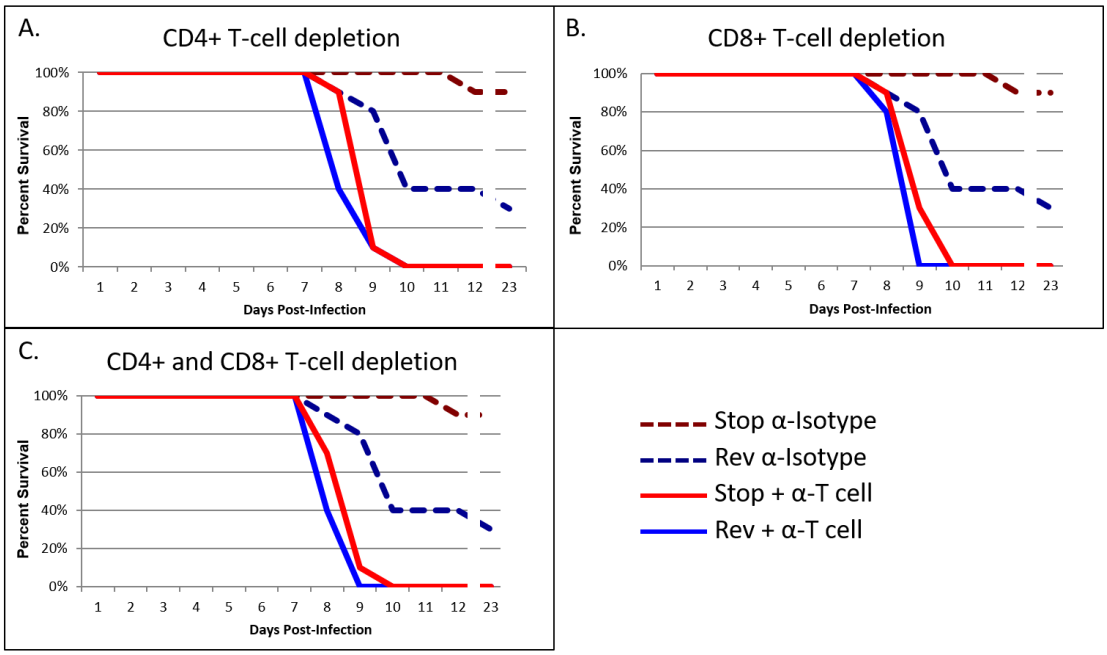

Figure 4.8 Effects of depletion of CD4+ and/or CD8+ T cells on survival

Female 8-week old mice were injected in the intraperitoneal cavity with isotype control antibody, anti-CD4, and/or anti-CD8 antibody at three and five days prior to infection. Infections were performed by injecting the left hind footpad with 10 µl of 1,000 PFU of C15Rev or C15Stop virus. Endpoints were determined by natural death, or in a few cases by determination of moribund status, followed by euthanasia. Combined data from two independent experiments each with five animals per group.

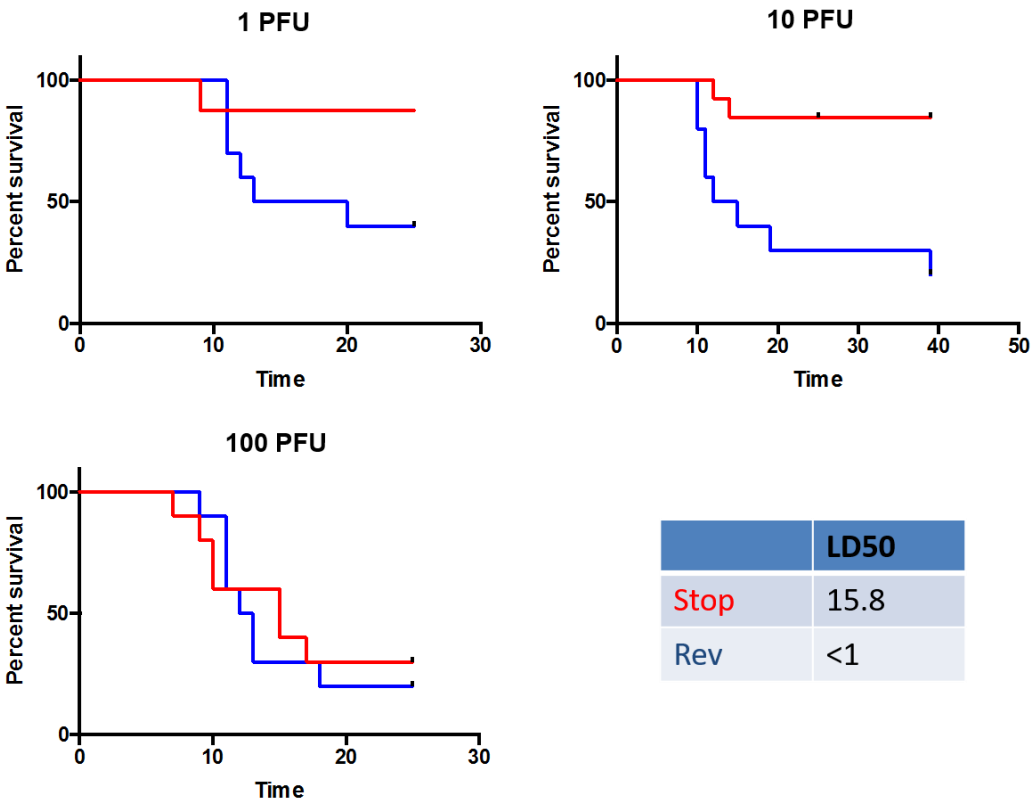

	LD50
Stop	15.8
Rev	<1

Figure 4.9 Mortality following intranasal infection

Ten BALB/c mice were infected intranasally and observed across two independent experiments. Infectious doses ranged from 1 to 100 PFU per mouse. At the highest dose of 100 PFU, animals succumb to mousepox in equal numbers and at the same time. However, at lower doses of 1 and 10 PFU there was less observed mortality in the absence of C15. This difference was significant at 10 PFU (Mantel-Cox $p = 0.2222$). The LD_{50} of C15Rev was less than 1 PFU per animal, and for C15Stop was 15.8 PFU per animal.

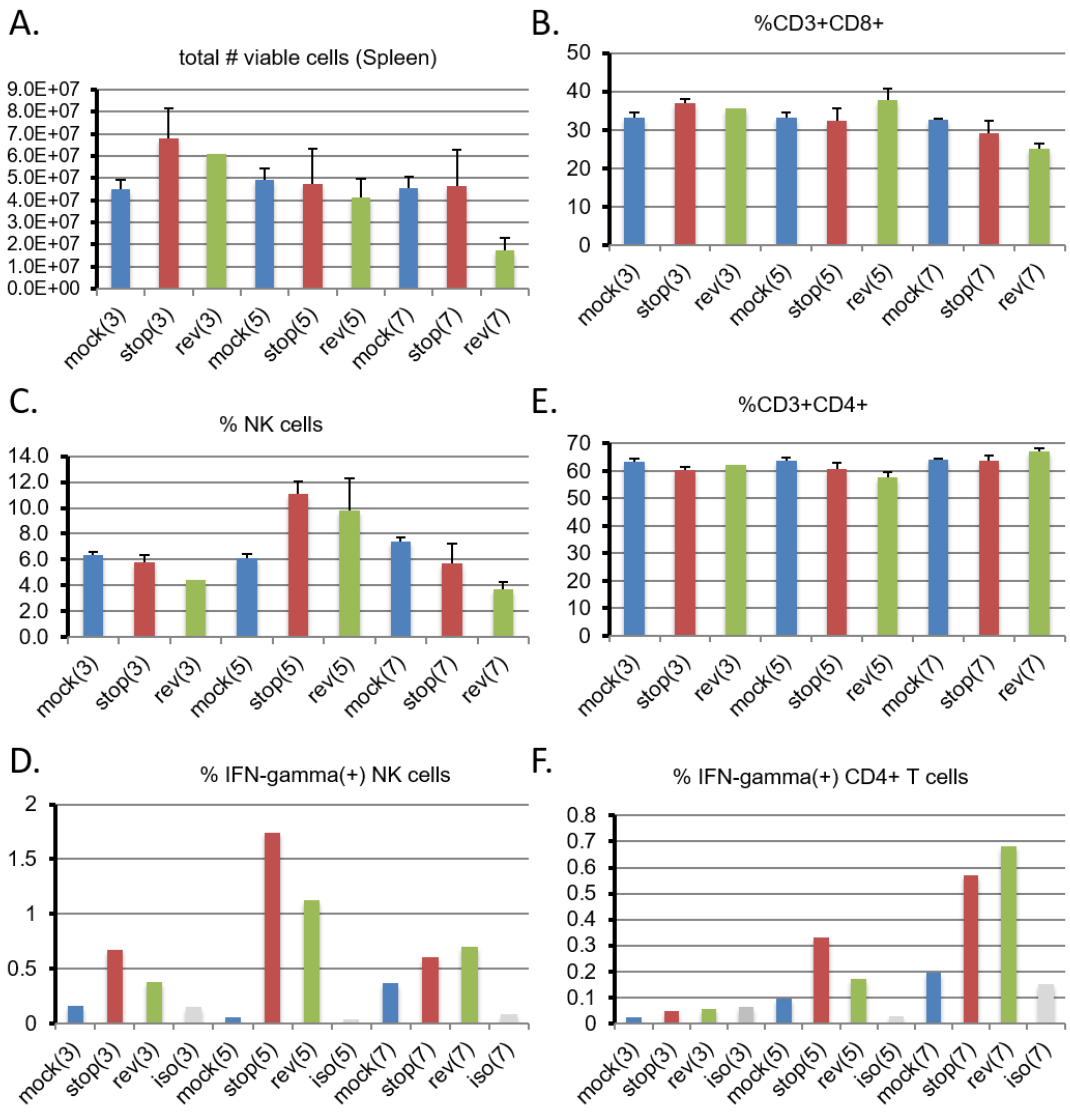

Figure 4.10 Minimal changes in IFN-γ staining of cells isolated from the spleens of infected mice.

Animals were infected via the footpad with 1,000 PFU of either C15Rev or C15Stop virus. Mock infected animals received only PBS+0.05% BSA. Animals were sacrificed 3, 5, and 7 DPI as labeled in parenthesis and spleens were harvested in RPMI on ice. Homogenates were treated to digest red blood cells and labeled with antibodies against extracellular markers. Cells were fixed and permeabilized prior to

labeling for intracellular IFN- γ. In (A), the total number of viable cells per spleen are shown. The percent of viable cells decreases 7 DPI, especially in the C15Rev infected animals. In (B), (C), and (E) the percent of viable cells that are CD8+ T cells, CD49+ NK cells, and CD4+ T cells, respectively, are shown. There is no detectable levels of IFN-γ in CD8+ T cells following stimulation via C15Stop infection. In (D), the levels of IFN-γ staining of NK cells is shown. At 5 DPI the highest levels of IFN-γ are observed, and about 50% higher in the C15Stop animals. In (F) the IFN-γ staining levels of CD4+ T cells are shown. These levels increase through 7 DPI. There is approximately 50% more IFN-γ staining at 5 DPI, but at only very low levels. At 7 DPI there appears to be very little difference between viruses. These data have not been repeated.

4.4 Discussion

The replicative ability of VACV, which lacks a B22 homolog, as well as CPXV (314) and MPXV (309) mutants had suggested that the protein is not required for an intrinsic viral function and likely has a role in host defense. However, the presence of B22 proteins in most poxviruses would mean that the host function has been conserved in fish, reptiles, birds and mammals. Nevertheless, deletion of the CPXV homolog did not attenuate pathogenicity in a mouse model (314). The latter hypothesis fit with the finding that the B22 proteins exhibits species specificity for inhibition of T cell activation and more specifically that the CPXV homolog does not inhibit murine T cells (309). Taken together, these results encouraged us to determine

whether the absence of the B22 homolog would attenuate pathogenicity of a poxvirus in a natural host e.g. footpad infection of mice by ECTV (121).

As expected from previous studies with CPXV and MPXV, the absence of C15 expression did not affect the replication of ECTV in cultured mouse cells and the particle to PFU ratios of control and mutant viruses were similar. However, greater mortality occurred at all doses tested when control virus was injected in the footpads of BALB/c mice compared to the C15 mutant. However, to our surprise mortality did not correlate with dose of the C15 mutant; at 1,000 PFU or more there was no mortality whereas approximately 50% of the mice died at doses of 10 to 100 PFU. To follow the course of infection, we determined the virus loads over time in the feet, popliteal and inguinal lymph nodes, liver and spleen. At the 1,000 PFU dose, in which all C15Rev mice died and all C15Stop mice survived, the titers of both viruses increased to the same extent in the foot indicating similar replication at the site of infection. However, there was significantly less C15Stop virus in the lymph nodes and internal organs compared to C15Rev accounting for the reduced mortality. For C15Rev the virus titers in the foot and organs generally increased with virus dose. The virus titers also increased with dose in the foot following infection with C15Stop; however, the titers generally decreased with dose in the organs. Taking the data on mortality and virus titers together, the attenuation of C15Stop appears to be due to decreased spread from the foot to the lymph nodes and beyond.

Since the B22 homologs localize to the plasma membrane, it seemed possible that one role of the protein is to enhance virus spread directly. Alternatively, the protein may only be involved in immune defense. Such a role was suggested by

inhibition of T cell activation in the MPXV model (309). If the role of the C15 protein is to prevent T cell activation, then one might expect the virulence of C15Rev and C15Stop to be similar if T cells were depleted. On the other hand, if the role of C15 is to enhance virus spread directly, then there might still be a difference in virulence after T cell depletion. We found that the mortality increased to 100% when either CD4+ or CD8+ T cells were depleted, indicating that T cells provide important protection against C15Stop. Although it remains to be directly demonstrated, a greater T cell response could explain the reduced spread and mortality of C15Stop compared to C15Rev. Along the same lines, the innate immune response might develop more rapidly with higher doses of C15Stop thereby reducing spread from the foot to the lymph nodes or preventing virus replication there leading to the paradoxical effect of virus dose and survival.

The present study highlights the importance of matching virus with a natural host when studying the potential role of a viral immune modulator. Nevertheless, further studies are needed to determine why the B22 homolog enhances virulence of ECTV but not CPXV. The most interesting possibility is that the ECTV homolog is better adapted to interact with the mouse immune system, even though they are 92% identical in amino acid sequence. Alternatively, the difference may be due to viral genome backgrounds e.g. CPXV has many more host defense genes and there may be redundancy. Still a third possibility is the route of infection, which was intranasal in the CPXV study and footpad in the present.

4.5 Materials and Methods

4.5.1 Cells

BS-C-1 cells were maintained at 37°C and 5% CO_2 in modified Eagle minimal essential medium (EMEM, Quality Biologicals, Inc., Gaithersburg, MD) supplemented with 10% fetal bovine serum, 2 mM L-glutamine, 10 U of penicillin/ml, and 10 mg of streptomycin/ml. HeLa and L929 cells were propagated in Dulbecco's modified Eagle's medium supplemented with 10% fetal bovine serum and antibiotics as described above.

4.5.2 Ectromelia virus

Ectromelia virus Moscow Strain was obtained from ATCC (VR-1374) and passaged. A clonal isolate was derived and shown to replicate equivalently to the uncloned parental virus in tissue culture, and to have similar pathogenicity via footpad infection (data not shown). Purified virus was prepared as previously described (320). Briefly, BS-C-1 cells were infected with 1 PFU/cell for 48 to 72 h and cells were obtained by centrifugation, Dounce homogenized, and purified through a 36% sucrose cushion. The pellet was suspended in 1 mM Tris-HCl for use in animal experiments. All viruses were tested for bacterial contamination by removing a small volume, inoculating in LB broth at 37°C with shaking, and observing for turbidity. All virus preparations were negative.

4.5.3 Generation of Recombinant Viruses

Recombinant viruses were constructed from the ECTV-Mos clonal isolate. DNA sequences used for homologous recombination were generated by overlapping PCR as previously described (314). In short, DNA from the C-terminal region of C15 was

amplified and used to flank the GFP open reading frame regulated by a VACV promoter, the unmodified C15 sequenve or a modified sequence containing two premature stop codons. To mutate the stop sequences the following primers were used with changes shown in bold: SR169.C15-R Stop 5'- GTA AG**C** TAT ATA GCC AGA GAT **T**AT TTC TGT AAA TTC ATG ATT G -3' and SR170.C15-F Stop 5'- CAA TCA TGA ATT TAC AGA AAT **A**AT CTC TGG CTA TAT A**G**C TTA C -3'. The ECTV-C15GFP was created by transfecting C15GFP DNA with Lipofectamine 2000 (Invitrogen) into HeLa cells followed after 1 h by infection with ECTV-Mos. After 5 – 7 days incubation under 5% MethylCellulose-EMEM, virus was isolated from fluorescent plaques and then re-plaqued to clonal homogeneity. A similar procedure was used to derive C15Rev and C15Stop except that the ECTV-C15GFP was used as the parental virus and virus was obtained from non-fluorescent plaques. The recombinant DNA sequences for each virus were verified by PCR and sequencing. Viruses were propagated in BS-C-1 cells and released through three repeated freeze/thaw cycles. Samples were sonicated prior to each use and virus titers were determined in duplicate using BS-C-1 cells.

4.5.4 Kinetics of virus growth in tissue culture.

Mouse L929 cells were infected in triplicate at with 3 PFU/cell at 37°C in EMEM for 1 h, washed three times with fresh, warm EMEM to remove the inoculum, and incubated at 37°C. Cells and media were harvested at appropriate times post-infection, frozen and thawed three times and sonicated prior to titration on BS-C-1 cells. The cell monolayers were overlaid with 5% Methylcellulose-EMEM for 6 days and stained with 2% crystal violet.

4.5.5 Mice

All experimental procedures involving mice were approved by the National Institutes of Allergy and Infectious Disease Animal Care and Use Committee and carried out in a humane manner. Female BALB/c mice were obtained from Taconic Biotechnology (Germantown, NY). Mice were maintained in a clean environment in small, static filter-top microisolator cages within an isolated room of an animal biosafety level 3 suite in accordance with protocols approved by NIAID Animal Care and Use committee.

The virus inoculum was sonicated and diluted in phosphate buffered saline + 0.05% bovine serum albumin and titered by plaque assay after each infection to confirm dosage. Groups of 5 female BALB/c mice 6 to 8 weeks old were sedated with isoflurane. A 25-27 gauge needle attached to a 25 µl gastight syringe (Hamilton) was inserted into the right hind footpad in the middle of the walking pads 8 to 10 mm beneath the skin. Mice were monitored daily and euthanized if they were determined to be moribund in accordance with NIAID Animal Care and Use protocols.

4.5.6 Evaluation of disease and virus spread

To monitor the progression of disease, animals were observed daily and given a score ranging from 0 (healthy) to 3 (severely ill) for each of the following categories: coat condition, movement/activity, eye condition, and limb swelling/necrosis. Veterinarians independently observed animals and made the determinations when one was moribund accordance to NIAID Animal Care and Use protocols. Foot measurements were performed using digital calipers to measure the thickest part of the foot and width at the base of the toes. The area of swelling was calculated by

multiplying these measurements.

Blood was collected from the mandibular vein in polypropylene tubes with EDTA and processed by centrifugation at 2,000 x *g* for 8 min to pellet cells; the plasma was aliquoted and stored at -80^{o}C. Animals were necropsied immediately after sacrifice and vital organs were collected including the inguinal and popliteal lymph node on the right side, the right hind foot, spleen and all lobes of the liver. Organs were placed in 1 to 2 ml of balanced salt solution containing 0.1% bovine serum albumin and stored at −80°C until use. Lymph nodes were Dounce homogenized and, other organs were homogenized with a GLH-1 mechanical grinder equipped with hard-tissue disposable probes and aerosol-proof caps (Omni International, Kennesaw, GA). After sonication, the homogenates were centrifuged for 10 s at 400 × g to remove cellular debris. Supernatants were aliquoted into fresh tubes and either frozen or used for virus titration by plaque assay on BS-C-1 cells.

Viral DNA was extracted through the use of the QIAamp MinElute Virus Spin Kit (Qiagen) according to the manufacturer's protocol and stored at -20 °C. Genome copy number was determined through droplet digital PCR (BioRad) according to the manufacturer's instructions. . Briefly, viral extracts from the MinElute spin kit were placed in a PCR plate with Evagreen supermix and primers targeting the E11 protein. Primer sequences were as follows: PXV(E11L)#2Rev_JA 5' – GGT TCG TCA AAG ACA TAA AAC TCA TT -3' and PXV(E11L)#3For_JA 5' – GAA TAC ATT CAC ATT GAC CAA TCA GAA – 3' Droplets were created in the automatic droplet generator, and genomes were amplified by PCR. Droplets were read in the BioRad QX200 droplet reader and analysis was preformed using the Quantasoft software.

4.5.7 Intranasal infection of animals.

For intranasal inoculation, groups of 5 BALB/c mice were anesthetized with isofluorane and inoculated slowly in a single nostril with a 20 µl suspension of sucrose-cushion purified virus. Animals were tilted backwards for 30 sec before lying on their back to wake up to improve infection efficiency. Mice were weighed daily following infection and euthanized if they reached 70% of their initial body weight in accordance with NIAID Animal Care and Use protocols. The infection inoculum was sonicated prior to each use, and titered by plaque assay to confirm dosages after each infection.

4.5.8 Quantitation of cytokines and chemokines in plasma of mice infected with ECTV

Quantitation of 25 cytokines and chemokines (G-CSF, GM-CSF, IFN-γ, IL-1α, IL-1β, IL-2, IL-3, IL-4, IL-5, IL-6, IL-7, IL-9, IL-10, IL-12p40, IL-12p70, IL-13, IL-15, IL-17 IP-10 (CXCL10), KC (CXCL1), MCP-1, MIP-1α, MIP-1β, MIP-2, RANTES (CCL5), and TNF-α) in the plasma of BALB/c was performed with a Milliplex MAP Mouse Cytokine/Chemokine immunoassay kit (Millipore Corp., Billerica, MA) using a BioPlex 200 Luminex (Bio-Rad, Hercules, CA) according to the manufacturer's instructions.

4.5.9 T cell depletion

MAbs against CD4 (clone GK1.5), CD8 (clone YTS 169.4), or KLH (isotype control, clone LTF-2)(Bio X Cell, Lebanon, NH) were utilized for T cell depletion. Mice were injected intraperitoneally with 0.2 mg of monoclonal antibody in 200 µl of PBS

on days 3 and 4 before virus challenge. The efficacy of depletion was tested by flow cytometry of cells harvested from whole blood on days 5 and 13 and spleen when terminated on day 29.

Chapter 5: Discussion and Future Directions

5.1 Characterization of CPX219

Our interest in the CPX219 protein emerged primarily from the uniqueness of its large size and the high level of conservation among chordopoxviruses for a protein in the variable region of the genome. The size of CPX219 posed unique challenges in the generation of recombinant viruses by homologous recombination and gel electrophoresis. Because early poxviral genes are transcribed from within the capsid, expression from a plasmid would require that expression be driven by a non-poxviral promoter, and so the ability to study the protein produced by the virus, not a plasmid, and was especially important for CPX219 which is regulated by an early promoter. Some early studies expressing CPX219 from a plasmid under a vaccinia early/late promoter led to significant over expression, accumulation in the ER, and thus improper glycosylation. This suggested to us expression from the viral genome was essential for future studies. Initial work was done using a mutant virus with only a C-terminal epitope tag. It wasn't until the addition of an N-terminal tag that a more complete picture of the biogenesis of CPX219 began to emerge.

The discovery of separate N- and C-terminal fragments was especially interesting and led to the use of BFA to confirm that this cleavage occurred intracellularly and not as an artifact *ex vivo*. These data also confirmed transport out of the ER, into the Golgi and there the further modification of the N-linked

glycosylation found on both fragments. As the cleave site(s) remain unknown, it is not possible to say if the two labeled fragments are the only fragments produced, or if additional internal fragments may exist due to multiple cleavage events. Indeed, on some western blots the C-terminal HA-tag is observed in multiple smaller bands. However, the sizes of deglycosylated fragments suggest that these two labeled fragments together are roughly the size of the full-length protein and would thus be the major fragments. Alzhanova et al (309) suggested that internal start sites could be responsible for the production of smaller fragments of CPX219. To test this we created a mutant in the first ATG allowing for the visualization of downstream, in frame, start site products but observed none.

Another important attribute of CPX219 is the transmembrane domains that anchor it in the plasma membrane. Software prediction strongly suggested a C-terminal transmembrane domain, as well as at least 3 additional possible domains towards the center of the protein. Which of these transmembrane domains are used, and how many are real, remains unknown. However, access to the protein extracellularly by antibody to epitope tags, and the glycosylation of fragments suggests at least 1 domain is responsible for looping the N-terminus and the majority of the protein to the extracellular space at the plasma membrane.

CPX219 was not essential for viral replication in tissue culture, which along with its location in the variable region of the genome suggested a role in host interactions. To assess the role of CPX219 during CPXV infection we first determined the LD_{50}

during intranasal infection of BALB/c mice and saw no difference in the absence of CPX219. This was also true in the CAST/EiJ mouse model, which has been shown in our lab to be highly susceptible to poxvirus infections (319).

5.2 Mousepox disease and ectromelia C15

Following our discovery that CPX219 did not influence pathogenicity in a mouse model, Alzhanova et al (309) demonstrated the ability of B22 homologs to reduce the activation state of both CD4+ and CD8+ T cells as measured by cytokine production. Interestingly, CPX219 was unable to enact this function on murine T cells. As Alzhanova et al. (309) examined the role of the MPXV B22 homolog, we next sought to examine the role of the B22 homolog in ECTV, C15.

As with the generation of CPX219 recombinant, the large size of C15 posed difficulties in the creation of mutant viruses. This was also complicated by the slower growth of ECTV. For example, VACV can form plaques visible by the naked eye within 24 hr, for CPXV this is about 36 – 48 hr, but for ECTV it can take 4-5 days. In part for this reason, biogenesis studies confirming an expression pattern similar to CPX219 were not performed. A mutant was created that, like the CPX219 mutant, had premature stop codons resulting in the lack of protein production despite maintaining the presence of the coding sequences in the genome.

Initial studies quickly highlighted a difference in the mortality resulting from the

C15Rev and C15Stop viruses, but unexpectedly we also observed reduced mortality at the highest doses with C15Stop. Stocks were tested to demonstrate the absence of bacterial contamination by incubation at 37 °C in LB with shaking, and the particle:PFU ratio was determined because infectious dosages were calculated solely by PFU. This ratio was equivalent whether determined by staining for DNA and protein positive particles via the ViroCyt, or by measuring the genome copy number of particles by droplet digital PCR following benzonase digest to remove nucleic acid material outside of particles. In addition, using analysis of genome copy number in the absence of benzonase as a measurement for the purity of preparation we observed variation between different viral stock preparations, but not between viruses prepared at the same time. By these measurements the virus and innocula given during infection was equivalent, and does not explain the differences in mortality.

Collection of organs at various DPI and following infection with different dosages provided some insight into the differences in mousepox disease progression in the absence of C15. Viral load at the site of infection (foot) was equivalent suggesting that changes in mortality were not due to reduced viral replication. In the lymph nodes viral load was reduced in the absence of C15, as well as in the critical spleen and liver. Significantly less virus in the liver in the absence of C15 may be the reason these animals can recover from the infection. Similarly, the higher mortality at lower doses of C15Stop may be due to higher viral loads in these key organs. These data were supported by histological analysis showing viral replication in key organs and resulting damage of the tissues. The mechanism of action for C15 that results in these

changes remains unknown.

Ectromelia virus spread has previously been demonstrated to be reduced in mouse strains inherently resistant to mousepox. One reason for this is the successful control of the infection and the generation of a strong and early type I response. To examine the immune response in the presence or absence of C15 we examined the cytokine levels in the blood. Although there are overall slightly higher cytokine levels in the blood in the presence of C15, we saw no shift in the cytokine profile to suggest that the immune response in the absence of C15 could explain the control of viral replication.

We also evaluated the intranasal model of infection to determine if this was a route-specific phenomenon. Although the mortality was less consistent than the footpad model of infection between experiments, we did observe reduced mortality in the absence of C15. However, unlike the footpad model, following intranasal infection mortality was reduced at lower doses. At higher doses the animals succumb to the disease at levels roughly equivalent to wildtype.

5.3 Future Directions

Much work remains before we will fully understand the role of B22 homologs during disease. Although Alzhanova et al (309) were able to determine that the MPXV homolog inhibits TCR-mediate stimulation upstream of PKC, the exact mechanism

remains unknown. T cells produce inhibitory signals, which could be engaged by the cell surface B22 homologs, although few direct viral-T cell inhibitory mechanisms have been described to date. In addition, the mousepox model provides a strong phenotype for the study of this homolog during disease and characterization of the mechanism of action, however the role of B22 needs to be confirmed at more physiologically relevant dosages.

The role of CPX219 during CPXV infection could be masked by the redundancy of other immunomodulatory proteins. Specifically, CPXV expresses two proteins capable of inhibiting the expression of MHC class I molecules, which stimulate the TCR on CD8+ T cells. One method to assess the influence of redundancy would be the generation of recombinant viruses where CPXV expresses the ECTV-C15 protein in place of CPX219, and vice versa. During these infections the viral environment would be swapped and redundant CPXV proteins would have the ability to inhibit the function of ECTV-C15 and in the mousepox model CPX219 would be able to act in an environment that could allow us to observe its potential role during disease. This is one possible explanation for the lack of phenotype observed during cowpox infection in the absence of CPX219. Another explanation is the possibility that these homologs have species-specific abilities, supported by the finding that CPX219 only poorly inhibits murine CD8+ T cell activation. This suggests that B22 homologs could directly affect the role of T cells during infection.

The suggestion of this species-specificity is especially intriguing as the amino acid

sequences between ECTV and CPXV are 92% identical, leaving little room for adaptation to the host. It is possible that this similarity could provide guidance in the determination of critical regions for species-specificity, host-interaction or performance of protein function. Amino acid alignment of B22 homologs has shown that the N-terminal region of the protein is more variable between viruses, and the C-terminal region is more conserved.

It would be interesting to preform studies on C15 similar to those carried out with CPX219 to determine if the cleavage event is conserved, or specific to the CPX219 protein. The topology of the protein and its localization at the plasma membrane may be essential for understanding the role of this protein and so it would be ideal to see the characterization of additional homologs.

Bibliography

1. **Riedel S.** 2005. Edward Jenner and the history of smallpox and vaccination. Proc (Bayl Univ Med Cent) **18:**21-25.

2. **Henderson DA.** 2009. Smallpox: The Death of a Disease - The Inside Story of Eradicating a Worldwide Killer. Prometheus Books, Amherst, New York, USA.

3. **Tack DM, Reynolds MG.** 2011. Zoonotic Poxviruses Associated with Companion Animals. Animals (Basel) **1:**377-395.

4. **Hendrickson RC, Wang C, Hatcher EL, Lefkowitz EJ.** 2010. Orthopoxvirus genome evolution: the role of gene loss. Viruses **2:**1933-1967.

5. **Gubser C, Hue S, Kellam P, Smith GL.** 2004. Poxvirus genomes: a phylogenetic analysis. J Gen Virol **85:**105-117.

6. **Theze J, Takatsuka J, Li Z, Gallais J, Doucet D, Arif B, Nakai M, Herniou EA.** 2013. New insights into the evolution of Entomopoxvirinae from the complete genome sequences of four entomopoxviruses infecting Adoxophyes honmai, Choristoneura biennis, Choristoneura rosaceana, and Mythimna separata. J Virol **87:**7992-8003.

7. **Xing K, Deng R, Wang J, Feng J, Huang M, Wang X.** 2006. Genome-based phylogeny of poxvirus. Intervirology **49:**207-214.

8. **Iyer LM, Aravind L, Koonin EV.** 2001. Common origin of four diverse families of large eukaryotic DNA viruses. J Virol **75:**11720-11734.

9. **Suzan-Monti M, La Scola B, Raoult D.** 2006. Genomic and evolutionary aspects of Mimivirus. Virus Res **117:**145-155.

10. **Anonymous.** 2015. International Committee on Taxonomy of Viruses, http://ictvonline.org/virusTaxonomy.asp.

11. **McInnes CJ, Wood AR, Thomas K, Sainsbury AW, Gurnell J, Dein FJ, Nettleton PF.** 2006. Genomic characterization of a novel poxvirus contributing to the decline of the red squirrel (Sciurus vulgaris) in the UK. J

Gen Virol **87:**2115-2125.

12. **Gjessing MC, Yutin N, Tengs T, Senkevich T, Koonin E, Ronning HP, Alarcon M, Ylving S, Lie KI, Saure B, Tran L, Moss B, Dale OB.** 2015. Salmon Gill Poxvirus, the Deepest Representative of the Chordopoxvirinae. J Virol **89:**9348-9367.

13. **Barnett J, Dastjerdi A, Davison N, Deaville R, Everest D, Peake J, Finnegan C, Jepson P, Steinbach F.** 2015. Identification of Novel Cetacean Poxviruses in Cetaceans Stranded in South West England. PLoS One **10:**e0124315.

14. **O'Dea MA, Tu SL, Pang S, De Ridder T, Jackson B, Upton C.** 2016. Genomic characterisation of a novel poxvirus from a flying fox; evidence for a new genus? J Gen Virol doi:10.1099/jgv.0.000538.

15. **Moss B.** 2007. Poxviridae: The Viruses and Their Replication. Fields Virology **2:**2905-2946.

16. **Pauli G, Blumel J, Burger R, Drosten C, Groner A, Gurtler L, Heiden M, Hildebrandt M, Jansen B, Montag-Lessing T, Offergeld R, Seitz R, Schlenkrich U, Schottstedt V, Strobel J, Willkommen H, von Konig CH.** 2010. Orthopox Viruses: Infections in Humans. Transfus Med Hemother **37:**351-364.

17. **Lyons ASaP, R.J.** 1997. Medicine—An Illustrated History. Abradale Press, Harry N Abrams Inc, New York.

18. **Christopher GW, Cieslak TJ, Pavlin JA, Eitzen EM, Jr.** 1997. Biological warfare. A historical perspective. JAMA **278:**412-417.

19. **Stark RB.** 1977. Immunization saves Washington's army. Surg Gynecol Obstet **144:**425-431.

20. **Sanchez-Sampedro L, Perdiguero B, Mejias-Perez E, Garcia-Arriaza J, Di Pilato M, Esteban M.** 2015. The evolution of poxvirus vaccines. Viruses **7:**1726-1803.

21. **Moss B, Carroll MW, Wyatt LS, Bennink JR, Hirsch VM, Goldstein S, Elkins WR, Fuerst TR, Lifson JD, Piatak M, Restifo NP, Overwijk W, Chamberlain R, Rosenberg SA, Sutter G.** 1996. Host range restricted, non-replicating vaccinia virus vectors as vaccine candidates. Adv Exp Med Biol

397:7-13.

22. **Kantele A, Chickering K, Vapalahti O, Rimoin AW.** 2016. Emerging diseases-the monkeypox epidemic in the Democratic Republic of the Congo. Clin Microbiol Infect doi:10.1016/j.cmi.2016.07.004.

23. **Jezek Z, Khodakevich LN.** 1987. Ten years of freedom from smallpox: lessons and experiences. Dedicated to the tenth anniversary of worldwide freedom from smallpox. J Hyg Epidemiol Microbiol Immunol **31:**237-244.

24. **Jezek Z, Grab B, Dixon H.** 1987. Stochastic model for interhuman spread of monkeypox. Am J Epidemiol **126:**1082-1092.

25. **Dabrowski PW, Radonic A, Kurth A, Nitsche A.** 2013. Genome-wide comparison of cowpox viruses reveals a new clade related to Variola virus. PLoS One **8:**e79953.

26. **Kinnunen PM, Holopainen JM, Hemmila H, Piiparinen H, Sironen T, Kivela T, Virtanen J, Niemimaa J, Nikkari S, Jarvinen A, Vapalahti O.** 2015. Severe Ocular Cowpox in a Human, Finland. Emerg Infect Dis **21:**2261-2263.

27. **Leite JA, Drumond BP, Trindade GS, Lobato ZI, da Fonseca FG, dos SJ, Madureira MC, Guedes MI, Ferreira JM, Bonjardim CA, Ferreira PC, Kroon EG.** 2005. Passatempo virus, a vaccinia virus strain, Brazil. Emerg Infect Dis **11:**1935-1938.

28. **Hoffmann D, Franke A, Jenckel M, Tamosiunaite A, Schluckebier J, Granzow H, Hoffmann B, Fischer S, Ulrich RG, Hoper D, Goller K, Osterrieder N, Beer M.** 2015. Out of the Reservoir: Phenotypic and Genotypic Characterization of a Novel Cowpox Virus Isolated from a Common Vole. J Virol **89:**10959-10969.

29. **Dahiya SS, Kumar S, Mehta SC, Narnaware SD, Singh R, Tuteja FC.** 2016. Camelpox: A brief review on its epidemiology, current status and challenges. Acta Trop **158:**32-38.

30. **Gallardo-Romero NF, Velasco-Villa A, Weiss SL, Emerson GL, Carroll DS, Hughes CM, Li Y, Karem KL, Damon IK, Olson VA.** 2011. Detection of North American orthopoxviruses by real time-PCR. Virol J **8:**313.

31. **Fleischauer C, Upton C, Victoria J, Jones GJ, Roper RL.** 2015. Genome sequence and comparative virulence of raccoonpox virus: the first North

American poxvirus sequence. J Gen Virol **96:**2806-2821.

32. **Cyrklaff M, Risco C, Fernandez JJ, Jimenez MV, Esteban M, Baumeister W, Carrascosa JL.** 2005. Cryo-electron tomography of vaccinia virus. Proc Natl Acad Sci U S A **102:**2772-2777.

33. **Heuser J.** 2005. Deep-etch EM reveals that the early poxvirus envelope is a single membrane bilayer stabilized by a geodetic "honeycomb" surface coat. J Cell Biol **169:**269-283.

34. **Matson J, Chou W, Ngo T, Gershon PD.** 2014. Static and dynamic protein phosphorylation in the Vaccinia virion. Virology **452-453:**310-323.

35. **Resch W, Hixson KK, Moore RJ, Lipton MS, Moss B.** 2007. Protein composition of the vaccinia virus mature virion. Virology **358:**233-247.

36. **Gray RD, Beerli C, Pereira PM, Scherer KM, Samolej J, Bleck CK, Mercer J, Henriques R.** 2016. VirusMapper: open-source nanoscale mapping of viral architecture through super-resolution microscopy. Sci Rep **6:**29132.

37. **Schmidt FI, Bleck CK, Reh L, Novy K, Wollscheid B, Helenius A, Stahlberg H, Mercer J.** 2013. Vaccinia virus entry is followed by core activation and proteasome-mediated release of the immunomodulatory effector VH1 from lateral bodies. Cell Rep **4:**464-476.

38. **Domi A, Moss B.** 2005. Engineering of a vaccinia virus bacterial artificial chromosome in Escherichia coli by bacteriophage lambda-based recombination. Nat Methods **2:**95-97.

39. **Baroudy BM, Venkatesan S, Moss B.** 1982. Incompletely base-paired flip-flop terminal loops link the two DNA strands of the vaccinia virus genome into one uninterrupted polynucleotide chain. Cell **28:**315-324.

40. **Merchlinsky M, Garon CF, Moss B.** 1988. Molecular cloning and sequence of the concatemer junction from vaccinia virus replicative DNA. Viral nuclease cleavage sites in cruciform structures. J Mol Biol **199:**399-413.

41. **Wittek R, Moss B.** 1980. Tandem repeats within the inverted terminal repetition of vaccinia virus DNA. Cell **21:**277-284.

42. **Wittek R, Cooper JA, Barbosa E, Moss B.** 1980. Expression of the vaccinia

virus genome: analysis and mapping of mRNAs encoded within the inverted terminal repetition. Cell **21:**487-493.

43. **Senkevich TG, Bruno D, Martens C, Porcella SF, Wolf YI, Moss B.** 2015. Mapping vaccinia virus DNA replication origins at nucleotide level by deep sequencing. Proc Natl Acad Sci U S A **112:**10908-10913.

44. **Upton C, Slack S, Hunter AL, Ehlers A, Roper RL.** 2003. Poxvirus orthologous clusters: toward defining the minimum essential poxvirus genome. J Virol **77:**7590-7600.

45. **Yang Z, Bruno DP, Martens CA, Porcella SF, Moss B.** 2010. Simultaneous high-resolution analysis of vaccinia virus and host cell transcriptomes by deep RNA sequencing. Proc Natl Acad Sci U S A **107:**11513-11518.

46. **Yang Z, Martens CA, Bruno DP, Porcella SF, Moss B.** 2012. Pervasive initiation and 3'-end formation of poxvirus postreplicative RNAs. J Biol Chem **287:**31050-31060.

47. **Yang Z, Reynolds SE, Martens CA, Bruno DP, Porcella SF, Moss B.** 2011. Expression profiling of the intermediate and late stages of poxvirus replication. J Virol **85:**9899-9908.

48. **DeFilippes FM.** 1982. Restriction enzyme mapping of vaccinia virus DNA. J Virol **43:**136-149.

49. **Chang SJ, Chang YX, Izmailyan R, Tang YL, Chang W.** 2010. Vaccinia virus A25 and A26 proteins are fusion suppressors for mature virions and determine strain-specific virus entry pathways into HeLa, CHO-K1, and L cells. J Virol **84:**8422-8432.

50. **Chung CS, Hsiao JC, Chang YS, Chang W.** 1998. A27L protein mediates vaccinia virus interaction with cell surface heparan sulfate. J Virol **72:**1577-1585.

51. **Hsiao JC, Chung CS, Chang W.** 1999. Vaccinia virus envelope D8L protein binds to cell surface chondroitin sulfate and mediates the adsorption of intracellular mature virions to cells. J Virol **73:**8750-8761.

52. **Lin CL, Chung CS, Heine HG, Chang W.** 2000. Vaccinia virus envelope H3L protein binds to cell surface heparan sulfate and is important for intracellular mature virion morphogenesis and virus infection in vitro and in

vivo. J Virol **74:**3353-3365.

53. **Chiu WL, Lin CL, Yang MH, Tzou DL, Chang W.** 2007. Vaccinia virus 4c (A26L) protein on intracellular mature virus binds to the extracellular cellular matrix laminin. J Virol **81:**2149-2157.

54. **Howard AR, Senkevich TG, Moss B.** 2008. Vaccinia virus A26 and A27 proteins form a stable complex tethered to mature virions by association with the A17 transmembrane protein. J Virol **82:**12384-12391.

55. **Kochan G, Escors D, Gonzalez JM, Casasnovas JM, Esteban M.** 2008. Membrane cell fusion activity of the vaccinia virus A17-A27 protein complex. Cell Microbiol **10:**149-164.

56. **Moss B.** 2012. Poxvirus cell entry: how many proteins does it take? Viruses **4:**688-707.

57. **Vanderplasschen A, Smith GL.** 1997. A novel virus binding assay using confocal microscopy: demonstration that the intracellular and extracellular vaccinia virions bind to different cellular receptors. J Virol **71:**4032-4041.

58. **Bengali Z, Satheshkumar PS, Moss B.** 2012. Orthopoxvirus species and strain differences in cell entry. Virology **433:**506-512.

59. **Bengali Z, Townsley AC, Moss B.** 2009. Vaccinia virus strain differences in cell attachment and entry. Virology **389:**132-140.

60. **Yao Y, Li P, Singh P, Thiele AT, Wilkes DS, Renukaradhya GJ, Brutkiewicz RR, Travers JB, Luker GD, Hong SC, Blum JS, Chang CH.** 2007. Vaccinia virus infection induces dendritic cell maturation but inhibits antigen presentation by MHC class II. Cell Immunol **246:**92-102.

61. **Carter GC, Rodger G, Murphy BJ, Law M, Krauss O, Hollinshead M, Smith GL.** 2003. Vaccinia virus cores are transported on microtubules. J Gen Virol **84:**2443-2458.

62. **Kilcher S, Schmidt FI, Schneider C, Kopf M, Helenius A, Mercer J.** 2014. siRNA screen of early poxvirus genes identifies the AAA+ ATPase D5 as the virus genome-uncoating factor. Cell Host Microbe **15:**103-112.

63. **Liu SW, Katsafanas GC, Liu R, Wyatt LS, Moss B.** 2015. Poxvirus decapping enzymes enhance virulence by preventing the accumulation of

dsRNA and the induction of innate antiviral responses. Cell Host Microbe **17:**320-331.

64. **Katsafanas GC, Moss B.** 2007. Colocalization of transcription and translation within cytoplasmic poxvirus factories coordinates viral expression and subjugates host functions. Cell Host Microbe **2:**221-228.

65. **Salzman NP.** 1960. The rate of formation of vaccinia deoxyribonucleic acid and vaccinia virus. Virology **10:**150-152.

66. **Paran N, De Silva FS, Senkevich TG, Moss B.** 2009. Cellular DNA ligase I is recruited to cytoplasmic vaccinia virus factories and masks the role of the vaccinia ligase in viral DNA replication. Cell Host Microbe **6:**563-569.

67. **Garcia AD, Moss B.** 2001. Repression of vaccinia virus Holliday junction resolvase inhibits processing of viral DNA into unit-length genomes. J Virol **75:**6460-6471.

68. **Morgan C.** 1976. The insertion of DNA into vaccinia virus. Science **193:**591-592.

69. **Szajner P, Jaffe H, Weisberg AS, Moss B.** 2004. A complex of seven vaccinia virus proteins conserved in all chordopoxviruses is required for the association of membranes and viroplasm to form immature virions. Virology **330:**447-459.

70. **Unger B, Mercer J, Boyle KA, Traktman P.** 2013. Biogenesis of the vaccinia virus membrane: genetic and ultrastructural analysis of the contributions of the A14 and A17 proteins. J Virol **87:**1083-1097.

71. **Ansarah-Sobrinho C, Moss B.** 2004. Role of the I7 protein in proteolytic processing of vaccinia virus membrane and core components. J Virol **78:**6335-6343.

72. **Moss B.** 2015. Poxvirus membrane biogenesis. Virology **479-480:**619-626.

73. **Maruri-Avidal L, Weisberg AS, Bisht H, Moss B.** 2013. Analysis of viral membranes formed in cells infected by a vaccinia virus L2-deletion mutant suggests their origin from the endoplasmic reticulum. J Virol **87:**1861-1871.

74. **Cassetti MC, Merchlinsky M, Wolffe EJ, Weisberg AS, Moss B.** 1998. DNA packaging mutant: repression of the vaccinia virus A32 gene results in

noninfectious, DNA-deficient, spherical, enveloped particles. J Virol **72:**5769-5780.

75. **Koonin EV, Senkevich TG, Chernos VI.** 1993. Gene A32 product of vaccinia virus may be an ATPase involved in viral DNA packaging as indicated by sequence comparisons with other putative viral ATPases. Virus Genes **7:**89-94.

76. **Grubisha O, Traktman P.** 2003. Genetic analysis of the vaccinia virus I6 telomere-binding protein uncovers a key role in genome encapsidation. J Virol **77:**10929-10942.

77. **DeMasi J, Du S, Lennon D, Traktman P.** 2001. Vaccinia virus telomeres: interaction with the viral I1, I6, and K4 proteins. J Virol **75:**10090-10105.

78. **Bisht H, Weisberg AS, Szajner P, Moss B.** 2009. Assembly and disassembly of the capsid-like external scaffold of immature virions during vaccinia virus morphogenesis. J Virol **83:**9140-9150.

79. **Moss B, Rosenblum EN.** 1973. Letter: Protein cleavage and poxvirus morphogenesis: tryptic peptide analysis of core precursors accumulated by blocking assembly with rifampicin. J Mol Biol **81:**267-269.

80. **Senkevich TG, White CL, Koonin EV, Moss B.** 2002. Complete pathway for protein disulfide bond formation encoded by poxviruses. Proc Natl Acad Sci U S A **99:**6667-6672.

81. **Howard AR, Weisberg AS, Moss B.** 2010. Congregation of orthopoxvirus virions in cytoplasmic A-type inclusions is mediated by interactions of a bridging protein (A26p) with a matrix protein (ATIp) and a virion membrane-associated protein (A27p). J Virol **84:**7592-7602.

82. **Schmelz M, Sodeik B, Ericsson M, Wolffe EJ, Shida H, Hiller G, Griffiths G.** 1994. Assembly of vaccinia virus: the second wrapping cisterna is derived from the trans Golgi network. J Virol **68:**130-147.

83. **Husain M, Moss B.** 2001. Vaccinia virus F13L protein with a conserved phospholipase catalytic motif induces colocalization of the B5R envelope glycoprotein in post-Golgi vesicles. J Virol **75:**7528-7542.

84. **Husain M, Moss B.** 2002. Similarities in the induction of post-Golgi vesicles by the vaccinia virus F13L protein and phospholipase D. J Virol **76:**7777-

7789.

85. **Sivan G, Weisberg AS, Americo JL, Moss B.** 2016. Retrograde Transport from Early Endosomes to the Trans-Golgi Network Enables Membrane Wrapping and Egress of Vaccinia Virions. J Virol doi:10.1128/JVI.01114-16.

86. **Lorenzo MM, Sanchez-Puig JM, Blasco R.** 2012. Mutagenesis of the palmitoylation site in vaccinia virus envelope glycoprotein B5. J Gen Virol **93:**733-743.

87. **Roper RL, Payne LG, Moss B.** 1996. Extracellular vaccinia virus envelope glycoprotein encoded by the A33R gene. J Virol **70:**3753-3762.

88. **Duncan SA, Smith GL.** 1992. Identification and characterization of an extracellular envelope glycoprotein affecting vaccinia virus egress. J Virol **66:**1610-1621.

89. **Parkinson JE, Smith GL.** 1994. Vaccinia virus gene A36R encodes a M(r) 43-50 K protein on the surface of extracellular enveloped virus. Virology **204:**376-390.

90. **Shida H.** 1986. Nucleotide sequence of the vaccinia virus hemagglutinin gene. Virology **150:**451-462.

91. **Zhang WH, Wilcock D, Smith GL.** 2000. Vaccinia virus F12L protein is required for actin tail formation, normal plaque size, and virulence. J Virol **74:**11654-11662.

92. **Hirt P, Hiller G, Wittek R.** 1986. Localization and fine structure of a vaccinia virus gene encoding an envelope antigen. J Virol **58:**757-764.

93. **Engelstad M, Smith GL.** 1993. The vaccinia virus 42-kDa envelope protein is required for the envelopment and egress of extracellular virus and for virus virulence. Virology **194:**627-637.

94. **Domi A, Weisberg AS, Moss B.** 2008. Vaccinia virus E2L null mutants exhibit a major reduction in extracellular virion formation and virus spread. J Virol **82:**4215-4226.

95. **Brum LM, Lopez MC, Varela JC, Baker HV, Moyer RW.** 2003. Microarray analysis of A549 cells infected with rabbitpox virus (RPV): a comparison of wild-type RPV and RPV deleted for the host range gene, SPI-1.

Virology **315:**322-334.

96. **Wagenaar TR, Moss B.** 2007. Association of vaccinia virus fusion regulatory proteins with the multicomponent entry/fusion complex. J Virol **81:**6286-6293.

97. **Sanderson CM, Hollinshead M, Smith GL.** 2000. The vaccinia virus A27L protein is needed for the microtubule-dependent transport of intracellular mature virus particles. J Gen Virol **81:**47-58.

98. **Ward BM, Moss B.** 2004. Vaccinia virus A36R membrane protein provides a direct link between intracellular enveloped virions and the microtubule motor kinesin. J Virol **78:**2486-2493.

99. **Jeshtadi A, Burgos P, Stubbs CD, Parker AW, King LA, Skinner MA, Botchway SW.** 2010. Interaction of poxvirus intracellular mature virion proteins with the TPR domain of kinesin light chain in live infected cells revealed by two-photon-induced fluorescence resonance energy transfer fluorescence lifetime imaging microscopy. J Virol **84:**12886-12894.

100. **Carpentier DC, Gao WN, Ewles H, Morgan GW, Smith GL.** 2015. Vaccinia virus protein complex F12/E2 interacts with kinesin light chain isoform 2 to engage the kinesin-1 motor complex. PLoS Pathog **11:**e1004723.

101. **Leite F, Way M.** 2015. The role of signalling and the cytoskeleton during Vaccinia Virus egress. Virus Res **209:**87-99.

102. **Marchal J.** 1930. Infectious Ectromelia. A Hitherto Undescribed Virus Disease of Mice. J of Path & Bact **33:**713-728.

103. **Fenner F.** 1947b. Studies in infectious ectromelia in mice; natural transmission; the portal of entry of the virus. Aust J Exp Biol Med Sci **25:**275-282.

104. **Briody BA.** 1955. Mouse pox (ectromelia) in the United States. Lab Anim Care **6:**1-8.

105. **Whitney RA, Jr.** 1974. Ectromelia in u. S. Mouse colonies. Science **184:**609.

106. **Lipman NS, Perkins S, Nguyen H, Pfeffer M, Meyer H.** 2000. Mousepox resulting from use of ectromelia virus-contaminated, imported mouse serum.

Comp Med **50:**426-435.

107. **Fenner F.** 1948b. The epizootic behaviour of mouse-pox, infectious ectromelia. Br J Exp Pathol **29:**69-91.

108. **Buller RM, Owens G, Schriewer J, Melman L, Beadle JR, Hostetler KY.** 2004. Efficacy of oral active ether lipid analogs of cidofovir in a lethal mousepox model. Virology **318:**474-481.

109. **Schriewer J, Buller RM, Owens G.** 2004. Mouse models for studying orthopoxvirus respiratory infections. Methods Mol Biol **269:**289-308.

110. **Andrewes CH, Elford WJ.** 1947. Infections ectromelia; experiments on interference and immunization. Br J Exp Pathol **28:**278-285.

111. **Fenner F.** 1949c. Studies in mousepox, infectious ectromelia of mice; a comparison of the virulence and infectivity of three strains of ectromelia virus. Aust J Exp Biol Med Sci **27:**31-43.

112. **Chen N, Danila MI, Feng Z, Buller RM, Wang C, Han X, Lefkowitz EJ, Upton C.** 2003. The genomic sequence of ectromelia virus, the causative agent of mousepox. Virology **317:**165-186.

113. **Flint J, Enquist, L., Racaniello, V., Skalka, A.** 2009. Principles of Virology, 3 ed. ASM Press, Washington D. C.

114. **McGaughey CA, and Whitehead, R.** 1933. Outbreaks of infectious ectromelia in laboratory and wild mice. J Pathol Bacteriol **37:**253-256.

115. **Wallace GD, Buller RM.** 1985. Kinetics of ectromelia virus (mousepox) transmission and clinical response in C57BL/6j, BALB/cByj and AKR/J inbred mice. Lab Anim Sci **35:**41-46.

116. **Jacoby RO, Bhatt PN.** 1987. Mousepox in inbred mice innately resistant or susceptible to lethal infection with ectromelia virus. II. Pathogenesis. Lab Anim Sci **37:**16-22.

117. **Bhatt PN, Jacoby RO.** 1987. Mousepox in inbred mice innately resistant or susceptible to lethal infection with ectromelia virus. I. Clinical responses. Lab Anim Sci **37:**11-15.

118. **Brownstein DG, Gras L.** 1997. Differential pathogenesis of lethal mousepox

in congenic DBA/2 mice implicates natural killer cell receptor NKR-P1 in necrotizing hepatitis and the fifth component of complement in recruitment of circulating leukocytes to spleen. Am J Pathol **150:**1407-1420.

119. **Fenner F.** 1949d. Studies in mousepox, infectious ectromelia of mice; the effect of the age of the host upon the response to infection. Aust J Exp Biol Med Sci **27:**45-53.

120. **Fenner F.** 1948a. The clinical features of mouse-pox (infectious ectromelia of mice) and the pathogenesis of the disease. J Pathol Bacteriol **60:**529-552.

121. **Fenner F.** 1948d. The pathogenesis of the acute exanthems; an interpretation based on experimental investigations with mousepox; infectious ectromelia of mice. Lancet **2:**915-920.

122. **Fenner F.** 1948c. The epizootic behaviour of mouse-pox (infectious ectromelia of mice) the course of events in long-continued epidemics. J Hyg (Lond) **46:**383-393.

123. **Roberts JA.** 1962. Histopathogenesis of mousepox. II. Cutaneous infection. Br J Exp Pathol **43:**462-468.

124. **Rous P, McMaster PD, Hudack SS.** 1935. The Fixation and Protection of Viruses by the Cells of Susceptible Animals. J Exp Med **61:**657-688.

125. **Allen AM, Clarke GL, Ganaway JR, Lock A, Werner RM.** 1981. Pathology and diagnosis of mousepox. Lab Anim Sci **31:**599-608.

126. **Dick EJ, Jr., Kittell CL, Meyer H, Farrar PL, Ropp SL, Esposito JJ, Buller RM, Neubauer H, Kang YH, McKee AE.** 1996. Mousepox outbreak in a laboratory mouse colony. Lab Anim Sci **46:**602-611.

127. **O'Neill HC, Blanden RV.** 1983. Mechanisms determining innate resistance to ectromelia virus infection in C57BL mice. Infect Immun **41:**1391-1394.

128. **Schell K.** 1960. Studies on the innate resistance of mice to infection with mousepox. I. Resistance and antibody production. Aust J Exp Biol Med Sci **38:**271-288.

129. **Fenner F.** 1949a. Mouse-pox; infectious ectromelia of mice; a review. J Immunol **63:**341-373.

130. **Mims CA.** 1964. Aspects of the Pathogenesis of Virus Diseases. Bacteriol Rev **28:**30-71.

131. **Esteban DJ, Buller RM.** 2005. Ectromelia virus: the causative agent of mousepox. J Gen Virol **86:**2645-2659.

132. **Wu J, Chen ZJ.** 2014. Innate immune sensing and signaling of cytosolic nucleic acids. Annu Rev Immunol **32:**461-488.

133. **Labzin LI, Lauterbach MA, Latz E.** 2016. Interferons and inflammasomes: Cooperation and counterregulation in disease. J Allergy Clin Immunol **138:**37-46.

134. **Gerlic M, Faustin B, Postigo A, Yu EC, Proell M, Gombosuren N, Krajewska M, Flynn R, Croft M, Way M, Satterthwait A, Liddington RC, Salek-Ardakani S, Matsuzawa S, Reed JC.** 2013. Vaccinia virus F1L protein promotes virulence by inhibiting inflammasome activation. Proc Natl Acad Sci U S A **110:**7808-7813.

135. **Brandt TA, Jacobs BL.** 2001. Both carboxy- and amino-terminal domains of the vaccinia virus interferon resistance gene, E3L, are required for pathogenesis in a mouse model. J Virol **75:**850-856.

136. **Kim YG, Muralinath M, Brandt T, Pearcy M, Hauns K, Lowenhaupt K, Jacobs BL, Rich A.** 2003. A role for Z-DNA binding in vaccinia virus pathogenesis. Proc Natl Acad Sci U S A **100:**6974-6979.

137. **Peters NE, Ferguson BJ, Mazzon M, Fahy AS, Krysztofinska E, Arribas-Bosacoma R, Pearl LH, Ren H, Smith GL.** 2013. A mechanism for the inhibition of DNA-PK-mediated DNA sensing by a virus. PLoS Pathog **9:**e1003649.

138. **Bowie A, Kiss-Toth E, Symons JA, Smith GL, Dower SK, O'Neill LA.** 2000. A46R and A52R from vaccinia virus are antagonists of host IL-1 and toll-like receptor signaling. Proc Natl Acad Sci U S A **97:**10162-10167.

139. **Stack J, Haga IR, Schroder M, Bartlett NW, Maloney G, Reading PC, Fitzgerald KA, Smith GL, Bowie AG.** 2005. Vaccinia virus protein A46R targets multiple Toll-like-interleukin-1 receptor adaptors and contributes to virulence. J Exp Med **201:**1007-1018.

140. **Harte MT, Haga IR, Maloney G, Gray P, Reading PC, Bartlett NW, Smith GL, Bowie A, O'Neill LA.** 2003. The poxvirus protein A52R targets

Toll-like receptor signaling complexes to suppress host defense. J Exp Med **197:**343-351.

141. **Graham SC, Bahar MW, Cooray S, Chen RA, Whalen DM, Abrescia NG, Alderton D, Owens RJ, Stuart DI, Smith GL, Grimes JM.** 2008. Vaccinia virus proteins A52 and B14 Share a Bcl-2-like fold but have evolved to inhibit NF-kappaB rather than apoptosis. PLoS Pathog **4:**e1000128.

142. **Gonzalez JM, Esteban M.** 2010. A poxvirus Bcl-2-like gene family involved in regulation of host immune response: sequence similarity and evolutionary history. Virol J **7:**59.

143. **Shchelkunov SN.** 2012. Orthopoxvirus genes that mediate disease virulence and host tropism. Adv Virol **2012:**524743.

144. **Neidel S, Maluquer de Motes C, Mansur DS, Strnadova P, Smith GL, Graham SC.** 2015. Vaccinia virus protein A49 is an unexpected member of the B-cell Lymphoma (Bcl)-2 protein family. J Biol Chem **290:**5991-6002.

145. **Smith GL, Benfield CT, Maluquer de Motes C, Mazzon M, Ember SW, Ferguson BJ, Sumner RP.** 2013. Vaccinia virus immune evasion: mechanisms, virulence and immunogenicity. J Gen Virol **94:**2367-2392.

146. **Oda S, Schroder M, Khan AR.** 2009. Structural basis for targeting of human RNA helicase DDX3 by poxvirus protein K7. Structure **17:**1528-1537.

147. **Schroder M, Baran M, Bowie AG.** 2008. Viral targeting of DEAD box protein 3 reveals its role in TBK1/IKKepsilon-mediated IRF activation. EMBO J **27:**2147-2157.

148. **Unterholzner L, Sumner RP, Baran M, Ren H, Mansur DS, Bourke NM, Randow F, Smith GL, Bowie AG.** 2011. Vaccinia virus protein C6 is a virulence factor that binds TBK-1 adaptor proteins and inhibits activation of IRF3 and IRF7. PLoS Pathog **7:**e1002247.

149. **Ferguson BJ, Benfield CT, Ren H, Lee VH, Frazer GL, Strnadova P, Sumner RP, Smith GL.** 2013. Vaccinia virus protein N2 is a nuclear IRF3 inhibitor that promotes virulence. J Gen Virol **94:**2070-2081.

150. **Maluquer de Motes C, Cooray S, Ren H, Almeida GM, McGourty K, Bahar MW, Stuart DI, Grimes JM, Graham SC, Smith GL.** 2011. Inhibition of apoptosis and NF-kappaB activation by vaccinia protein N1 occur via distinct binding surfaces and make different contributions to

virulence. PLoS Pathog **7:**e1002430.

151. **Chen RA, Ryzhakov G, Cooray S, Randow F, Smith GL.** 2008. Inhibition of IkappaB kinase by vaccinia virus virulence factor B14. PLoS Pathog **4:**e22.

152. **Benfield CT, Mansur DS, McCoy LE, Ferguson BJ, Bahar MW, Oldring AP, Grimes JM, Stuart DI, Graham SC, Smith GL.** 2011. Mapping the IkappaB kinase beta (IKKbeta)-binding interface of the B14 protein, a vaccinia virus inhibitor of IKKbeta-mediated activation of nuclear factor kappaB. J Biol Chem **286:**20727-20735.

153. **Mansur DS, Maluquer de Motes C, Unterholzner L, Sumner RP, Ferguson BJ, Ren H, Strnadova P, Bowie AG, Smith GL.** 2013. Poxvirus targeting of E3 ligase beta-TrCP by molecular mimicry: a mechanism to inhibit NF-kappaB activation and promote immune evasion and virulence. PLoS Pathog **9:**e1003183.

154. **Shisler JL, Jin XL.** 2004. The vaccinia virus K1L gene product inhibits host NF-kappaB activation by preventing IkappaBalpha degradation. J Virol **78:**3553-3560.

155. **Gedey R, Jin XL, Hinthong O, Shisler JL.** 2006. Poxviral regulation of the host NF-kappaB response: the vaccinia virus M2L protein inhibits induction of NF-kappaB activation via an ERK2 pathway in virus-infected human embryonic kidney cells. J Virol **80:**8676-8685.

156. **Hinthong O, Jin XL, Shisler JL.** 2008. Characterization of wild-type and mutant vaccinia virus M2L proteins' abilities to localize to the endoplasmic reticulum and to inhibit NF-kappaB activation during infection. Virology **373:**248-262.

157. **Mohamed MR, Rahman MM, Lanchbury JS, Shattuck D, Neff C, Dufford M, van Buuren N, Fagan K, Barry M, Smith S, Damon I, McFadden G.** 2009. Proteomic screening of variola virus reveals a unique NF-kappaB inhibitor that is highly conserved among pathogenic orthopoxviruses. Proc Natl Acad Sci U S A **106:**9045-9050.

158. **Rubio D, Xu RH, Remakus S, Krouse TE, Truckenmiller ME, Thapa RJ, Balachandran S, Alcami A, Norbury CC, Sigal LJ.** 2013. Crosstalk between the type 1 interferon and nuclear factor kappa B pathways confers resistance to a lethal virus infection. Cell Host Microbe **13:**701-710.

159. **Wang Q, Burles K, Couturier B, Randall CM, Shisler J, Barry M.** 2014.

Ectromelia virus encodes a BTB/kelch protein, EVM150, that inhibits NF-kappaB signaling. J Virol **88:**4853-4865.

160. **Xu RH, Wong EB, Rubio D, Roscoe F, Ma X, Nair S, Remakus S, Schwendener R, John S, Shlomchik M, Sigal LJ.** 2015. Sequential Activation of Two Pathogen-Sensing Pathways Required for Type I Interferon Expression and Resistance to an Acute DNA Virus Infection. Immunity **43:**1148-1159.

161. **Sutherland DB, Ranasinghe C, Regner M, Phipps S, Matthaei KI, Day SL, Ramshaw IA.** 2011. Evaluating vaccinia virus cytokine co-expression in TLR GKO mice. Immunol Cell Biol **89:**706-715.

162. **Samuelsson C, Hausmann J, Lauterbach H, Schmidt M, Akira S, Wagner H, Chaplin P, Suter M, O'Keeffe M, Hochrein H.** 2008. Survival of lethal poxvirus infection in mice depends on TLR9, and therapeutic vaccination provides protection. J Clin Invest **118:**1776-1784.

163. **Sigal LJ.** 2016. The Pathogenesis and Immunobiology of Mousepox. Adv Immunol **129:**251-276.

164. **Marie I, Durbin JE, Levy DE.** 1998. Differential viral induction of distinct interferon-alpha genes by positive feedback through interferon regulatory factor-7. EMBO J **17:**6660-6669.

165. **Stark GR, Darnell JE, Jr.** 2012. The JAK-STAT pathway at twenty. Immunity **36:**503-514.

166. **Perdiguero B, Esteban M.** 2009. The interferon system and vaccinia virus evasion mechanisms. J Interferon Cytokine Res **29:**581-598.

167. **Silverman RH.** 2007. Viral encounters with 2',5'-oligoadenylate synthetase and RNase L during the interferon antiviral response. J Virol **81:**12720-12729.

168. **Schoggins JW, Rice CM.** 2011. Interferon-stimulated genes and their antiviral effector functions. Curr Opin Virol **1:**519-525.

169. **Najarro P, Traktman P, Lewis JA.** 2001. Vaccinia virus blocks gamma interferon signal transduction: viral VH1 phosphatase reverses Stat1 activation. J Virol **75:**3185-3196.

170. **Moss B.** 1968. Inhibition of HeLa cell protein synthesis by the vaccinia

virion. J Virol **2:**1028-1037.

171. **Rice AP, Roberts BE.** 1983. Vaccinia virus induces cellular mRNA degradation. J Virol **47:**529-539.

172. **Parrish S, Moss B.** 2006. Characterization of a vaccinia virus mutant with a deletion of the D10R gene encoding a putative negative regulator of gene expression. J Virol **80:**553-561.

173. **Carroll K, Elroy-Stein O, Moss B, Jagus R.** 1993. Recombinant vaccinia virus K3L gene product prevents activation of double-stranded RNA-dependent, initiation factor 2 alpha-specific protein kinase. J Biol Chem **268:**12837-12842.

174. **Ueda Y, Morikawa S, Matsuura Y.** 1990. Identification and nucleotide sequence of the gene encoding a surface antigen induced by vaccinia virus. Virology **177:**588-594.

175. **Alcami A, Smith GL.** 1992. A soluble receptor for interleukin-1 beta encoded by vaccinia virus: a novel mechanism of virus modulation of the host response to infection. Cell **71:**153-167.

176. **Symons JA, Alcami A, Smith GL.** 1995. Vaccinia virus encodes a soluble type I interferon receptor of novel structure and broad species specificity. Cell **81:**551-560.

177. **Waibler Z, Anzaghe M, Frenz T, Schwantes A, Pohlmann C, Ludwig H, Palomo-Otero M, Alcami A, Sutter G, Kalinke U.** 2009. Vaccinia virus-mediated inhibition of type I interferon responses is a multifactorial process involving the soluble type I interferon receptor B18 and intracellular components. J Virol **83:**1563-1571.

178. **Mossman K, Upton C, Buller RM, McFadden G.** 1995. Species specificity of ectromelia virus and vaccinia virus interferon-gamma binding proteins. Virology **208:**762-769.

179. **Alcami A.** 2003. Viral mimicry of cytokines, chemokines and their receptors. Nat Rev Immunol **3:**36-50.

180. **Symons JA, Tscharke DC, Price N, Smith GL.** 2002. A study of the vaccinia virus interferon-gamma receptor and its contribution to virus

virulence. J Gen Virol **83:**1953-1964.

181. **Smith VP, Bryant NA, Alcami A.** 2000. Ectromelia, vaccinia and cowpox viruses encode secreted interleukin-18-binding proteins. J Gen Virol **81:**1223-1230.

182. **Smith CA, Davis T, Wignall JM, Din WS, Farrah T, Upton C, McFadden G, Goodwin RG.** 1991. T2 open reading frame from the Shope fibroma virus encodes a soluble form of the TNF receptor. Biochem Biophys Res Commun **176:**335-342.

183. **Jacoby RO, Bhatt PN, Brownstein DG.** 1989. Evidence that NK cells and interferon are required for genetic resistance to lethal infection with ectromelia virus. Arch Virol **108:**49-58.

184. **Xu RH, Rubio D, Roscoe F, Krouse TE, Truckenmiller ME, Norbury CC, Hudson PN, Damon IK, Alcami A, Sigal LJ.** 2012. Antibody inhibition of a viral type 1 interferon decoy receptor cures a viral disease by restoring interferon signaling in the liver. PLoS Pathog **8:**e1002475.

185. **Karupiah G, Fredrickson TN, Holmes KL, Khairallah LH, Buller RM.** 1993. Importance of interferons in recovery from mousepox. J Virol **67:**4214-4226.

186. **Colamonici OR, Domanski P, Sweitzer SM, Larner A, Buller RM.** 1995. Vaccinia virus B18R gene encodes a type I interferon-binding protein that blocks interferon alpha transmembrane signaling. J Biol Chem **270:**15974-15978.

187. **Smith VP, Alcami A.** 2002. Inhibition of interferons by ectromelia virus. J Virol **76:**1124-1134.

188. **Xu RH, Cohen M, Tang Y, Lazear E, Whitbeck JC, Eisenberg RJ, Cohen GH, Sigal LJ.** 2008. The orthopoxvirus type I IFN binding protein is essential for virulence and an effective target for vaccination. J Exp Med **205:**981-992.

189. **Karupiah G, Xie QW, Buller RM, Nathan C, Duarte C, MacMicking JD.** 1993. Inhibition of viral replication by interferon-gamma-induced nitric oxide synthase. Science **261:**1445-1448.

190. **Sakala IG, Chaudhri G, Buller RM, Nuara AA, Bai H, Chen N, Karupiah G.** 2007. Poxvirus-encoded gamma interferon binding protein dampens the

host immune response to infection. J Virol **81:**3346-3353.

191. **Chaudhri G, Panchanathan V, Buller RM, van den Eertwegh AJ, Claassen E, Zhou J, de Chazal R, Laman JD, Karupiah G.** 2004. Polarized type 1 cytokine response and cell-mediated immunity determine genetic resistance to mousepox. Proc Natl Acad Sci U S A **101:**9057-9062.

192. **Siciliano NA, Hersperger AR, Lacuanan AM, Xu RH, Sidney J, Sette A, Sigal LJ, Eisenlohr LC.** 2014. Impact of distinct poxvirus infections on the specificities and functionalities of CD4+ T cell responses. J Virol **88:**10078-10091.

193. **Szulc L, Gierynska M, Winnicka A, Martyniszyn L, Boratynska-Jasinska A, Niemialtowski M.** 2012. T cell cytokine synthesis at the single-cell level in BALB/c and C57BL/6 mice infected with ectromelia virus. Postepy Hig Med Dosw (Online) **66:**222-230.

194. **Alcami A, Smith GL.** 1996. A mechanism for the inhibition of fever by a virus. Proc Natl Acad Sci U S A **93:**11029-11034.

195. **Smith VP, Alcami A.** 2000. Expression of secreted cytokine and chemokine inhibitors by ectromelia virus. J Virol **74:**8460-8471.

196. **Spriggs MK, Koller BH, Sato T, Morrissey PJ, Fanslow WC, Smithies O, Voice RF, Widmer MB, Maliszewski CR.** 1992. Beta 2-microglobulin-, CD8+ T-cell-deficient mice survive inoculation with high doses of vaccinia virus and exhibit altered IgG responses. Proc Natl Acad Sci U S A **89:**6070-6074.

197. **Turner SJ, Silke J, Kenshole B, Ruby J.** 2000. Characterization of the ectromelia virus serpin, SPI-2. J Gen Virol **81:**2425-2430.

198. **Symons JA, Adams E, Tscharke DC, Reading PC, Waldmann H, Smith GL.** 2002. The vaccinia virus C12L protein inhibits mouse IL-18 and promotes virus virulence in the murine intranasal model. J Gen Virol **83:**2833-2844.

199. **Ray CA, Black RA, Kronheim SR, Greenstreet TA, Sleath PR, Salvesen GS, Pickup DJ.** 1992. Viral inhibition of inflammation: cowpox virus encodes an inhibitor of the interleukin-1 beta converting enzyme. Cell **69:**597-604.

200. **Fujino M, Kawasaki M, Funeshima N, Kitazawa Y, Kosuga M, Okabe K,**

Hashimoto M, Yaginuma H, Mikoshiba K, Okuyama T, Suzuki S, Li XK. 2003. CrmA gene expression protects mice against concanavalin-A-induced hepatitis by inhibiting IL-18 secretion and hepatocyte apoptosis. Gene Ther **10:**1781-1790.

201. **Born TL, Morrison LA, Esteban DJ, VandenBos T, Thebeau LG, Chen N, Spriggs MK, Sims JE, Buller RM.** 2000. A poxvirus protein that binds to and inactivates IL-18, and inhibits NK cell response. J Immunol **164:**3246-3254.

202. **Esteban DJ, Buller RM.** 2004. Identification of residues in an orthopoxvirus interleukin-18 binding protein involved in ligand binding and species specificity. Virology **323:**197-207.

203. **Wang Y, Chaudhri G, Jackson RJ, Karupiah G.** 2009. IL-12p40 and IL-18 play pivotal roles in orchestrating the cell-mediated immune response to a poxvirus infection. J Immunol **183:**3324-3331.

204. **Smith CA, Farrah T, Goodwin RG.** 1994. The TNF receptor superfamily of cellular and viral proteins: activation, costimulation, and death. Cell **76:**959-962.

205. **Ruby J, Bluethmann H, Peschon JJ.** 1997. Antiviral activity of tumor necrosis factor (TNF) is mediated via p55 and p75 TNF receptors. J Exp Med **186:**1591-1596.

206. **Pontejo SM, Alejo A, Alcami A.** 2015. Comparative Biochemical and Functional Analysis of Viral and Human Secreted Tumor Necrosis Factor (TNF) Decoy Receptors. J Biol Chem **290:**15973-15984.

207. **Saraiva M, Alcami A.** 2001. CrmE, a novel soluble tumor necrosis factor receptor encoded by poxviruses. J Virol **75:**226-233.

208. **Saraiva M, Smith P, Fallon PG, Alcami A.** 2002. Inhibition of type 1 cytokine-mediated inflammation by a soluble CD30 homologue encoded by ectromelia (mousepox) virus. J Exp Med **196:**829-839.

209. **Alejo A, Saraiva M, Ruiz-Arguello MB, Viejo-Borbolla A, de Marco MF, Salguero FJ, Alcami A.** 2009. A method for the generation of ectromelia virus (ECTV) recombinants: in vivo analysis of ECTV vCD30 deletion mutants. PLoS One **4:**e5175.

210. **Sharma DP, Ramsay AJ, Maguire DJ, Rolph MS, Ramshaw IA.** 1996.

Interleukin-4 mediates down regulation of antiviral cytokine expression and cytotoxic T-lymphocyte responses and exacerbates vaccinia virus infection in vivo. J Virol **70:**7103-7107.

211. **Hou W, Jin YH, Kang HS, Kim BS.** 2014. Interleukin-6 (IL-6) and IL-17 synergistically promote viral persistence by inhibiting cellular apoptosis and cytotoxic T cell function. J Virol **88:**8479-8489.

212. **Muller U, Steinhoff U, Reis LF, Hemmi S, Pavlovic J, Zinkernagel RM, Aguet M.** 1994. Functional role of type I and type II interferons in antiviral defense. Science **264:**1918-1921.

213. **Ramshaw IA, Andrew ME, Phillips SM, Boyle DB, Coupar BE.** 1987. Recovery of immunodeficient mice from a vaccinia virus/IL-2 recombinant infection. Nature **329:**545-546.

214. **O'Gorman WE, Sampath P, Simonds EF, Sikorski R, O'Malley M, Krutzik PO, Chen H, Panchanathan V, Chaudhri G, Karupiah G, Lewis DB, Thorne SH, Nolan GP.** 2010. Alternate mechanisms of initial pattern recognition drive differential immune responses to related poxviruses. Cell Host Microbe **8:**174-185.

215. **Alcami A, Symons JA, Collins PD, Williams TJ, Smith GL.** 1998. Blockade of chemokine activity by a soluble chemokine binding protein from vaccinia virus. J Immunol **160:**624-633.

216. **Bahar MW, Kenyon JC, Putz MM, Abrescia NG, Pease JE, Wise EL, Stuart DI, Smith GL, Grimes JM.** 2008. Structure and function of A41, a vaccinia virus chemokine binding protein. PLoS Pathog **4:**e5.

217. **Chen N, Buller RM, Wall EM, Upton C.** 2000. Analysis of host response modifier ORFs of ectromelia virus, the causative agent of mousepox. Virus Res **66:**155-173.

218. **Graham KA, Lalani AS, Macen JL, Ness TL, Barry M, Liu LY, Lucas A, Clark-Lewis I, Moyer RW, McFadden G.** 1997. The T1/35kDa family of poxvirus-secreted proteins bind chemokines and modulate leukocyte influx into virus-infected tissues. Virology **229:**12-24.

219. **Lalani AS, Masters J, Graham K, Liu L, Lucas A, McFadden G.** 1999. Role of the myxoma virus soluble CC-chemokine inhibitor glycoprotein, M-T1, during myxoma virus pathogenesis. Virology **256:**233-245.

220. **Arnold PL, Fremont DH.** 2006. Structural determinants of chemokine binding by an Ectromelia virus-encoded decoy receptor. J Virol **80:**7439-7449.

221. **Ruiz-Arguello MB, Smith VP, Campanella GS, Baleux F, Arenzana-Seisdedos F, Luster AD, Alcami A.** 2008. An ectromelia virus protein that interacts with chemokines through their glycosaminoglycan binding domain. J Virol **82:**917-926.

222. **Moulton EA, Bertram P, Chen N, Buller RM, Atkinson JP.** 2010. Ectromelia virus inhibitor of complement enzymes protects intracellular mature virus and infected cells from mouse complement. J Virol **84:**9128-9139.

223. **Girgis NM, Dehaven BC, Fan X, Viner KM, Shamim M, Isaacs SN.** 2008. Cell surface expression of the vaccinia virus complement control protein is mediated by interaction with the viral A56 protein and protects infected cells from complement attack. J Virol **82:**4205-4214.

224. **Vanderplasschen A, Mathew E, Hollinshead M, Sim RB, Smith GL.** 1998. Extracellular enveloped vaccinia virus is resistant to complement because of incorporation of host complement control proteins into its envelope. Proc Natl Acad Sci U S A **95:**7544-7549.

225. **Moulton EA, Atkinson JP, Buller RM.** 2008. Surviving mousepox infection requires the complement system. PLoS Pathog **4:**e1000249.

226. **Silverman GA, Bird PI, Carrell RW, Church FC, Coughlin PB, Gettins PG, Irving JA, Lomas DA, Luke CJ, Moyer RW, Pemberton PA, Remold-O'Donnell E, Salvesen GS, Travis J, Whisstock JC.** 2001. The serpins are an expanding superfamily of structurally similar but functionally diverse proteins. Evolution, mechanism of inhibition, novel functions, and a revised nomenclature. J Biol Chem **276:**33293-33296.

227. **Bratke KA, McLysaght A, Rothenburg S.** 2013. A survey of host range genes in poxvirus genomes. Infect Genet Evol **14:**406-425.

228. **Luttge BG, Moyer RW.** 2005. Suppressors of a host range mutation in the rabbitpox virus serpin SPI-1 map to proteins essential for viral DNA replication. J Virol **79:**9168-9179.

229. **Kvansakul M, Yang H, Fairlie WD, Czabotar PE, Fischer SF, Perugini MA, Huang DC, Colman PM.** 2008. Vaccinia virus anti-apoptotic F1L is a

novel Bcl-2-like domain-swapped dimer that binds a highly selective subset of BH3-containing death ligands. Cell Death Differ **15:**1564-1571.

230. **Aoyagi M, Zhai D, Jin C, Aleshin AE, Stec B, Reed JC, Liddington RC.** 2007. Vaccinia virus N1L protein resembles a B cell lymphoma-2 (Bcl-2) family protein. Protein Sci **16:**118-124.

231. **Lanier LL.** 2005. NK cell recognition. Annu Rev Immunol **23:**225-274.

232. **Lanier LL.** 2005. NKG2D in innate and adaptive immunity. Adv Exp Med Biol **560:**51-56.

233. **Delano ML, Brownstein DG.** 1995. Innate resistance to lethal mousepox is genetically linked to the NK gene complex on chromosome 6 and correlates with early restriction of virus replication by cells with an NK phenotype. J Virol **69:**5875-5877.

234. **Martinez J, Huang X, Yang Y.** 2010. Direct TLR2 signaling is critical for NK cell activation and function in response to vaccinia viral infection. PLoS Pathog **6:**e1000811.

235. **Chisholm SE, Reyburn HT.** 2006. Recognition of vaccinia virus-infected cells by human natural killer cells depends on natural cytotoxicity receptors. J Virol **80:**2225-2233.

236. **Kirwan S, Merriam D, Barsby N, McKinnon A, Burshtyn DN.** 2006. Vaccinia virus modulation of natural killer cell function by direct infection. Virology **347:**75-87.

237. **Brooks CR, Elliott T, Parham P, Khakoo SI.** 2006. The inhibitory receptor NKG2A determines lysis of vaccinia virus-infected autologous targets by NK cells. J Immunol **176:**1141-1147.

238. **Williams KJ, Wilson E, Davidson CL, Aguilar OA, Fu L, Carlyle JR, Burshtyn DN.** 2012. Poxvirus infection-associated downregulation of C-type lectin-related-b prevents NK cell inhibition by NK receptor protein-1B. J Immunol **188:**4980-4991.

239. **Seet BT, Johnston JB, Brunetti CR, Barrett JW, Everett H, Cameron C, Sypula J, Nazarian SH, Lucas A, McFadden G.** 2003. Poxviruses and immune evasion. Annu Rev Immunol **21:**377-423.

240. **Alzhanova D, Fruh K.** 2010. Modulation of the host immune response by cowpox virus. Microbes Infect **12:**900-909.

241. **Byun M, Wang X, Pak M, Hansen TH, Yokoyama WM.** 2007. Cowpox virus exploits the endoplasmic reticulum retention pathway to inhibit MHC class I transport to the cell surface. Cell Host Microbe **2:**306-315.

242. **Jarahian M, Fiedler M, Cohnen A, Djandji D, Hammerling GJ, Gati C, Cerwenka A, Turner PC, Moyer RW, Watzl C, Hengel H, Momburg F.** 2011. Modulation of NKp30- and NKp46-mediated natural killer cell responses by poxviral hemagglutinin. PLoS Pathog **7:**e1002195.

243. **Lazear E, Peterson LW, Nelson CA, Fremont DH.** 2013. Crystal structure of the cowpox virus-encoded NKG2D ligand OMCP. J Virol **87:**840-850.

244. **Brownstein DG, Bhatt PN, Gras L.** 1993. Ectromelia virus replication in major target organs of innately resistant and susceptible mice after intravenous infection. Arch Virol **129:**65-75.

245. **Kawano T, Cui J, Koezuka Y, Toura I, Kaneko Y, Sato H, Kondo E, Harada M, Koseki H, Nakayama T, Tanaka Y, Taniguchi M.** 1998. Natural killer-like nonspecific tumor cell lysis mediated by specific ligand-activated Valpha14 NKT cells. Proc Natl Acad Sci U S A **95:**5690-5693.

246. **Karupiah G, Buller RM, Van Rooijen N, Duarte CJ, Chen J.** 1996. Different roles for CD4+ and CD8+ T lymphocytes and macrophage subsets in the control of a generalized virus infection. J Virol **70:**8301-8309.

247. **Parker AK, Parker S, Yokoyama WM, Corbett JA, Buller RM.** 2007. Induction of natural killer cell responses by ectromelia virus controls infection. J Virol **81:**4070-4079.

248. **Fang M, Lanier LL, Sigal LJ.** 2008. A role for NKG2D in NK cell-mediated resistance to poxvirus disease. PLoS Pathog **4:**e30.

249. **Moutaftsi M, Tscharke DC, Vaughan K, Koelle DM, Stern L, Calvo-Calle M, Ennis F, Terajima M, Sutter G, Crotty S, Drexler I, Franchini G, Yewdell JW, Head SR, Blum J, Peters B, Sette A.** 2010. Uncovering the interplay between CD8, CD4 and antibody responses to complex pathogens. Future Microbiol **5:**221-239.

250. **Panchanathan V, Chaudhri G, Karupiah G.** 2005. Interferon function is not required for recovery from a secondary poxvirus infection. Proc Natl Acad

Sci U S A **102:**12921-12926.

251. **Xu R, Johnson AJ, Liggitt D, Bevan MJ.** 2004. Cellular and humoral immunity against vaccinia virus infection of mice. J Immunol **172:**6265-6271.

252. **Kindt T, Osborne, B., Goldsby, R.** 2007. Kuby Immunology, 6 ed. W. H. Freeman, New York.

253. **Jellison ER, Kim SK, Welsh RM.** 2005. Cutting edge: MHC class II-restricted killing in vivo during viral infection. J Immunol **174:**614-618.

254. **Warrington R, Watson W, Kim HL, Antonetti FR.** 2011. An introduction to immunology and immunopathology. Allergy Asthma Clin Immunol **7 Suppl 1:**S1.

255. **Hu Z, Molloy MJ, Usherwood EJ.** 2016. CD4(+) T-cell dependence of primary CD8(+) T-cell response against vaccinia virus depends upon route of infection and viral dose. Cell Mol Immunol **13:**82-93.

256. **Xu RH, Remakus S, Ma X, Roscoe F, Sigal LJ.** 2010. Direct presentation is sufficient for an efficient anti-viral CD8+ T cell response. PLoS Pathog **6:**e1000768.

257. **Gasteiger G, Kastenmuller W, Ljapoci R, Sutter G, Drexler I.** 2007. Cross-priming of cytotoxic T cells dictates antigen requisites for modified vaccinia virus Ankara vector vaccines. J Virol **81:**11925-11936.

258. **Yates NL, Alexander-Miller MA.** 2007. Vaccinia virus infection of mature dendritic cells results in activation of virus-specific naive CD8+ T cells: a potential mechanism for direct presentation. Virology **359:**349-361.

259. **Calvo-Calle JM, Strug I, Nastke MD, Baker SP, Stern LJ.** 2007. Human CD4+ T cell epitopes from vaccinia virus induced by vaccination or infection. PLoS Pathog **3:**1511-1529.

260. **Blanden RV.** 1970. Mechanisms of recovery from a generalized viral infection: mousepox. I. The effects of anti-thymocyte serum. J Exp Med **132:**1035-1054.

261. **Blanden RV.** 1971. Mechanisms of recovery from a generalized viral infection: mousepox. II. Passive transfer of recovery mechanisms with

immune lymphoid cells. J Exp Med **133:**1074-1089.

262. **Fang M, Remakus S, Roscoe F, Ma X, Sigal LJ.** 2015. CD4+ T cell help is dispensable for protective CD8+ T cell memory against mousepox virus following vaccinia virus immunization. J Virol **89:**776-783.

263. **Fang M, Sigal LJ.** 2005. Antibodies and CD8+ T cells are complementary and essential for natural resistance to a highly lethal cytopathic virus. J Immunol **175:**6829-6836.

264. **Buller RM, Holmes KL, Hugin A, Frederickson TN, Morse HC, 3rd.** 1987. Induction of cytotoxic T-cell responses in vivo in the absence of CD4 helper cells. Nature **328:**77-79.

265. **Panchanathan V, Chaudhri G, Karupiah G.** 2006. Protective immunity against secondary poxvirus infection is dependent on antibody but not on CD4 or CD8 T-cell function. J Virol **80:**6333-6338.

266. **Chaudhri G, Panchanathan V, Bluethmann H, Karupiah G.** 2006. Obligatory requirement for antibody in recovery from a primary poxvirus infection. J Virol **80:**6339-6344.

267. **Fang M, Siciliano NA, Hersperger AR, Roscoe F, Hu A, Ma X, Shamsedeen AR, Eisenlohr LC, Sigal LJ.** 2012. Perforin-dependent CD4+ T-cell cytotoxicity contributes to control a murine poxvirus infection. Proc Natl Acad Sci U S A **109:**9983-9988.

268. **Wang B, Norbury CC, Greenwood R, Bennink JR, Yewdell JW, Frelinger JA.** 2001. Multiple paths for activation of naive CD8+ T cells: CD4-independent help. J Immunol **167:**1283-1289.

269. **Demkowicz WE, Jr., Ennis FA.** 1993. Vaccinia virus-specific CD8+ cytotoxic T lymphocytes in humans. J Virol **67:**1538-1544.

270. **Fang M, Sigal LJ.** 2006. Direct CD28 costimulation is required for CD8+ T cell-mediated resistance to an acute viral disease in a natural host. J Immunol **177:**8027-8036.

271. **Tscharke DC, Karupiah G, Zhou J, Palmore T, Irvine KR, Haeryfar SM, Williams S, Sidney J, Sette A, Bennink JR, Yewdell JW.** 2005. Identification of poxvirus CD8+ T cell determinants to enable rational design

and characterization of smallpox vaccines. J Exp Med **201:**95-104.

272. **Remakus S, Rubio D, Lev A, Ma X, Fang M, Xu RH, Sigal LJ.** 2013. Memory CD8(+) T cells can outsource IFN-gamma production but not cytolytic killing for antiviral protection. Cell Host Microbe **13:**546-557.

273. **Edghill-Smith Y, Golding H, Manischewitz J, King LR, Scott D, Bray M, Nalca A, Hooper JW, Whitehouse CA, Schmitz JE, Reimann KA, Franchini G.** 2005. Smallpox vaccine-induced antibodies are necessary and sufficient for protection against monkeypox virus. Nat Med **11:**740-747.

274. **Boulter EA, Appleyard G.** 1973. Differences between extracellular and intracellular forms of poxvirus and their implications. Prog Med Virol **16:**86-108.

275. **Law M, Putz MM, Smith GL.** 2005. An investigation of the therapeutic value of vaccinia-immune IgG in a mouse pneumonia model. J Gen Virol **86:**991-1000.

276. **Duke-Cohan JS, Wollenick K, Witten EA, Seaman MS, Baden LR, Dolin R, Reinherz EL.** 2009. The heterogeneity of human antibody responses to vaccinia virus revealed through use of focused protein arrays. Vaccine **27:**1154-1165.

277. **Putz MM, Midgley CM, Law M, Smith GL.** 2006. Quantification of antibody responses against multiple antigens of the two infectious forms of Vaccinia virus provides a benchmark for smallpox vaccination. Nat Med **12:**1310-1315.

278. **Benhnia MR, McCausland MM, Laudenslager J, Granger SW, Rickert S, Koriazova L, Tahara T, Kubo RT, Kato S, Crotty S.** 2009. Heavily isotype-dependent protective activities of human antibodies against vaccinia virus extracellular virion antigen B5. J Virol **83:**12355-12367.

279. **Cohen ME, Xiao Y, Eisenberg RJ, Cohen GH, Isaacs SN.** 2011. Antibody against extracellular vaccinia virus (EV) protects mice through complement and Fc receptors. PLoS One **6:**e20597.

280. **Bidgood SR, Mercer J.** 2015. Cloak and Dagger: Alternative Immune Evasion and Modulation Strategies of Poxviruses. Viruses **7:**4800-4825.

281. **Smith GL, Vanderplasschen A, Law M.** 2002. The formation and function

of extracellular enveloped vaccinia virus. J Gen Virol **83:**2915-2931.

282. **Zinkernagel RM, Hengartner H.** 2006. Protective 'immunity' by pre-existent neutralizing antibody titers and preactivated T cells but not by so-called 'immunological memory'. Immunol Rev **211:**310-319.

283. **Fenner F.** 1949b. Studies in mousepox, infectious ectromelia of mice; quantitative investigations on the spread of virus through the host in actively and passively immunized animals. Aust J Exp Biol Med Sci **27:**1-18.

284. **Ma X, Xu RH, Roscoe F, Whitbeck JC, Eisenberg RJ, Cohen GH, Sigal LJ.** 2013. The mature virion of ectromelia virus, a pathogenic poxvirus, is capable of intrahepatic spread and can serve as a target for delayed therapy. J Virol **87:**7046-7053.

285. **Tscharke DC, Smith GL.** 1999. A model for vaccinia virus pathogenesis and immunity based on intradermal injection of mouse ear pinnae. J Gen Virol **80 (Pt 10):**2751-2755.

286. **Lin LC, Flesch IE, Tscharke DC.** 2013. Immunodomination during peripheral vaccinia virus infection. PLoS Pathog **9:**e1003329.

287. **Williamson JD, Reith RW, Jeffrey LJ, Arrand JR, Mackett M.** 1990. Biological characterization of recombinant vaccinia viruses in mice infected by the respiratory route. J Gen Virol **71 (Pt 11):**2761-2767.

288. **Flesch IE, Hollett NA, Wong YC, Quinan BR, Howard D, da Fonseca FG, Tscharke DC.** 2015. Extent of Systemic Spread Determines CD8+ T Cell Immunodominance for Laboratory Strains, Smallpox Vaccines, and Zoonotic Isolates of Vaccinia Virus. J Immunol **195:**2263-2272.

289. **Brinton MA, Nathanson N.** 1981. Genetic determinants of virus susceptibility: epidemiologic implications of murine models. Epidemiol Rev **3:**115-139.

290. **Yokoyama WM, Ryan JC, Hunter JJ, Smith HR, Stark M, Seaman WE.** 1991. cDNA cloning of mouse NKR-P1 and genetic linkage with LY-49. Identification of a natural killer cell gene complex on mouse chromosome 6. J Immunol **147:**3229-3236.

291. **Vance RE, Jamieson AM, Cado D, Raulet DH.** 2002. Implications of CD94 deficiency and monoallelic NKG2A expression for natural killer cell

development and repertoire formation. Proc Natl Acad Sci U S A **99:**868-873.

292. **Fang M, Orr MT, Spee P, Egebjerg T, Lanier LL, Sigal LJ.** 2011. CD94 is essential for NK cell-mediated resistance to a lethal viral disease. Immunity **34:**579-589.

293. **Rapaport AS, Schriewer J, Gilfillan S, Hembrador E, Crump R, Plougastel BF, Wang Y, Le Friec G, Gao J, Cella M, Pircher H, Yokoyama WM, Buller RM, Colonna M.** 2015. The Inhibitory Receptor NKG2A Sustains Virus-Specific CD8(+) T Cells in Response to a Lethal Poxvirus Infection. Immunity **43:**1112-1124.

294. **Brownstein DG, Bhatt PN, Gras L, Budris T.** 1992. Serial backcross analysis of genetic resistance to mousepox, using marker loci for Rmp-2 and Rmp-3. J Virol **66:**7073-7079.

295. **Brownstein DG, Gras L.** 1995. Chromosome mapping of Rmp-4, a gonad-dependent gene encoding host resistance to mousepox. J Virol **69:**6958-6964.

296. **Damon I.** 2013. Poxviruses, p 2160-2184. *In* Knipe DM, Howley PM (ed), Fields Virology, Sixth ed, vol 2. Wolters Kluwer/ Lippincott Williams &Wilkins, Philadelphia.

297. **Moss B.** 2013. Poxvirus DNA replication. Cold Spring Harb Perspect Biol **5**.

298. **Haller SL, Peng C, McFadden G, Rothenburg S.** 2014. Poxviruses and the evolution of host range and virulence. Infect Genet Evol **21:**15-40.

299. **Xu Z, Zikos D, Osterrieder N, Tischer BK.** 2014. Generation of a complete single-gene knockout bacterial artificial chromosome library of cowpox virus and identification of its essential genes. J Virol **88:**490-502.

300. **Byrd CM, Hruby DE.** 2005. A conditional-lethal vaccinia virus mutant demonstrates that the I7L gene product is required for virion morphogenesis. Virol J **2:**4.

301. **Ansarah-Sobrinho C, Moss B.** 2004. Vaccinia virus G1 protein, a predicted metalloprotease, is essential for morphogenesis of infectious virions but not for cleavage of major core proteins. J Virol **78:**6855-6863.

302. **Hedengren-Olcott M, Byrd CM, Watson J, Hruby DE.** 2004. The vaccinia virus G1L putative metalloproteinase is essential for viral replication in vivo. J

Virol **78:**9947-9953.

303. **Doms RW, Russ G, Yewdell JW.** 1989. Brefeldin A redistributes resident and itinerant Golgi proteins to the endoplasmic reticulum. J Cell Biol **109:**61-72.

304. **Lippincott-Schwartz J, Yuan LC, Bonifacino JS, Klausner RD.** 1989. Rapid redistribution of Golgi proteins into the ER in cells treated with brefeldin A: evidence for membrane cycling from Golgi to ER. Cell **56:**801-813.

305. **Husain M, Weisberg AS, Moss B.** 2006. Existence of an operative pathway from the endoplasmic reticulum to the immature poxvirus membrane. Proc Natl Acad Sci U S A **103:**19506-19511.

306. **Shaw AS, Rottier PJ, Rose JK.** 1988. Evidence for the loop model of signal-sequence insertion into the endoplasmic reticulum. Proc Natl Acad Sci U S A **85:**7592-7596.

307. **Americo JL, Moss B, Earl PL.** 2010. Identification of wild-derived inbred mouse strains highly susceptible to monkeypox virus infection for use as small animal models. J Virol **84:**8172-8180.

308. **Americo JL, Sood CL, Cotter CA, Vogel JL, Kristie TM, Moss B, Earl PL.** 2014. Susceptibility of the wild-derived inbred CAST/Ei mouse to infection by orthopoxviruses analyzed by live bioluminescence imaging. Virology **449:**120-132.

309. **Alzhanova D, Hammarlund E, Reed J, Meermeier E, Rawlings S, Ray CA, Edwards DM, Bimber B, Legasse A, Planer S, Sprague J, Axthelm MK, Pickup DJ, Lewinsohn DM, Gold MC, Wong SW, Sacha JB, Slifka MK, Fruh K.** 2014. T cell inactivation by poxviral B22 family proteins increases viral virulence. PLoS Pathog **10:**e1004123.

310. **Kay BK, Williamson MP, Sudol M.** 2000. The importance of being proline: the interaction of proline-rich motifs in signaling proteins with their cognate domains. FASEB J **14:**231-241.

311. **Alzhanova D, Edwards DM, Hammarlund E, Scholz IG, Horst D, Wagner MJ, Upton C, Wiertz EJ, Slifka MK, Fruh K.** 2009. Cowpox virus inhibits the transporter associated with antigen processing to evade T cell recognition. Cell Host Microbe **6:**433-445.

312. **Byun M, Verweij MC, Pickup DJ, Wiertz EJ, Hansen TH, Yokoyama WM.** 2009. Two mechanistically distinct immune evasion proteins of cowpox virus combine to avoid antiviral CD8 T cells. Cell Host Microbe **6:**422-432.

313. **Lustig S, Fogg C, Whitbeck JC, Eisenberg RJ, Cohen GH, Moss B.** 2005. Combinations of polyclonal or monoclonal antibodies to proteins of the outer membranes of the two infectious forms of vaccinia virus protect mice against a lethal respiratory challenge. J Virol **79:**13454-13462.

314. **Reynolds SE, Moss B.** 2015. Characterization of a large, proteolytically processed cowpox virus membrane glycoprotein conserved in most chordopoxviruses. Virology **483:**209-217.

315. **Szulc L GM, Winnicka A, Martyniszyn L, Boratyńska-Jasińska A, Niemiałtowski M.** 2010. T cell cytokine synthesis at the single-cell level in BALB/c and C57BL/6 mice infected with ectromelia virus. Postepy Hig Med Dosw (Online) **66:**222-230.

316. **Karupiah G.** 1998. Type 1 and type 2 cytokines in antiviral defense. Vet Immunol Immunopathol **63:**105-109.

317. **Sakala IG, Chaudhri G, Eldi P, Buller RM, Karupiah G.** 2015. Deficiency in Th2 cytokine responses exacerbate orthopoxvirus infection. PLoS One **10:**e0118685.

318. **Demetri GD, Griffin JD.** 1991. Granulocyte colony-stimulating factor and its receptor. Blood **78:**2791-2808.

319. **Earl PL, Americo JL, Moss B.** 2012. Lethal monkeypox virus infection of CAST/EiJ mice is associated with a deficient gamma interferon response. J Virol **86:**9105-9112.

320. **Cotter CA, Earl PL, Wyatt LS, Moss B.** 2015. Preparation of Cell Cultures and Vaccinia Virus Stocks. Curr Protoc Microbiol **39:**14A 13 11-18.